



**PROMOTING ACCESS TO HAEMOSTASIS TESTING IN RESOURCE-SCARCE AND  
EMERGENCY SETTINGS USING PAPER-BASED LATERAL FLOW DIAGNOSTIC  
SCREENING ASSAYS FOR COAGULATION DISORDERS**

**JERRO SAIDYKHAN**

**A thesis submitted in partial fulfilment of the requirement of the University  
of the West of England, Bristol for the degree of Doctor of Philosophy**

**Director of Studies: Prof Tony Killard**

**Co-supervisor: Dr. Jennifer May**

**School of Applied Sciences  
University of the West of England, Bristol**

**October 2023**

## ABSTRACT

Haemostatic disorders cause excessive bleeding and clotting and result in high morbidity and mortality worldwide, but especially in low-income areas which often lack suitable facilities and expertise for affordable diagnosis and treatment. Simple and low-cost haemostasis tests in such areas would permit diagnosis and effective treatment and thus reduce the associated morbidity and mortality. In a quest to provide simple, affordable, and yet effective haemostasis tests for low resource areas, this project utilised simple materials in the form of chromatography paper, coupled with inexpensive fabrication techniques such as wax printing and drop-casting to develop a number of low-cost and easy-to-use lateral flow devices for testing for haemostasis dysfunctions.

The devices developed in this project were all fabricated using the same basic techniques and procedures. Firstly, lateral flow test strip formats were designed using Microsoft PowerPoint and printed onto chromatography papers using wax printing. The printed papers were cured in an oven at 100°C for two minutes, allowing wax to sink to make a hydrophobic boundary. The strips were then modified with appropriate reagent(s) via drop-casting and allowed to air dry before being cut and inserted into test strip holders. The strip holders were fabricated using 3D printing and were equipped with elevated rails to ensure that samples only flowed through the paper, a millimetric graduation scale to measure the distances travelled by the samples, and an opening for sample deposition and the visual monitoring of sample flow.

In all, two paper-based lateral flow coagulation assay devices were developed, and the effect of platelet aggregation on sample flow was also investigated, and which were all based on the principle that coagulation or aggregation would alter the flow rate, or distance travelled by the sample. Assay development for each device began with isolating the effect of either coagulation or platelet adhesion/aggregation on sample flow rates from other contributions such as sample viscosity or reagent deposition. These coagulation or aggregation effects were then enhanced via optimising the relevant analytical parameters such as the type and amount of reagent immobilised on assay strips, sample volume, and strip geometry. Optimized formats of the devices were then calibrated and validated against routine reference methods using artificially constructed and clinical samples.

The first coagulation testing device was developed to measure fibrinogen concentration in blood plasma and provided results within five minutes. This device had good

agreement with an established reference method for fibrinogen concentrations of 0.5 to 7.0 mg/mL. The second coagulation testing device was a prothrombin assay and measured the effect on clotting in distance rather than in time. The distance values from the device had a good correlation with prothrombin time (PT) values from a reference routine hospital method ( $r=0.849$ ) for samples with PT values  $\leq 40.0$  s. The device for platelet aggregation on lateral flow strips could distinguish dysfunctional platelet samples from normal ones ( $p<0.05$ ) based on the difference in their travel distances. In addition, it showed a strong correlation between platelet count and sample distance ( $r=0.996$ ) and Aggregation Effect ( $r=0.886$ ). This means it could also potentially test for quantitative platelet disorders.

In summary, two novel paper-based lateral flow coagulation testing devices have been developed. In addition, platelet aggregation and its effect on sample flow have been determined thus laying the foundation for development of a lateral flow platelet function analyser. These devices have the potential for deployment and incorporation into healthcare delivery systems in low-income areas to alleviate morbidity and mortality associated with bleeding and clotting disorders.

**To my dear parents,  
my mum, Queen Sonko, and my dad, Ebrahim Saidykhan**

## **ACKNOWLEDGEMENTS**

I wish to recognise the support offered by the people in making this project a success. I will first of all thank Prof Tony Killard, director of studies and Dr. Jennifer May, the supervisor for this project for their direction, advice, support, and encouragement as well as their patience and understanding during the entire time I was working on this PhD project. I can't thank you enough.

I also wish to express my sincere gratitude to the UK Commonwealth Scholarship Commission for providing the funding for this PhD project which included funds for tuition, living expenses, laboratory equipment and chemical reagents.

My thanks go to the UWE School of Applied Sciences and its laboratory technical support team for providing the space, equipment and other necessary facilities and services during the implementation of this project.

I wish to thank the University of the Gambia for offering me study leave to pursue my PhD. I'm really grateful for this.

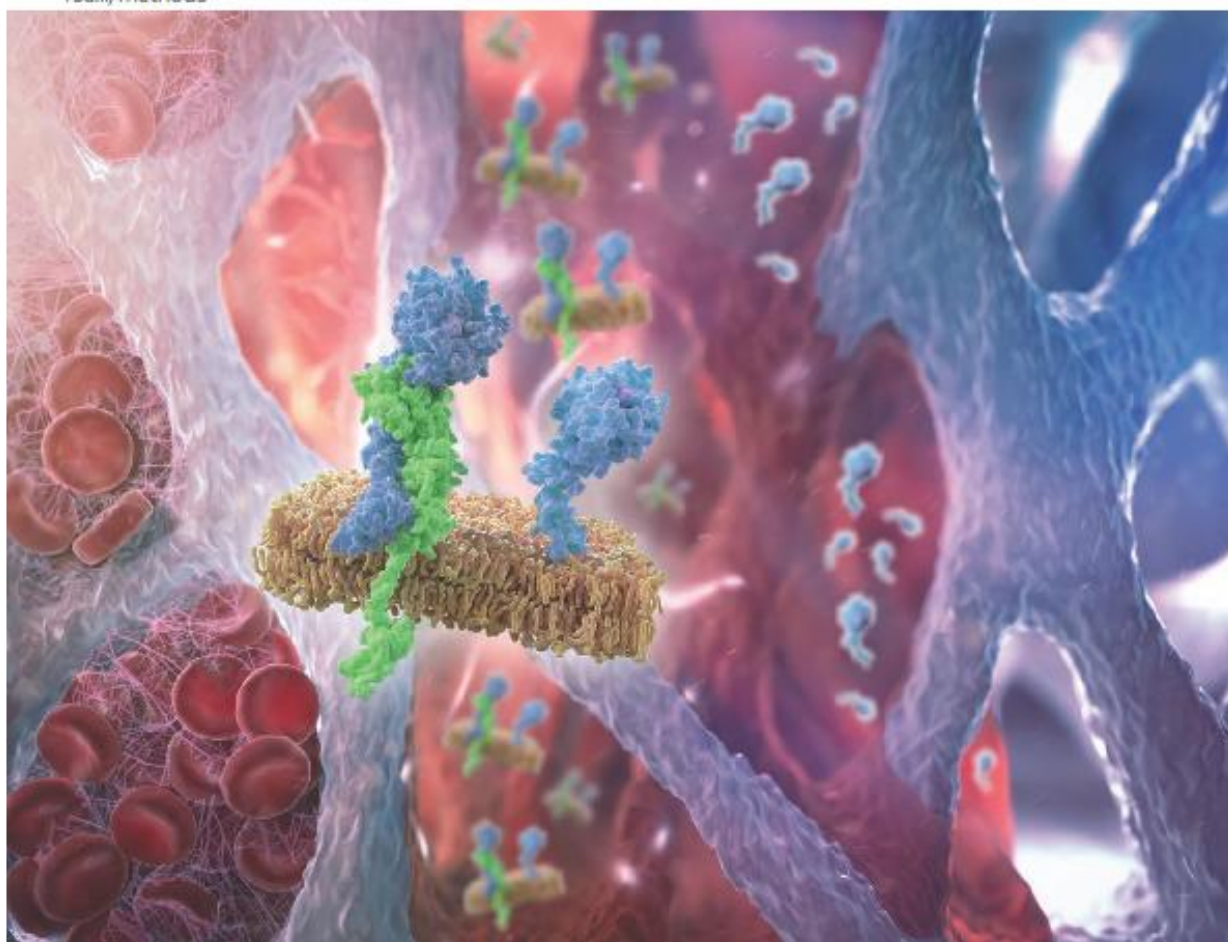
I cannot conclude without thanking my wife, Khaddijation Saidykhan, and my children. A big thanks to you all for your patience and understanding while I was away for such a long period of time working on this PhD project.

Finally, I wish to thank everyone else not mentioned, and who in one way or another rendered support in whatever form and whatever degree during the conduct of this PhD project.

# Analytical Methods

Volume 14  
Number 38  
14 October 2022  
Pages 3711–3816

rsc.li/methods



ISSN 1759-9679



ROYAL SOCIETY  
OF CHEMISTRY

#### PAPER

Anthony J. Killard et al.  
Development of a paper-based lateral flow prothrombin  
assay

Indexed in  
Medline!

Analytical Methods journal cover article for Saidykhan, J., Pointon, L., Cinti, S., May, J.E., and Killard, A.J. (2022). Development of a paper-based lateral-flow prothrombin assay. *Analytical Methods*, DOI: 10.1039/D2AY00965J.

Artwork depicts blood sample moving through paper matrix and undergoing coagulation in response to extrinsic pathway activation with extrinsic tenase activation of factor X.

# TABLE OF CONTENTS

Abstract .....	1
Dedication .....	3
Acknowledgements .....	4
Cover artwork .....	5
List of abbreviations .....	10
<b>1. INTRODUCTION .....</b>	<b>13</b>
1.1 An overview of haemostasis .....	14
1.2 Bleeding and coagulation disorders .....	18
1.3 Thrombotic disorders .....	19
1.4 Conventional haemostasis tests .....	20
1.4.1 Thrombin time/quantitative fibrinogen (Clauss) assay .....	21
1.4.2 Prothrombin time .....	22
1.4.3 Activated partial thromboplastin time .....	23
1.4.4 Mixing tests .....	24
1.4.5 Platelet function tests .....	25
1.5 Point of care haemostasis testing devices .....	27
1.5.1 Detection techniques used in POC haemostasis testing devices .....	28
1.5.2 Limitations to the use of POC haemostasis testing devices in resource scarce areas .....	30
1.6 Lateral flow haemostasis testing devices .....	30
1.6.1 Design and fabrication of lateral flow haemostasis testing devices .....	31
1.6.2 Materials used in fabrication of lateral flow haemostasis testing devices .....	32
1.6.3 Principles of detection used in lateral flow haemostasis testing devices .....	34
1.6.4 Challenges and drawbacks of lateral flow haemostasis testing devices .....	36
1.7 Aims and objectives .....	37

<b>2. MATERIALS AND METHODS .....</b>	<b>39</b>
<b>2.1 Materials .....</b>	<b>40</b>
<b>2.2 Methods .....</b>	<b>41</b>
2.2.1 Standardisation of thrombin activity .....	41
2.2.2 Preparation of fibrinogen standards and samples .....	42
2.2.3 Measurement of fibrinogen concentration .....	42
2.2.4 Preparation of standards and samples for prothrombin time measurement .....	42
2.2.5 Measurement of prothrombin time .....	43
2.2.6 Preparation of platelet suspensions .....	43
2.2.7 Determination of platelet count .....	43
2.2.8 Staining and microscopic analysis of platelets .....	43
2.2.9 Scanning electron microscopy of lateral flow strips .....	44
2.2.10 Fabrication of lateral flow test strips .....	44
2.2.11 Fabrication of strip holders .....	45
2.2.12 General lateral flow assay development procedure .....	46
2.2.13 Storage and stability studies of test strips .....	47
2.2.14 Statistical and numeral analysis .....	47
<b>3. DEVELOPMENT OF A PAPER-BASED LATERAL FLOW FIBRINOGEN ASSAY DEVICE .....</b>	<b>49</b>
3.1 Introduction .....	50
3.2 Results and discussion .....	55
3.2.1 Design of the paper-based lateral flow fibrinogen assay strip ....	55
3.2.2 Assessing the effect of thrombin clotting on sample flow rate ...	55
3.2.3 Investigation the deposition of thrombin on paper strips .....	57
3.2.4 Determination of the effect of thrombin activity on sample flow rate .....	59
3.2.5 Optimization of thrombin Activity and sample volume .....	62
3.2.6 Calibration of paper-based lateral flow fibrinogen assay device ..	63
3.2.7 Validation of paper-based lateral flow fibrinogen assay device ..	65
3.2.8 Investigation of the effect of temperature on device storage and operational stability .....	68



3.3 Conclusion .....	70
<b>4. DEVELOPMENT OF A PAPER-BASED LATERAL FLOW PROTHROMBIN ASSAY DEVICE .....</b>	<b>72</b>
4.1 Introduction .....	73
4.2 Results and discussion .....	77
4.2.1 Investigation of paper substrates for lateral flow prothrombin assay .....	77
4.2.2 Investigation of sample flow rates on thromboplastin-modified substrates .....	79
4.2.3 Optimization of thromboplastin and sample volume .....	81
4.2.4 Optimization of strip format and calcium chloride deposition ....	83
4.2.5 Investigation of the effect of thromboplastin reagent type .....	85
4.2.6 Determination of optimised lateral flow prothrombin assay in calibration plasmas .....	90
4.2.7 Validation of the paper-based lateral flow prothrombin assay device .....	92
4.2.8 Investigation of the storage and operational stability of the prothrombin assay device .....	95
4.3 Conclusion .....	98
<b>5. INVESTIGATION OF PLATELET AGGREGATION ON PAPER-BASED LATERAL FLOW STRIPS .....</b>	<b>99</b>
5.1 Introduction .....	100
5.2 Results and discussion .....	105
5.2.1 Study of lyophilised platelet viability using staining and light microscopy .....	105
5.2.2 Study of platelet adhesion and aggregation on test strips using light and electron microscopy .....	106
5.2.3 Assessment of the effect of platelet aggregation on sample flow rate .....	107
5.2.4 Investigation of agonist on strip-based aggregation .....	111

5.2.5	Investigation of the enhancement of aggregation using fibrinogen .....	114
5.2.6	Optimization of ADP concentration .....	114
5.2.7	Experimental and mathematical reduction of errors in Aggregation Effect .....	115
5.2.8	Investigation of the plasma sample matrix on the Aggregation Effect .....	117
5.2.9	Optimization of sample volume .....	118
5.2.10	Study of the effect of platelet count on the aggregation effect ..	118
5.2.11	The effect of the platelet antagonist aspirin on platelet aggregation on strip .....	120
5.3	Conclusion .....	122
<b>6.</b>	<b>OVERALL CONCLUSIONS AND FUTURE WORK .....</b>	<b>123</b>
6.1	Overall conclusions .....	124
6.2	Future work .....	125
6.2.1	Improving the performance of the developed assay devices ....	125
6.2.2	Development of a paper-based lateral flow activated partial thromboplastin assay .....	127
6.2.3	Development of a multiplexed lateral flow coagulation analyser .....	128
6.2.4	Development of lateral flow assay for detection of Von Willebrand Disease (vWD) .....	129
6.2.5	Development of a multiplexed lateral flow platelet function analyser .....	130
6.2.6	Deployment of the coagulation testing devices into low resource areas .....	131
	References .....	133
	List of publications and presentations .....	146

## LIST OF ABBREVIATIONS

$\alpha_2$ AP	$\alpha_2$ -antiplasmin
A	Abnormal plasma
ABS	Absorbance
ACT	Activated clotting time
ADP	Adenosine diphosphate
APC	Activated protein C
aPTT	Activated partial thromboplastin time
AT	Anti-thrombin
ATP	Adenosine triphosphate
BSS	Bernard-Soulier syndrome
CA	Contact activator
CI	Confidence interval
COX-1	Cyclooxygenase-1
CRP	C-reactive protein
CV	Coefficient of variation
CVT	Cerebrovascular thrombosis
DIC	Disseminated intravascular coagulation
DMSO	Dimethyl sulfoxide
DVT	Deep vein thrombosis
ECG	Electrocardiogram
EDTA	Ethylenediaminetetraacetic acid
ELISA	Enzyme-linked immunosorbent assay
EPCR	Endothelial protein C receptor
FDP	Fibrin degradation product
FIB	Fibrinogen
FPA	Fibrinopeptide A
FPB	Fibrinopeptide B
FVIID	Factor VII deficient plasma
GP	Glycoprotein
hCG	Human chorionic gonadotrophin
INR	International normalised ratio
IRP	International reference preparation
ISI	International sensitivity index
L CL	Lower confidence limit

L LOA	Lower limit of agreement
LFA	Lateral flow assay
MI	Myocardial infarction
N	Normal plasma
NIH	National Institute of Health
PAI	Plasminogen activator inhibitor
PBS	Phosphate-buffered saline
VASP-P	Phosphorylated Vasodilator-stimulated phosphoprotein
PC	Protein-C
PDGF	Platelet derived growth factor
PE	Pulmonary embolism
PFA	Platelet function analyser
PL	Phospholipid
POC	Point-of-care
PPH	Postpartum haemorrhage
PPP	Platelet poor plasma
PRP	Platelet rich plasma
PS	Protein-S
PT	Prothrombin time
QC	Quality control
QCM	Quartz crystal microbalance
RHTF	Recombinant human tissue factor
ROTEM	Rotational thromboelastometry
RSD	Relative standard deviation
SA	Severe abnormal plasma
SD	Standard deviation
SE	Standard error
SEM	Scanning electron microscopy
SPD	Storage pool disease
SV	Sample variance
TAFI	Thrombin-activatable fibrinolysis inhibitor
TBS	Tris-buffered saline
TCT	Thrombin clotting time
TEG	Thromboelastography
TF	Tissue factor

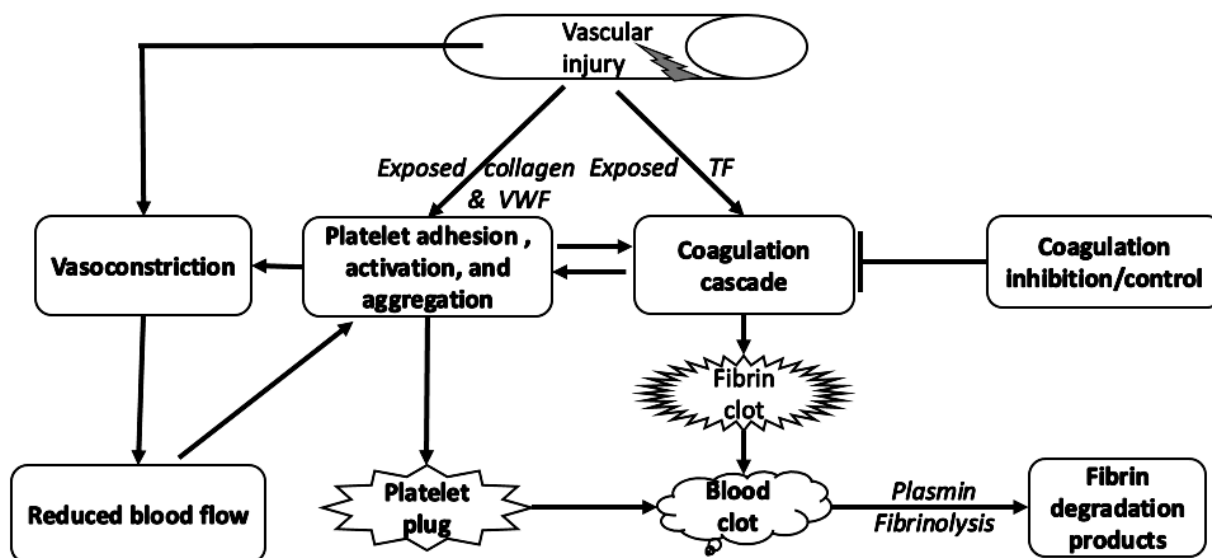
TFPI	Tissue factor pathway inhibitor
TM	Thrombomodulin
tPA	Tissue plasminogen activator
TT	Thrombin time
U CL	Upper confidence limit
U LOA	Upper limit of agreement
uPA	Urokinase plasminogen activator
UV	Ultraviolet
VT	Venous thrombosis
vWD	Von Willebrand disease
vWF	Von Willebrand factor

## **1. INTRODUCTION**

## 1.1 An overview of haemostasis

Haemostasis is the body's innate mechanism to minimise and halt bleeding in the event of injury. A malfunction of this process results in either excessive bleeding or clotting. Disorders of haemostasis lead to excessive blood loss, e.g., post-partum haemorrhage (PPH), prolonged menstrual periods, intestinal bleeding, and frequent epistaxis; or excessive clotting which results in venous thromboembolism (VT), myocardial infarction (MI), and thromboembolic strokes (Hoffbrand and Steensma, 2019). Haemostatic disorders are among the leading causes of morbidity and mortality worldwide. Identification and proper management of these disorders require the use of reliable and rapid testing methods to allow appropriate and effective treatment. Mortality rates are especially high in resource scarce settings, partly due to a lack of access to testing and treatment. This has prompted the development of haemostasis testing technologies that are appropriate for resource poor regions such as low cost, and simplicity (Guler *et al.*, 2018; Dudek *et al.*, 2010). Successful development of such technologies depends on a clear understanding of the physiological processes involved in the haemostatic response and the abnormalities that lead to haemostatic disorders.

Haemostasis is a balance between clot formation and clot prevention/removal and is brought about by complex interactions involving vascular endothelium, platelets, and coagulation proteins (Hoffbrand *et al.*, 2015) (Fig. 1.1). In response to vascular damage, haemostasis occurs in three main stages – primary and secondary haemostasis and fibrinolysis. The initial response to injury, termed primary haemostasis is brought about by blood vessels and platelets. It starts with the localised contraction of smooth vascular muscle cells (vasoconstriction) to reduce blood flow to the area. Vasoconstriction is mainly triggered by the sympathetic nervous system and endothelin-1, a peptide released from endothelial cells and platelets. The exposure of sub-endothelial matrix (collagen, laminin, microfibrils, and Von Willebrand Factor (vWF)) stimulates platelet adhesion and aggregation at the site of vascular damage, leading to the formation of the primary haemostatic plug (Hoffbrand *et al.*, 2015). This plug temporarily stops bleeding and provides phospholipid (PL) membrane surface for assembly of the coagulation factors and deposition of fibrin fibres in the formation of the secondary haemostatic plug. Platelets also promote wound healing by producing platelet-derived growth factor (PDGF) which stimulates cell division in vascular smooth muscle cells (Hoffbrand and Steensma, 2019).



**Fig. 1.1.** The haemostatic response. Vascular damage triggers vasoconstriction causing reduced blood flow. Endothelial damage exposes collagen and releases Von Willebrand Factor (vWF), resulting in platelet adhesion and activation. Release of tissue factor (TF) results in the initiation of the coagulation cascade. Aggregated platelets form a plug which is cross-linked by fibrin produced from the coagulation cascade, leading to formation of the secondary haemostatic plug (blood clot). The extent of coagulation is controlled and limited to the site of damage by coagulation inhibitors. Clot is removed after healing by fibrinolysis involving plasmin. Adopted with permission from Hoffbrand's Essential Haematology, 8th ed (Hoffbrand and Steensma, 2019).

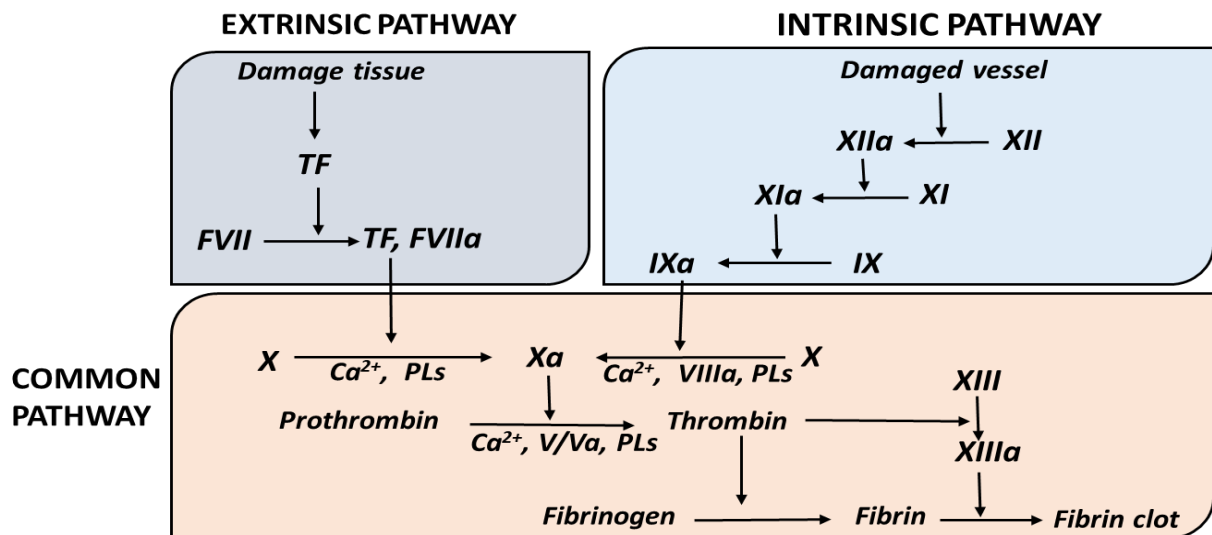
Secondary haemostasis is the stage during which the fibrin clot is formed over and within the platelet plug, converting it into a stronger haemostatic plug which permanently stops bleeding. This involves the coagulation cascade (Fig. 1.2), which is a series of reactions involving sequential activation of proteolytic enzymes called coagulation factors (Table 1.1), that generates thrombin and forms the fibrin clot. The inactive forms of these enzymes, called zymogens are named using Roman numerals and their active forms are indicated by adding the suffix "a" to the numeral (Palta *et al.*, 2014). Coagulation is predominantly initiated by the exposure of tissue factor (TF) from the damaged endothelium to the circulating blood, which then binds with, and activates Factor VII (FVII) (the extrinsic tenase complex). In the presence of  $\text{Ca}^{2+}$  and the PL surface. This, in turn activates FX to FXa. The reactions from exposure of TF down to the activation of FX is termed the 'extrinsic pathway'. The coagulation cascade is also initiated through an 'intrinsic pathway' which starts from activation of FXII via its interaction with collagen from the damaged endothelium. FX is activated by FIXa, VIIIa,  $\text{Ca}^{2+}$  and PLs (intrinsic tenase complex) via this pathway.



**Table 1.1.** Coagulation factors and their functions (Palta et al., 2014).

Factor	Other name	Function
FI	Fibrinogen	Clot formation, platelet adhesion & aggregation
FII	Prothrombin	Activates FI, FV, FVII, FVIII, FXI, FXIII, Protein C and platelets
FIII	Tissue factor	Activates VII, VIIa co factor
FIV	Calcium	Co factor, facilitates factor binding to phospholipids
FV	Labile factor	X-prothrombinase co factor
FVII	Proconvertin	Activates FIX and FX
FVIII	Antihaemophilia factor A	IX-tenase complex co factor
FIX	Christmas factor	Activates FX, component of FVIII-FIX tenase complex
FX	Stuart factor	Activates FII, forms prothrombinase complex with FV
FXI	Plasma thromboplastin antecedent	Activates FIX
FXII	Hageman factor	Activates FXI, FVII, and prekallikrein
FXIII	Fibrin stabilizing factor	Fibrin crosslinking, wound healing
HMWK	High molecular weight kininogen	Co factor, binding fibrinogen to phospholipid surface
PKK	Prekallikrein	Serine protease, vasodilation

From prothrombin, the common pathway generates thrombin which then converts fibrinogen into fibrin molecules (Douglas, 2000). Fibrin molecules bind non-covalently with one another to form fibres and the fibres are stabilised via covalent crosslinking by FXIII.

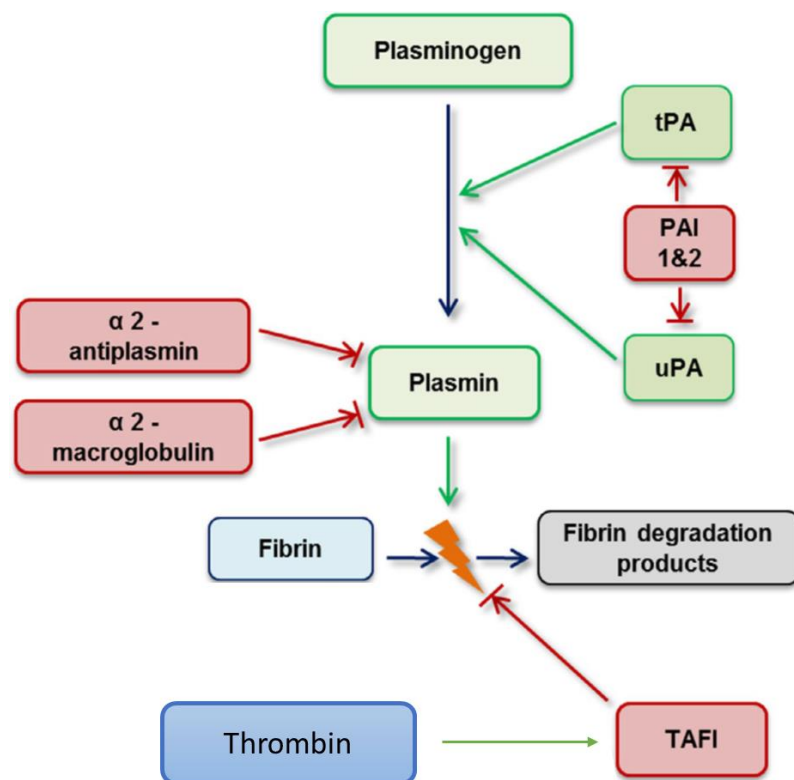


**Fig. 1.2.** The coagulation cascade. Coagulation is triggered predominantly through the extrinsic pathway, initiated by exposure of TF, and also through the intrinsic pathway, initiated by exposure of FXII to the damaged vessel. Both pathways converge into a common pathway which generates thrombin that converts fibrinogen into fibrin fibres. The fibrin fibres are stabilised through cross linking by FXIII. Adopted with permission from “Laboratory Evaluation of Hemostasis Disorders” (Leonardi, 2019a).

The extent of clot formation is regulated by anticoagulants (Table 1.2) such as antithrombin, tissue factor pathway inhibitor (TFPI), protein C (PC) and protein S (PS).

**Table 1.2.** Natural anticoagulants (Dorgalaleh, Danshi and Rashidpanah, 2018).

Name	Function
Antithrombin (AT)	Inhibits Thrombin, FXa, FIXa, and FVIIa
Tissue factor pathway inhibitor (TFPI)	Inhibits TF/FVIIa complex, FVa, and FXa
Protein C (PC)	Degrades FVa and FVIIIa
Protein S (PS)	Protein C cofactor
Thrombomodulin (TM)	Binds to thrombin and enhance PC activation
Endothelial protein C receptor (EPCR)	Promotes activated protein C (APC) generation
Heparin	Enhances the effect of AT
Heparin sulphate	Enhances the effect of AT
Heparin cofactor II	Inhibits thrombin
Dermatan sulphate	Enhances inhibitory effect of heparin cofactor II



**Fig. 1.3.** The fibrinolytic system. Plasminogen is activated to plasmin by plasminogen activators: tissue plasminogen activator (tPA) and urokinase plasminogen activator (uPA). Plasmin then breaks down the fibrin clot into fibrin degradation products (FDPs). Fibrinolysis is controlled by plasminogen activator inhibitors (PAI 1 & PAI 2) which deactivate plasminogen activators;  $\alpha_2$ -antiplasmin ( $\alpha_2$ AP) and  $\alpha_2$ -macroglobulin ( $\alpha_2$ MG), which directly inhibits plasmin, and thrombin-activatable fibrinolysis inhibitor (TAFI, activated by Thrombin), which inhibits the conversion of fibrin clot into FDPs (Mehic et al., 2021).

After tissue repair, the fibrin clot breaks down into fibrin degradation products in a process called fibrinolysis. The fibrinolytic system (Fig. 1.3) consists of plasminogen (plasmin precursor), plasminogen activators, plasmin (which breaks down the fibrin clot), and fibrinolytic inhibitors:  $\alpha_2$ -antiplasmin ( $\alpha_2$ AP)  $\alpha_2$ -macroglobulin ( $\alpha_2$ -MG), plasminogen activator inhibitors I and II (PAI 1 and PAI 2), and thrombin-activatable fibrinolysis inhibitor (TAFI) (Mehic et al., 2021; Chapin and Hajjar, 2015).

Abnormalities in any of the components/processes involved in haemostasis can upset the haemostatic balance and potentially lead to excessive bleeding, excessive clotting, or a combination of the two i.e., disseminated intravascular coagulation (DIC).

## **1.2 Bleeding and coagulation disorders**

Bleeding and coagulation disorders are haemostatic problems characterised by a wide range of symptoms including: easy bruising, frequent and prolonged epistaxis, gastrointestinal bleeding, prolonged menstrual periods, recurrent bleeding from wounds, and extended bleeding after minor traumas such as small cuts, injections, and dental procedures. These cause mild to excessive blood loss depending on the severity of the condition which are due to either slow/inadequate clot formation or increased clot lysis. Severe sequelae such as haematoma, heavy postpartum haemorrhage, and intracerebral haemorrhage can be life threatening or even fatal (Hoffbrand and Steensma, 2019).

Bleeding and coagulation disorders are a result of a malfunction or deficiency of at least one of the components of the haemostatic system, e.g., vascular abnormalities, platelet abnormalities, or deficiency of coagulation factors. Vascular abnormalities include: haemorrhagic telangiectasia, Ehlers-Danlos syndrome, pseudoxanthoma and giant cavernous haemangioma (McKenzie and Williams, 2010). Platelet abnormalities result from either low platelet count (thrombocytopenia) or abnormal platelet function (e.g., Glanzmann's disease, Bernard-Soulier syndrome, and storage pool disease). Coagulation factor deficiencies are quantitative or functional abnormalities of the proteins involved in the coagulation cascades that result in clotting failure or abnormal clotting. Notable abnormalities are: deficiency of FVIII (Haemophilia A), FIX (Haemophilia B) and vWF (Von Willebrand disease [vWD]). Both Haemophilia A and B are recessive X-linked genetic disorders while vWD is a heterogeneous autosomal

dominant disorder. Deficiency of other coagulation factors such as FV, FII and FI also exist but are comparatively rare (Hoffbrand and Steensma, 2019).

Fibrinolytic and anticoagulant disorders also result in bleeding problems depending on the nature of the disorder. For instance, excessive activity of coagulation inhibitors e.g. antithrombin, TFPI, PC etc. lead to reduced clot formation while decreased activity of fibrinolysis inhibitors (PAI-1 & 2, TAFI, and  $\alpha_2$ AP) (Fig. 1.3) result in excessive clot lysis (Leonardi, 2019a). Development of antibodies to coagulation factors such as FVIII and vWF are also reported to cause bleeding abnormalities (Hoffbrand and Steensma, 2019).

Illnesses such as cancers, liver disease and kidney disease, bone marrow disorder, hypothyroidism and vitamin K deficiency are associated causes of haemostatic abnormalities since they influence the production or activity of components of the haemostatic system, especially platelets, coagulation factors and inhibitors. Heavy blood loss and massive transfusion can also significantly contribute to bleeding disorders due to loss and dilution of coagulation factors and reduced activity of stored platelets used in transfusion (Hoffbrand and Steensma, 2019).

### **1.3 Thrombotic disorders**

Thrombotic disorders are characterised by inappropriate or excessive clotting that forms solid masses (thrombi) in circulation, which potentially obstruct blood vessels and lead to ischaemia and eventually tissue damage. The tendency to form thrombi in circulation (thrombophilia) increases the risk of thrombotic events including: deep vein thrombosis (DVT), cerebrovascular thrombosis (CVT), pulmonary embolism (PE) and myocardial infarction (MI) as well as arterial thrombosis (Hoffbrand and Steensma, 2019). It is believed that over two million people in the USA die every year from thrombotic conditions (Shirlyn, 2010). Venous thrombosis e.g., DVT result from slow blood flow/stasis, vessel wall damage and blood hypercoagulability. Reduction or cessation in blood flow which is often due to immobility, paralysis, or ventricular dysfunction, allows accumulation of clotting factors and the formation of thrombi in veins. Vessel wall damage from trauma, surgery, venepuncture, and chemical irritation exposes TF and PAI-1, activates the coagulation system, and leads to spontaneous clot formation in some individuals. Hypercoagulable states are due either to increased activity/production of coagulation factors or deficiency in activity of coagulation inhibitors. Other conditions

associated with venous thrombosis include: pregnancy, malignancy, anti-phospholipid syndrome, inflammation, blood disorders, hyperhomocysteinaemia, and oestrogen therapy (Leonardi, 2019a).

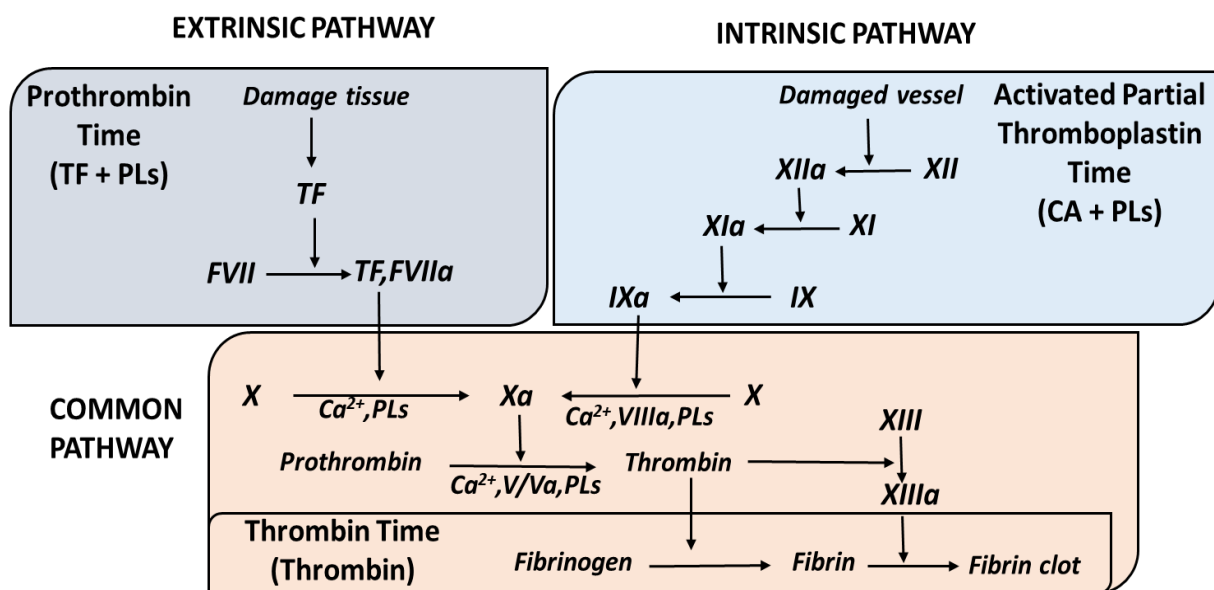
Arterial thromboses mainly result from the formation of atherosclerotic plaques in arteries which sometimes rupture, exposing procoagulants such as TF, collagen and vWF. This leads to platelet adhesion/activation and formation of clots that extend into vessel lumen, obstructing blood flow. Recurrent clotting and healing also cause regrowth of endothelial cells and thickening of the vessel wall, further inhibiting blood flow and causing ischaemia (Shirlyn, 2010). Risk factors include diabetes, hyperlipidaemia, gout, hyperhomocysteinaemia, Behçet's disease, ECG abnormalities, obesity, physical inactivity, and cigarette smoking. Indicators of arterial thrombosis include elevated fibrinogen, D-dimer, C-reactive protein (CRP), and PAI-1 as well as decreased tPA. However, these signs are not specific for arterial thrombosis, but thromboses in general.

DIC is the combined effect of thrombosis and haemorrhage and is the result of uncontrolled and widespread activation of the coagulation system that emanates from loss of localisation and inability of the anticoagulants to regulate thrombin generation (Wada *et al.*, 2014). It is typically a consequence of an underlying condition such as: sepsis, severe infections, trauma, malignancy, obstetric problems, vascular malfunctions, liver disease, and immunological reactions (Levi, 2018; Wada *et al.*, 2014). The underlying disease causes over-expression of TF, driving uncontrolled and disseminated generation of thrombin and results in excessive consumption of platelets, coagulation factors, and anticoagulants, as well as deposition and lysis of fibrin clots in blood vessels, consequently resulting in bleeding and thrombosis (Levi, 2018; Papageorgiou *et al.*, 2018).

#### **1.4 Conventional haemostasis tests**

Investigation of haemostatic disorders starts with physical examination of the patient for symptoms; checking patient history for bleeding patterns; and family history for inherited disorders. This guides subsequent laboratory investigations which may include full blood count, blood film, and clotting time tests (Leonardi, 2019; Shirlyn, 2010). Testing for bleeding disorders was first performed using the bleeding time test, measuring the time it takes for blood to stop flowing from pierced skin, about 3,000 years ago.

However, it was not until the 1900s when coagulation disorders were determined using a bedside bleeding time test, following the discovery that clotting is accelerated when blood comes into contact with surfaces such as glass and certain biological tissues like placenta (Harris *et al.*, 2013). Improved understanding of the coagulation system has led to the development of the current clotting time tests: thrombin time (TT), prothrombin time (PT), and activated partial thromboplastin time (aPTT) which are used to assess the different pathways of the coagulation cascade (Fig. 1.4). Abnormal clotting times indicate a quantitative or functional deficiency of the clotting factors or the presence of an inhibitor (Harris, Castro-López and Killard, 2013). Further understanding of the coagulation system has led to the emergence of many new assay techniques, including those based on platelet adhesion and aggregation. Principles and techniques used in these clot-based and platelet-based assays have further been used to develop automated coagulation tests to reduce human error and assay time (Harris *et al.*, 2016).



**Fig. 1.4.** Clotting time tests. Prothrombin time assesses the extrinsic and common pathways; Activated partial thromboplastin time, the intrinsic and common pathways; and Thrombin time, the rate of conversion of fibrinogen to fibrin clot respectively. Adopted with permission from “Laboratory Evaluation of Hemostasis Disorders” (Leonardi, 2019; Harris, Castro-López and Killard, 2013). TF = Tissue factor, PLs = Phospholipids, CA = Contact activator.

### 1.4.1 Thrombin time/quantitative fibrinogen (Clauss) assay

Also called thrombin clotting time (TCT), thrombin time (TT) is a measure of the rate of conversion of fibrinogen to fibrin clot in the presence of excess thrombin. An exogenous thrombin is added to citrated plasma and the time it takes for clotting to start is measured. Depending on the reagent used, the reference range for TT is around 10 to

16 seconds, with a prolonged TT indicating low fibrinogen concentration, low fibrinogen activity, or the presence of a thrombin inhibitor. TT is also used in qualitative monitoring of thrombin inhibition-based anticoagulants such as dabigatran and argatroban (Leonardi, 2019a).

The fibrinogen assay is the quantitative measurement of functional fibrinogen in plasma, and it is based on the thrombin time test. In the assay, the thrombin times of various fibrinogen standards are produced and plotted onto a graph of TT versus fibrinogen concentration. With the fibrinogen level inversely proportional to thrombin time, the fibrinogen level in the unknown sample is determined from the graph using the TT value of the unknown. The unknown and each of the fibrinogen standards is typically diluted to 1/10 with imidazole prior to taking the measurements (Shirlyn, 2010). The normal range of fibrinogen in human plasma is 2 to 4 mg/mL. A low fibrinogen concentration may indicate disorders such as dysfibrinogenaemia, hypofibrinogenaemia, afibrinogenaemia, DIC, or liver disease. Increased fibrinogen concentration could be due to inflammatory disorders, pregnancy, or use of certain contraceptives. Antigenic fibrinogen assay (which determines total fibrinogen concentration) and functional fibrinogen assay (which determines active fibrinogen concentration), when used together, distinguish dysfibrinogenaemia from hypofibrinogenaemia (Shirlyn 2010).

#### **1.4.2 Prothrombin time**

As indicated in Fig. 1.4, prothrombin time (PT) is used to evaluate the extrinsic and common coagulation pathways. It uses tissue thromboplastin (TF and PLs) which has been traditionally extracted from animal sources such as rabbit brain, to trigger the coagulation cascade. Currently, many commercial PT reagents contain a recombinant TF, synthetic PLs, and calcium. A typical PT experiment involves adding a thromboplastin reagent to a citrated platelet poor plasma (PPP) at 37°C and the time it takes for the first sign of fibrin clot to appear is measured in seconds. Calcium enables TF to bind with FVII to form TF-VIIa complex which activates the extrinsic pathway while PLs provide the surface for binding of coagulation factors involved in activating prothrombin to thrombin (Shirlyn, 2010). Calcium also enables the coagulation factors to bind to the PLs. The blood sample used to make the PPP was previously collected in a tube containing citrate which removes calcium from the sample and render it anticoagulated. The reference range for PT is 10 to 13 seconds, depending on the reagent used (Leonardi, 2019; Shirlyn, 2010), with prolonged PT results indicative of a

deficiency of an extrinsic or a common pathway factor or presence of an inhibitor. Prolonged PT can also be a result of DIC, vitamin K deficiency, liver disease or presence of an anticoagulant drug such as warfarin.

PT results tend to vary between labs depending on the reagent used. To minimise this inter-laboratory variability, PT results are often expressed in a standardised format called the International Normalised Ratio (INR) which is derived from PT results of the patient using the formula:

$$INR = \left( \frac{\textit{Patient PT}}{\textit{Mean normal PT}} \right)^{ISI}$$

Where ISI is the international sensitivity index of the PT reagent used. Optimum ISI value lies within 0.9 to 1.1 and smaller the ISI value the more sensitive the PT reagent. Normal INR values range from 0.8 to 1.2, also depending on reagent.

PT/INR is used in monitoring oral anticoagulant (e.g. warfarin) therapy, in which an INR values of 2 to 3 is the most common target (Leonardi, 2019a). Warfarin works by interfering with the bioavailability of vitamin K by inhibiting vitamin K epoxide reductase. This hinders coagulation and enables warfarin to be used in treating patients with thrombotic disorders. However, warfarin therapy requires frequent monitoring due to the variable half-life of the drug and its dependency on individual patients and diet (Leonardi, 2019a).

### **1.4.3 Activated partial thromboplastin time**

Activated partial thromboplastin time (aPTT) is a laboratory-based method for assessing the intrinsic and common coagulation pathway factors. It uses a mixture of negatively charged contact activator e.g., kaolin, ground glass, celite, or ellagic acid and PLs to activate the intrinsic pathway, leading to clotting. Since it uses PLs without TF, the reagent is termed partial thromboplastin. PLs function as in the PT assay while the activator triggers the cascade by activating FXII (Leonardi, 2019; Shirlyn, 2010). In an aPTT assay, the PL/activator mixture is incubated with citrated PPP at 37°C, a solution of calcium is added and the time it takes for the first sign of clotting to appear is measured in seconds. Normal aPTT results ranges from 35 to 45 seconds (Shirlyn , 2010).



The aPTT assay can detect deficiencies in all coagulation factors apart from FVII, and TF, but is particularly sensitive to deficiency of FVIII (haemophilia A), FIX (haemophilia B), FXI (Haemophilia C) and FXII (which is asymptomatic). Due to interpatient variability, aPTT is also used to monitor unfractionated heparin (UFH) therapy. UFH works by inhibiting thrombin as well as FIX, FX, and FXII, making aPTT more sensitive for monitoring heparin therapy than PT (Shirlyn, 2010). Generally, aPTT values for patients on UFH should be 1.5 to 2.5 times above the upper limit of the normal aPTT range.

Results from the screening tests (TT, PT, and aPTT), when used in combination as shown in Table 1.3, can provide significant information on the possible cause of the disorder, helping to guide decisions on subsequent specific tests to be carried out (Leonardi, 2019a).

**Table 1.3.** Interpretation of coagulation assays.

Test			PACF	Other possible causes
TT	PT	APTT		
Normal	Prolonged	Normal	FVII	
Normal	Normal	Prolonged	FVIII, FIX, FXI, FXII	Lupus anticoagulant, vWD
Normal	Prolonged	Prolonged	FII, FV, FX	Liver disease, VKD
Prolonged	Prolonged	Prolonged	Fibrinogen	Liver disease
Normal	Normal	Normal	FXIII	Plt dysfunction, vWD, excess fibrinolysis

*PACF* Potentially affected coagulation factor, *TT* = Thrombin time, *PT* = Prothrombin time, *aPTT* = Activated partial thromboplastin time, *vWD* = Von Willebrand disease, *VKD* = Vitamin K deficiency, *Plt* = Platelet, (Leonardi, 2019a).

#### 1.4.4 Mixing tests

Mixing studies follow abnormal screening test results to further narrow down the abnormality to a specific cause. Abnormal patient plasma and normal plasma are mixed in a 1:1 ratio and analysed in a screening test. Correction of an abnormal result indicates deficiency of a clotting factor, while an uncorrected result indicates presence of a coagulation inhibitor (Leonardi, 2019; McKenZie, 2010). Incubation is sometimes necessary because it takes time for the action of some inhibitors to have full effect. To specify the particular factor that is deficient, the patient plasma can then be mixed 1:1 with various plasmas, each deficient in one of the suspected factors. Table 1.4 shows the interpretation of mixing studies (Leonardi, 2019a).

Confirmation of a factor deficiency is also performed using factor specific tests such as enzyme immunoassay, which can determine the factor protein concentration (although not necessarily the functional protein); or a chromogenic technique, which measures the functional factor level. Together, results from both techniques can help specify the abnormality i.e., a dysfunctional factor or low level of a specific factor (McKenZie, 2010).

**Table 1.4.** Interpretation of mixing studies.

Sample	Before Incubation	After incubation	Interpretation
Normal : Patient	Normal PT, aPTT or TT	Normal PT, aPTT or TT	Factor deficiency
Normal : patient	Normal/prolonged PT, aPTT, or TT	Prolonged PT, APTT, or TT	Presence of an inhibitor
Patient : FVIII deficient	Prolonged aPTT, normal PT	Prolonged aPTT, normal PT	Haemophilia A
Patient : FIX deficient	Prolonged aPTT, normal PT	Prolonged aPTT, normal PT	Haemophilia B
Patient: FVII deficient	Prolonged PT, normal aPTT	Prolonged PT, normal aPTT	Factor FVII deficiency
Patient plasma with excess PLs	Normal aPTT , PT	Normal aPTT , PT	Presence of lupus anticoagulant

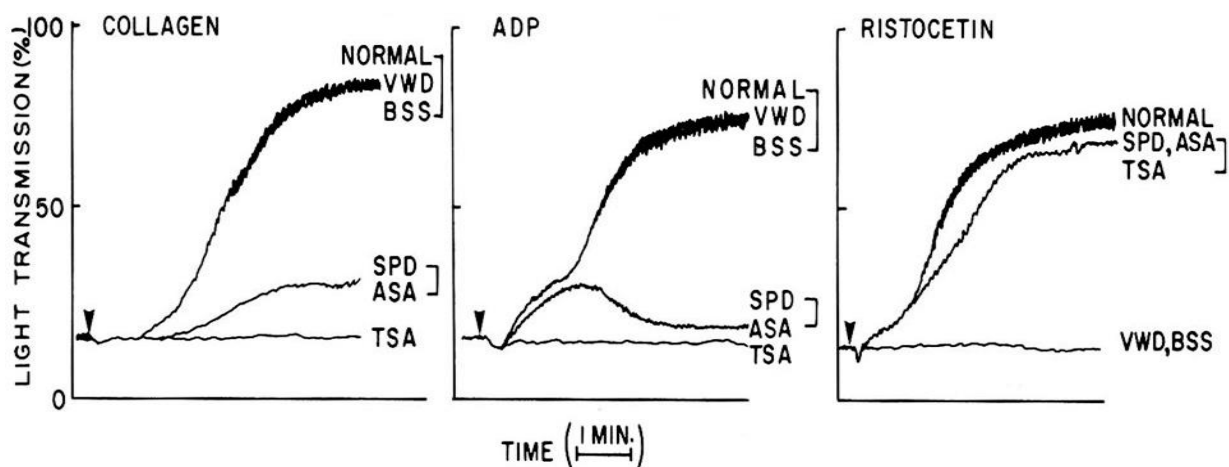
*PT = Prothrombin time, aPTT = Activated partial thromboplastin time, TT = Thrombin time, PLs = Phospholipids (Leonardi, 2019).*

#### 1.4.5 Platelet function tests

Assessment of platelet function was first performed using the bleeding time test which relates to platelet function, platelet count, and vascular integrity with abnormality in any aspect potentially leading to prolonged bleeding time. It is performed by applying pressure on the patient's arm and measuring the time it takes for blood to stop flowing from shallow cuts on the lower arm which normally ranges from 1 to 9 min. Due to the many variables such as the amount of pressure applied; location, size, and depth of cuts; and arm movements influencing the results, bleeding time is no longer conducted in most hospitals. It has been replaced to some extent by the Platelet Function Analyser (PFA-100), a standardised *in vitro* technique that eliminates most of the variables affecting the bleeding time test (Shirlyn, 2010). PFA measures platelet function by aspirating citrated whole blood through an aperture coated with a mixture of platelet agonists (collagen/epinephrine or collagen/ADP) and measuring the time it takes for the aperture to occlude (Leonardi, 2019; Shirlyn, 2010). PFA is sensitive to platelet count, platelet function, vWD, and haematocrit level.

More detailed platelet function testing is performed using platelet aggregometry, which employs either citrated whole blood or citrated platelet rich plasma (PRP). Whole blood

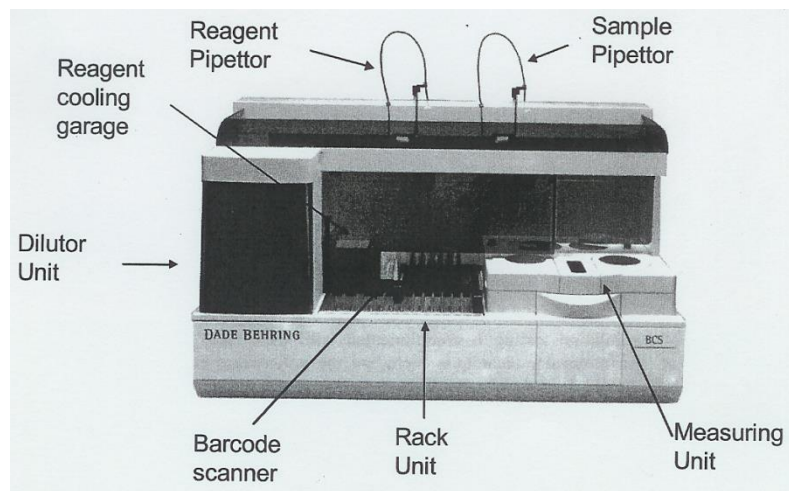
platelet aggregometry is performed by measuring electrical impedance changes induced by aggregating platelets on the surfaces of two wires placed within the sample. An agonist is initially added to the sample and the two wires previously coated with platelets before running the test. PRP platelet aggregometry on the other hand, is based on increased light transmission through the sample as platelets aggregate, leaving a clear liquid above. After adding an agonist, the optical density of the sample is measured over time (Leonardi, 2019a). As shown in Fig.1.5, different agonists produce different curves which are examined for abnormalities such as Bernard Soulier syndrome (BSS), Thrombasthenia, vWD, storage-pool disease (SPD) and aspirin ingestion. Ristocetin in particular is sensitive to vWD and BSS ( Shirlyn, 2010).



**Fig. 1.5.** Platelet aggregation patterns with various agonists (collagen, ADP, and ristocetin). Adopted from *Clinical Laboratory Hematology* (Shirlyn, 2010) ADP= Adenosine diphosphate, ASA = Aspirin ingestion and aspirin like disorders, BSS = Bernard Soulier syndrome, SPD = Storage-pool disease, TSA = Thrombasthenia, vWD = Von Willebrand disease.

Most hospital laboratories now use automated coagulation analysers and instruments that use a variety of detection techniques including electrochemical (impedance), optical (turbidimetry and nephelometry), and mechanical using rotating steel balls. The invention of automated analysers led to high throughput analysis, improved precision and accuracy, and reduced turn-around times. These analysers also offered the advantage of standardised testing among laboratories using the same instruments and reagents (Harris *et al.*, 2016). Automated and semi-automated coagulation analysers are ubiquitous in laboratories worldwide, from many different manufacturers, including devices that conduct multiple tests. Components of a typical state-of-the-art automated coagulation analyser include the robotic hardware which comprises the sample rack, reagent garage, barcode scanner, sample pipettor, reagent pipettor, dilution unit, and the measuring unit; and the software that enables communication between the operator

and the robotic hardware (Fig. 1.6). They are often capable of carrying out multiple coagulation tests based on different methods including clotting, chromogenic, and immunochemical methods (Qari, 2005). Clot based methods measure the time it takes for a sample to clot. Chromogenic methods assess the functional activity of target clotting factors, while immunochemical methods measure the concentration of coagulation factors within the sample. The main drawbacks of automated analysers are that they are relatively expensive, not very portable, and they often require technical expertise to operate. These may prevent their use in point of care settings and limit their use in low resource environments.



**Fig. 1.6.** Components of a typical automated coagulation analyser (Qari, 2005).

### 1.5 Point-of-care (POC) haemostasis testing devices

Traditional manual laboratory-based coagulation assays are relatively less precise, inconvenient to conduct, have long turn-around times and consume large volumes of samples and reagents while automated analysers are laboratory-based (i.e., not portable), expensive and require technical expertise to operate. This has prompted the development of techniques and devices that could eliminate these limitations and be conducted near the patient, thus allowing fast diagnosis and treatment, and reducing unnecessary delays. Point-of-care (POC) testing involves the use devices and assays to conduct medical diagnosis at the patient's bedside. An ideal POC device should be portable, handheld/benchttop and easily operatable by a non-laboratory personnel. They have the potential to reduce hospitalisations and the burden on healthcare resources and improve patient satisfaction especially, for example, in the administration and monitoring of anticoagulant therapy. POC devices are able to provide results within and

outside normal working hours, allowing more rapid decision making on treatment (Harris *et al.*, 2013; Srivastava and Kelleher, 2013).

### 1.5.1 Detection techniques used in POC haemostasis testing devices

Haemostatic POC devices have been typically based on the detection principles and reagents used in classical clotting time and platelet function tests and miniaturising them into portable, fast, and simple to operate procedures. The range of detection and measurement approaches employed include optical, electrochemical, viscoelastic, and ultrasound/acoustic techniques. Devices may measure single or multiple coagulation parameters (Table 1.5).

**Table 1.5.** Some current POC coagulation monitoring devices (Srivastava & Kelleher, 2013).

Name	Detection Technique	What is measured	Manufacturer
Yumizen G200	Optical	Fibrinogen, PT/INR, aPTT, D-Dimer	Horiba Medical
CoaguChek S	Optical	PT/INR,	Roche Diagnostics Cooperation
Hemochron Jr. Signature	Optical	PT/INR	Accriva Diagnostics Inc Instrumentation Laboratory, Bedford, US
GEM®PCL Plus	Optical	PT/INR, aPTT	Laboratory, Bedford, US
The VerifyNow® system	Optical	Platelet aggregation	Accumetrics Inc Roche
CoaguChek XS	Electrochemical	PT, Thrombin Activity	Diagnostics Cooperation Abbott
I-STAT	Electrochemical	ACT	Laboratories,
Xprezia Stride™ Coagulation system	Electrochemical	PT/INR	Siemens Medical Solutions USA, Inc.
Plateletworks®	Electrochemical	Platelet dysfunction	Helena Bioscience Roche
The Multiplate® device	Electrochemical	Platelet dysfunction	Diagnostics
CoagMax	Viscoelastic	PT/INR	Microvisk Ltd Sienco Inc
Sonoclot SCI	Viscoelastic	ACT, Clotting rate	(Arvada, CO, USA)
TEG® Platelet Mapping Assay	Viscoelastic	Platelet dysfunction	Haemoscope Corporation, Niles, Illinois, US)
Quantra™ Hemostasis Analyzer	Ultrasound	Clotting time, Clot stiffness	HemoSonics

Optical POC coagulation testing devices measure changes in light absorption (turbidimetry), light scattering (nephelometry) and/or light emission (chromogenic) by the sample to assess coagulation abnormalities. This is based on the fact that coagulation is accompanied by changes in optical properties of the sample and the rate and magnitude of the change furnish information about the clotting capacity of the sample (Louka and Kaliviotis, 2021).

Electrochemical POC coagulation monitoring devices measure the impedance or capacitance as a blood/plasma sample coagulates. This principle has been utilised in measuring PT/INR (CoaguChek XS, Roche Diagnostics Cooperation), activated clotting time (I-STAT, Abbott Laboratories), and detecting platelet dysfunction (Plateletworks®, Helena Bioscience). Detection relies on the principle that the impedance/capacitance increases as a sample of blood coagulates and the rate of increase as well as the maximum values of capacitance/impedance indicates the ability of the sample to coagulate (Louka and Kaliviotis, 2021).

Other properties of blood that change as it coagulates are mechanical characteristics such as viscosity and elasticity. Viscoelastic methods are often termed global assays because they measure real time changes in many characteristics, often of whole blood as the clot is formed and may provide more information than the other detection techniques including clot initiation, fibrinogen level, platelet function and fibrinolysis. POC devices that use this principle include Thromboelastography (TEG<sup>(r)</sup>, Haemonetics, Braintree, USA) and Rotational Thromboelastometry (ROTEM<sup>(r)</sup>, Werfen). They both measure the torque exerted on a pin immersed in a sample as the sample coagulates. In TEG, the container is rotated along with the sample while in ROTEM, the pin is rotated instead (National Institute for Health and Care Excellence, 2014). Sonoclot (Arvada, CO, USA) is also a viscoelastic device, but it measures the mechanical impedance of a vibrating probe placed in clotting sample.

Acoustic wave coagulation testing devices use piezoelectric transduction to measure coagulation parameters. A typical example using quartz crystal microbalance (QCM), consists of a piezoelectric material between two electrodes and by applying electric current to the electrodes, generates a mechanical wave whose resonant frequency and damping are functions of the mass or viscosity of a material at the surface. Changes in the resonant frequency/dissipation due to accumulation of fibrin or increases in viscosity

during coagulation are used to measure coagulation parameters such as prothrombin time, fibrinogen concentration, platelet aggregation ( Aria, Erten, and Yalcin, 2019) and clot retraction (Efremov *et al.*, 2021).

Ultrasound-based POC coagulation testing devices such as the Quantra™ Hemostasis Analyser, use ultrasound transducers to measure viscoelastic properties of a clotting sample from which clotting time and clot stiffness are derived. It is based on Sonic Estimation of Elasticity via Resonance (SEER) Sonorheometry in which high frequency ultrasound pulses are used to determine shear modulus of a clotting blood sample. In a typical experiment, an ultrasound pulse directed to the sample causes a shear wave, making the sample resonate as clotting progresses (Ferrante *et al.*, 2016). The motion of the sample is monitored as a function of time, producing dynamic changes in the sample shear modulus. The curve is then used to generate clot time and clot stiffness.

### **1.5.2 Limitations to the use of POC haemostasis testing devices in resource scarce areas**

As with any other analytical device, POC coagulation analysers also have drawbacks. The cost of analysis by most POC devices are comparable to those of laboratory-based analysers, meaning the cost of analysis is still high. In addition, the cost of acquisition and maintenance of many POC instruments and reagents are also high. It is also challenging comparing results across different methods and also many POC devices may only offer a limited menu of test per device. Operation of most POC devices also requires power and technical expertise. These issues of cost, power, and expertise particularly hinder the use of POC analysers in low-income settings. To overcome result variability, some devices are supplied with quality control (QC) reagents and samples, while others have automatic pipetting to reduce operator error (Hyatt and Brainard, 2016). For low resource settings, inexpensive, instrument-free, easy to operate, and yet robust POC coagulation analysers that can produce clinically reliable results are needed. A potential approach to addressing these challenges is the use of instrument-free lateral flow devices as coagulation testing devices. These types of analytical devices are inexpensive, easy to use and do not require power to operate.

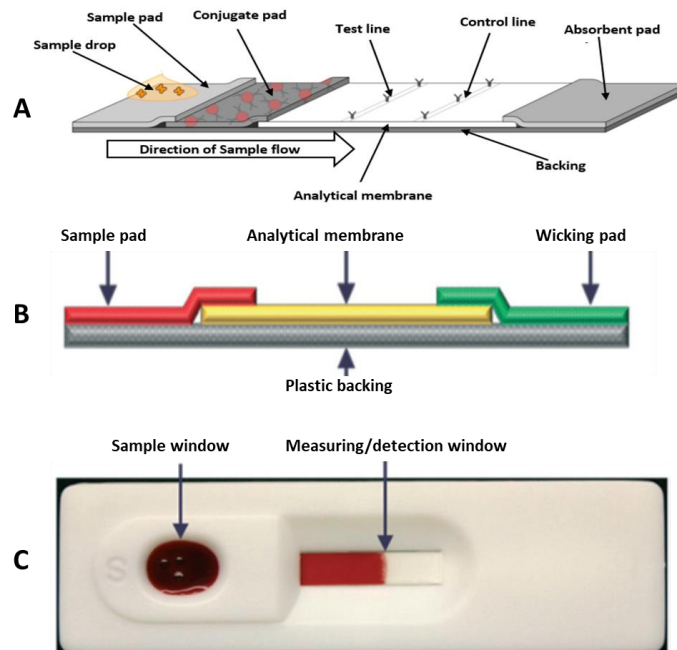
## **1.6 Lateral flow haemostasis devices**

Lateral flow assays (LFAs) are assay systems that rely on capillary action for the passive movement of a sample and its interaction with assay reagents in a controlled manner

through the control of volume, flow rates and reaction stoichiometries. They do not generally require power or an instrument to operate. LFA devices afford many potential advantages over other analytical methods such as reduced cost, ease of use, portability and short analysis time, among others (Bahadır and Sezgintürk, 2016). LFAs employing immunochromatographic approaches were first developed in the late 1960s with the first home-based LFA for detecting human chorionic gonadotropin (hCG) in urine conducted in 1976. Afterwards, they became increasingly used in the detection of various analytes including biomarkers for different diseases, microorganisms, toxins, pesticides, and heavy metals. With high potentials for miniaturization and on-site testing, LFAs have attracted increased attention as a rapid, qualitative and quantitative approach to blood coagulation monitoring and screening (Li *et al.*, 2014; Gerbers, 2013; Jiang *et al.*, 2019). They have been demonstrated in measuring fibrinogen in blood and blood plasma (Dudek *et al.*, 2010; Bialkower *et al.*, 2020), PT/INR based anticoagulation monitoring (Hegener *et al.*, 2017), D-dimer detection (Ruivo *et al.*, 2017), and aPTT (Dudek, *et al.*, 2011). The detection principle utilised in most lateral flow assays is either immunochromatography or change in sample flow dynamics, explained in section 1.6.3.

### 1.6.1 Design and fabrication of lateral flow haemostasis testing devices

There many different designs and shapes used in fabricating lateral flow devices. A typical LFA device is composed of a sample application pad made of cellulose or glass



**Fig. 1.7.** **A)** Generalized structure of lateral flow device (Helen *et al.*, 2017), **B)** Device with three flow components, **C)** Plastic casing showing the sample and detection windows (Han *et al.*, 2014).



fiber; a conjugate pad made of polyesters, cellulose, or glass fiber; an analytical membrane made of nitrocellulose or chromatography paper; and an adsorbent pad which acts as a sink for sample fluid for supporting forward flow of sample (Fig. 1.7). The conjugate pad bears the labelled analyte recognition molecules while the analytical membrane bears immobilized analyte capturing molecules and secondary capturing molecules arranged in test and control lines respectively (Sajid *et al.*, 2015; Bahadır and Sezgintürk, 2016).

Other designs may be simpler, composing of fewer flow components e.g., the sample pad, analytical membrane, and wicking pad (Han *et al.*, 2014). Others still may have just two flow parts, the sample zone and analytical zone, both on the same substrate i.e., excluding the conjugate and absorbent/wicking pads. The flow components may be housed in a plastic casing, which has openings for dispensing the sample and reading the results.

In the fabrication of these devices, techniques such as photolithography,, wax printing, or ink stamping is used in designing strips while drop casting, inkjet printing, and spray coating are use in immobilising the assay reagents on the substrate (Akyazi *et al.*, 2018). Inkjet printing and spray coating may be more precisely controlled and can be scaled up for mass production, however drop-casting is much cheaper. The plastic housings are mainly fabricated using 3D-printing.

### **1.6.2 Materials used in fabrication of lateral flow haemostasis testing devices**

Lateral flow devices for coagulation monitoring have employed a range of substrate materials to transport the sample, including nitrocellulose, cellulose, and synthetic polymers. The properties of these materials such as porosity/density, thickness, hydrophobicity etc, directly influence the sensitivity and precision of these devices. Devices using polymer substrates have been applied to the quantification of fibrinogen in plasma and whole blood (Dudek, *et al.*, 2010), detecting onset of coagulation (Dudek, *et al.*, 2011a) and in measuring aPTT (Dudek, *et al.*, 2011b). Polymeric substrates have the advantages of high material uniformity and allowing reproducible, mass fabrication, and so potentially improving assay precision. In such assays, the sample moves across the polymer surface by capillary action. However, due to their hydrophobic nature, polymer substrates require modification to induce lateral flow. This has been achieved using embossed micropillar arrays and the addition of surface modifications such as plasma treatment or addition of surfactants (Dudek *et al.*, 2010). In addition to these

disadvantages, polymers are also persistent environmental pollutants and so are not ideal for use as single use, disposable coagulation testing devices (Chen *et al.*, 2021).

Paper-based materials i.e., nitrocellulose and cellulose-based papers are more suitable and more widely used as substrates in lateral flow coagulation testing devices. Among the two, nitrocellulose is the most widely used. It has been used in; determining clotting capacity of blood samples (Han *et al.*, 2014), animal blood coagulation monitoring (Li *et al.*, 2018) and in warfarin-based anticoagulant monitoring (Hegener *et al.*, 2017). Nitrocellulose is attractive for its biocompatibility and its ability to strongly bind with assay reagents. However, nitrocellulose is relatively hydrophobic compared to cellulose papers due to the cellulose acetate blended into its structure. This often makes it necessary to treat it with surfactants to make it more wettable (Yetisen *et al.*, 2013). Also, nitrocellulose papers are more expensive than cellulose papers. The less expensive and more hydrophilic material used as a substrate in coagulation testing devices is cellulose-based filter papers. There are several types that differ in thickness, pore size and water flow rate. Whatman no. 1 filter paper with a thickness of 0.18 mm, water flow rate of 130 mm/30 min, pore size of 11  $\mu\text{m}$  and a smooth surface, is probably the most widely used. It has been used in plasma separation and fibrinogen quantification (Guan *et al.*, 2020). Employing a vertical flow configuration, the use of filter paper (Whatman 41) and tissue paper (comprising eucalyptus fibres) in measuring fibrinogen in plasma was demonstrated (Bialkower *et al.*, 2019). A sample is added to a paper strip modified with thrombin and after it clotted and dried, a blue dye is then added to the strip. The wicking length of the dye is inversely proportional the sample fibrinogen concentration. High fibrinogen level makes the strip more hydrophobic than samples with less fibrinogen. According to the team, sensitivity was found to be a function of paper density i.e., the less dense tissue paper gave better sensitivity than the denser filter paper. In lateral flow platform, eucalyptus-based tissue paper have also been demonstrated in measuring fibrinogen in whole blood by the same research group (Bialkower, *et al.*, 2020).

An ideal substrate for coagulation testing devices intended for low resource environments should therefore have the following properties:

- i. Relatively low cost and widely available
- ii. Be biodegradable and easy to dispose of
- iii. Have uniform thickness, porosity, and density

- iv. Compatible with assay reagents and plasma/blood samples

### **1.6.3 Principles of detection used in lateral flow haemostasis testing devices**

Different principles and techniques have been employed for detecting and measuring coagulation in lateral flow-based testing devices. These include colorimetric, fluorescence, electrochemical, and travel distance. The detection and readout method used affects portability, cost, ease of operation, turnaround time, and reliability of the device (Akyazi *et al.*, 2018). An ideal detection technique is one that does not add cost and complexity to the device and its operation; is sensitive, precise, robust, and has a short turnaround time. Wide linearity and low detection and quantification limits are also very important. However, few, if any techniques currently available meets all of these requirements.

Colorimetric-based lateral devices for coagulation testing are those that use colour change as a detection signal and colour intensity as a quantification signal. They essentially take the format of a conventional immunochromatographic lateral flow device that uses test and control lines on the analytical membrane. Colour formation at the test line indicates presence of the analyte while intensity of colour is a function of analyte concentration in the sample. Colour formation at the control line indicates validity of the test result. Development of colour can be due to the accumulation of gold or other colour-based particles which can be qualitatively read visually or quantitatively by reflectance photometry (Rifai, 2018). This principle has been successfully demonstrated for measuring D-dimer in simulated plasma samples (Ruivo *et al.*, 2017). This approach employed a sandwich type colorimetric immunoassay in which anti D-dimer gold nanoparticle conjugate D-dimers from the sample, the complex flows with the sample and is captured at the test line by immobilised anti D-dimer antibody. An image of the test line is processed and correlated with D-dimer concentration. This device had a detection limit of 15 ng/mL and a linearity up to 100 ng/mL. Use of colorimetric lateral flow devices have also been demonstrated in measuring dabigatran etexilate in blood which is used in anticoagulant therapy (Alnajrani *et al.*, 2022). Here, they used gold nanoparticles as label, an aptamer as recognition unit and streptavidin as capturing unit (at the test line). Colorimetric-based lateral flow devices are attractive because they can be easily interpreted by un-skilled persons using the naked eye. However, quantitation/semi quantitation requires image analysis which could take time and more

resources. Fabrication and operation of Immuno-colorimetric types also require use of antibodies/aptamer which are expensive and difficult to handle.

Fluorescence-based detection methods have also been applied to POC lateral flow assays for coagulation. Dudek *et al.* (2011a and 2011b) demonstrated that fluorescently labelled fibrinogen present in a plasma sample was cleaved and progressively incorporated into a fibrin clot during coagulation following activation with partial thromboplastin. This resulted in the redistribution of the fluorescence, the intensity of which could be measured using a fluorescence microscope with a charge coupled device. Harris *et al.* (2013) deposited a fluorogenic FXa substrate into a polymer microchannel-based anti-FXa assay device for measuring novel anti-coagulants. Excess FXa not inactivated by anti-coagulant cleaved the fluorogen. However, while fluorescence detection techniques have the potential to be very sensitive and reliable, this approach adds significant cost, complexity, and bulkiness to miniaturised devices which limits its use in POC devices.

Electrochemical techniques for coagulation testing have been based on the concept that blood coagulation is accompanied by changes in ionic mobility and movement of cells, which alters parameters such as conductivity and resistance. These electrochemical properties appear to correlate well with clotting time values. For instance, impedance technique in PT test has been demonstrated using a paper substrate and two electrodes imprinted by deposition of pencil graphite (Saha and Bhattacharya, 2020). The points of maximum change in resistance mark the onset of clotting from which coagulation time is derived. Furthermore, an Impedance-based technique was utilised for measuring aPTT and heparin in whole blood using a microfluidic device (Ramaswamy *et al.*, 2013). The HemoSense InRatio device also measured electrochemical impedance changes that took place during coagulation; however, it is now discontinued due to issues with accuracy. Other electrochemical detection techniques measure current rather than resistance. Most voltametric/amperometric measurements use either a natural or synthetic clotting factor substrate tagged with an electrochemically active compound such as ferrocene. The action of a clotting factor on the substrate either releases the electrochemical moiety or causes coagulation which leads to accumulation of the compound on the electrode surface. This method has been used in the detection of thrombin (Ko *et al.*, 2015) and FXa inhibitors (Doerge *et al.*, 2009). Electrochemical techniques are sensitive and satisfactorily reliable but still require an instrument-based

reader and in some cases, a signal amplifier which adds cost, complexity and power requirements which are in contradiction to requirements for devices suitable for use in low resource environments.

Distance based readout formats are instrument free and can be used for both qualitative and quantitative clotting measurements. They appear to be the most ideal detection technique for simple and low-cost use in resource limited areas. It has been successfully used in measuring fibrinogen in plasma (Dudek *et al.*, 2010), calcium in whole blood, prothrombin time test in plasma (Guler *et al.*, 2018) and warfarin-based anti-coagulant monitoring (Hegener *et al.*, 2017). Its main drawback especially for those that use paper substrates, is the inherent variability in sample flow rates which leads to low precision. This can be minimised by using flow control techniques such as changing the geometry of the fluidic channel which would not necessarily add much complexity and cost to the device as in the other detection methods.

#### **1.6.4 Challenges and drawbacks of lateral flow haemostasis testing devices**

Devices that use paper substrates have issues with precision due the variations in the production of these materials (Killard, 2010) which leads to variability in density and porosity of the material which directly affect sample flow rates and consequently, cause variation in travel distances. Flow control techniques such as altering channel dimensions, introducing fluidic valves and absorbent pads can be used (Jeong *et al.*, 2016).

For those that use open lateral flow and distance-based readouts, fluctuations in conditions of the operational environment such as humidity and temperature may influence the assay results especially for devices that require longer periods to operate. Low humidity for instance, encourages high evaporation rates which tend to shorten the travel distance, while high humidity has the opposite effect. Temperature influences both enzymatic reaction and evaporation rates which consequently affect distance travelled. To overcome the issue with humidity, a stimulated environment with a constant known humidity could be used for conducting tests. However, this would increase the cost of the assay. As for temperature, different reading scales for different temperatures could be used.

Durability/stability of reagents immobilised on test strips also present problems for simple lateral flow devices designed for coagulation testing. Most of them last for only two to three weeks even when stored in a freezer (Killard, 2010), and for a few, three months (Hegener *et al.*, 2017). Some use either a two to three step analysis protocol, requiring mixing the reagent and sample and then applying the mixture on the strip (Bialkower, *et al.*, 2020) or preparing the test strip and using it immediately (Bialkower *et al.*, 2019) which is not ideal for mass production and low-cost usage. These environmental and stability issues are challenging to address in low resource areas which often have extreme conditions such as high temperatures and also lack reliable power supply to preserve the assay strips. Effective and efficient stabilisers could be employed to prolong their working lives.

Ensuring low-cost production and usage of these devices also demand limited or no power usage and instrument free operation. Some devices require power to actively move the sample by pumping, while others need instrument-based readers which need power to operate (Chen *et al.*, 2020; Guler *et al.*, 2018). The use of power and expensive instrument readers would limit accessibility and affordability of these devices to the intended end-users. This makes passive movement of samples by capillary action and visual detection very attractive.

## **1.7 Aims and objectives**

The main aim of this programme of research was to develop several haemostasis assays with the potential for deployment in low resource environments. Such devices would have the potential to detect coagulation and platelet function abnormalities while being very low cost, simple to use, field deployable as well as environmentally sustainable.

In this regard, an extremely simple approach was taken to employ a low-cost cellulosic paper as the substrate of a lateral flow assay device, upon which the extent of clotting or aggregation could be determined visually by changes in the flow properties of the sample in response to activation. The development of three assays was investigated. These were a fibrinogen assay, a PT assay, and a platelet function assay. This involved several objectives:

- Develop and transfer coagulation (in the case of clotting time tests) and aggregation (in the case of platelet) assay principles to lateral flow assay formats.
- Understand the fluid dynamic properties of coagulating/aggregating and non-coagulating/aggregating samples and assay reagents on paper substrates.
- Optimise the design configurations of the lateral flow strip formats in terms of their dimensions and assay zonal structures.
- Optimise the assay reagent configurations with respect to reagent composition, concentrations, volumes, and deposition locations.
- Undertake analytical characterisation of assay performance using lateral flow motion capture techniques.
- Regarding platelet aggregation studies, undertake additional physical characterisation to enhance the understanding of assay behaviour at a microscopic level.
- Demonstrate the performance of the optimised assay configurations in artificial or clinical samples with appropriate statistical analysis.

## **2. MATERIALS AND METHODS**



## 2.1 Materials

Chromozym TH, lyophilised fibrinogen from human plasma (F3879), acetylsalicylic acid (A5376), glutaraldehyde (G6403), May-Grunwald solution (63590), Giemsa solution (48900), and Whatman No. 1 chromatography paper (460 x 570 mm, 1001-917) were sourced from Sigma-Aldrich, UK. Eosin Y (1% aqueous, HS250) was from TCS Biosciences Ltd UK. Calcium chloride fused granules (10043-52-4), methanol ( $\geq 99.9\%$ , CAS: 67-56-1, Code: M/4000/PB08), Whatman SG81 grade chromatography paper (11370744), microscope slides (T/F Ground, CAT. No 7107, 1.0-1.2 mm) and Whatman grade 3MM chromatography paper (10085370) were from Fisher Scientific, UK. The citrated human plasma standards: Routine Control N (normal) (5186, PT approx. 9 s), Routine Control A (abnormal) (5187, PT approx. 17 s), Routine Control SA (severe abnormal) (5183, PT approx. 34 s), immunodepleted factor VII-deficient plasma (5792), pooled normal human plasma (5185), Thromboplastin L (5265HL), calibration plasmas (5185), containing approx. 2.8 mg/mL fibrinogen (5185) and lyophilised bovine thrombin (50 NIH unit/ mL) from Clauss fibrinogen 50 kit (5556) were from Helena Biosciences, UK. Lyophilised platelets (5371), lyophilised adenosine diphosphate (5366), lyophilised epinephrine (5367), 100  $\mu\text{g/mL}$  collagen (5368), lyophilised arachidonic acid (5364) and Tris-buffered saline (TBS, 5365) were also purchased from Helena Biosciences, UK. Yumizen G FIB 2 (130036383), Yumizen G imidazol (130036385), Yumizen G PT Reco 10 (1300036376) and control plasmas: Yumizen G CTRL I & II (1300036412) were from Horiba, UK. Hemosil low-fibrinogen content plasma with approx. 0.75 mg/mL fibrinogen (0020004200) and Hemosil RecombiPlasTin 2G (0020003050) were from Instrumentation Laboratory, UK. Defibrinated plasma with approx. 1.5 mg/mL fibrinogen was purchased from BioIVI, UK. Thromborel® S and Dade® Innovin® (B4212-40) were from Sysmex. Silica gel desiccant sachets (10 g) were from CelloExpress, 0.2  $\mu\text{m}$  filter (Ref 83.1826.001, Filtropur S 0.2) was from Sartedt AG & Co. KG, Germany, while aluminium foil Mylar bags (X000Y9UA0L, 12 x 8 cm) were purchased from Fresherpack, UK. Sixty fresh citrated human plasmas used in the validation of the paper-based prothrombin assay (Chapter 4) were supplied by North Bristol NHS Trust (IRAS ID: 263472).

## 2.2 Methods

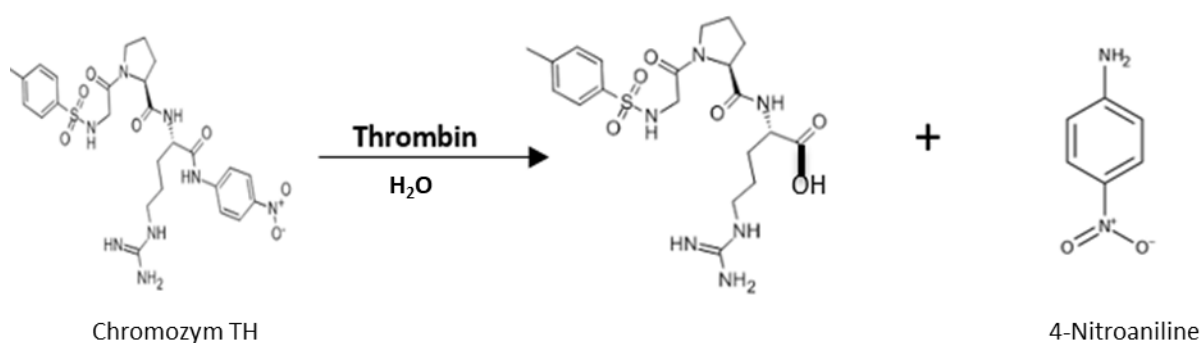
### 2.2.1 Standardisation of thrombin activity

In the fibrinogen assay development (Chapter 3), the activity of thrombin immobilised on the assay strips was monitored and standardised using a chromogenic method where Chromozym TH was used as a substrate for thrombin (Herrmann, 1979). The method was based on the principle that when thrombin cleaves the chromozyme, a chromophore (4-nitroaniline) that absorbs light at 405 nm is released (Fig 2.1). The gradient or rate of change of absorbance ( $\Delta ABS/min$ ) was used to calculate activity of thrombin using the formular:

$$A = \frac{V}{v \times \epsilon \times d} \times \Delta ABS$$

Where  $V$  = assay volume (3.2 mL),  $v$  = sample volume (0.1mL),  $\epsilon_{405} = 10.4(\text{mm}^{-1}\text{cm}^{-1})$ ,  $d$  = path length (1cm) and  $\Delta ABS$  = change in absorbance ( $\text{min}^{-1}$ )

In a typical standardization experiment, 10  $\mu\text{L}$  of thrombin reconstituted with deionised water was diluted to 1000  $\mu\text{L}$  using Tris buffer (50 mM, pH 8.3). 0.1 mL of this was added to a 1 cm plastic cuvette containing the buffer (2.8 mL) and the Chromozym TH (0.3 mL, 1.9 mM) and tested with a UV spectrophotometer. The absorbance as a function of time was recorded in a 25-minute period at 25°C.



**Fig. 2.1.** Generation of a chromophore (4-nitroaniline) from Chromozym TH by action of thrombin.

### **2.2.2 Preparation of fibrinogen standards and samples**

The fibrinogen standards and samples used in the development and validation of the fibrinogen assay (Chapter 3) were prepared by reconstituting vials of calibration plasma, plasma calibrator from Clauss Fibrinogen 50 kit, low fibrinogen control plasma, human plasma K<sub>2</sub>EDTA, as well as supplementing the human plasma K<sub>2</sub>EDTA with lyophilised fibrinogen. Assay development and calibration was conducted using fibrinogen standards within the range of 0.8 to 7.4 mg/mL.

### **2.2.3 Measurement of fibrinogen concentration**

Fibrinogen concentrations of plasma standards and samples were determined using the Yumizen G200 coagulation analyser (Horiba) according to manufacturer's protocol. Samples with 1.0 to 4.9 mg/mL fibrinogen were diluted to 1/10 in imidazol, while those with fibrinogen content  $\geq 5$  mg/mL were diluted to 1/20, those  $\leq 1.0$  mg/mL fibrinogen were diluted to 1/5 and the results calculated using the appropriate dilution factor.

### **2.2.4 Preparation of standards and samples for prothrombin time measurement**

The artificial plasma samples and standards used in the development and laboratory validation of the paper-based prothrombin assay (Chapter 4) were prepared by reconstituting commercial plasma samples i.e., calibration plasma, Routine control N, Routine control A, Routine control SA and FVII-deficient plasma according to manufacturer's instructions. To ensure adequate dissolution, the artificially constructed samples were set aside at room ambient temperature for 15 min and homogenised thoroughly before use.

The plasma samples received from the North Bristol NHS Trust (NBT) and used in clinical validation of the lateral flow prothrombin assay device (IRAS ID: 263472) were prepared from patient blood samples collected into sodium citrate (0.109 M) evacuated tubes (BD Plymouth UK Ltd). The blood samples, as soon as received, were centrifuged at 2,000 x g for 15 minutes and the plasma samples collected and immediately frozen at  $\leq 20^{\circ}\text{C}$ . Prior to prothrombin time measurement, these samples were thawed at  $37^{\circ}\text{C}$  for 5 min and then mixed thoroughly.

### **2.2.5 Measurement of prothrombin time**

The PT values of the artificially constructed plasma samples and standards used in the paper-based lateral flow prothrombin assay development and validation were also measured using the Yumizen G200 with the Yumizen G PT method. Typically, 50  $\mu\text{L}$  of the sample was placed in a cuvette in the instrument, and incubated at 37°C for 2 min. 100  $\mu\text{L}$  PT reagent, prepared by reconstituting it with imidazol, and kept at 37°C was then added. The PT and their corresponding INR values were displayed digitally.

The PT values for patient plasma samples used in the clinical validation of the lateral prothrombin time assay device were determined using Sysmex CS-5100 System at NBT following the manufacturer's protocol, and the anonymised samples were received at UWE on ice.

### **2.2.6 Preparation of platelet suspensions**

The platelet samples used in the study of platelet behaviour on later flow assay strips (Chapter 5) were prepared from lyophilised human platelets. Typically, a vial of lyophilised platelets was reconstituted in 5 mL of a solution of 2.1 mg/mL fibrinogen in TBS, or calibration plasma. Samples with different platelet counts were prepared by either reconstituting or diluting vials of lyophilised platelets with different volumes of buffer or calibration plasma.

### **2.2.7 Determination of platelet count**

The platelet counts of platelet suspensions were determined using the Yumizen H500 analyser (Horiba, UK). The reconstituted platelet samples were first equilibrated to ambient temperature for 10 min, mixed well and then measured with the analyser according to the manufacturer's protocol.

### **2.2.8 Staining and microscopic analysis of platelets**

The viability of the lyophilised platelets was tested by treating them with agonists and checking for aggregation using staining and microscopy. The reconstituted platelet samples were treated with a solution of an agonist (ADP [200  $\mu\text{M}$ ], epinephrine [3 mM], or collagen [100  $\mu\text{g}/\text{mL}$ ]) or TBS buffer control in a 1:9 v/v agonist to sample ratio, and incubated at 37°C for 3 min. Smears of the platelet suspensions were prepared on glass microscope slides, fixed with methanol (100%) for five minutes, stained with eosin for ten minutes, and then washed with phosphate buffer (pH 6.8). After air drying, the slides

were viewed with a light microscope (Nikon ECLIPSE 50i Microscope, DS-U3 DS Camera Control Unit, Nikon Metrology Europe NV) and the images saved.

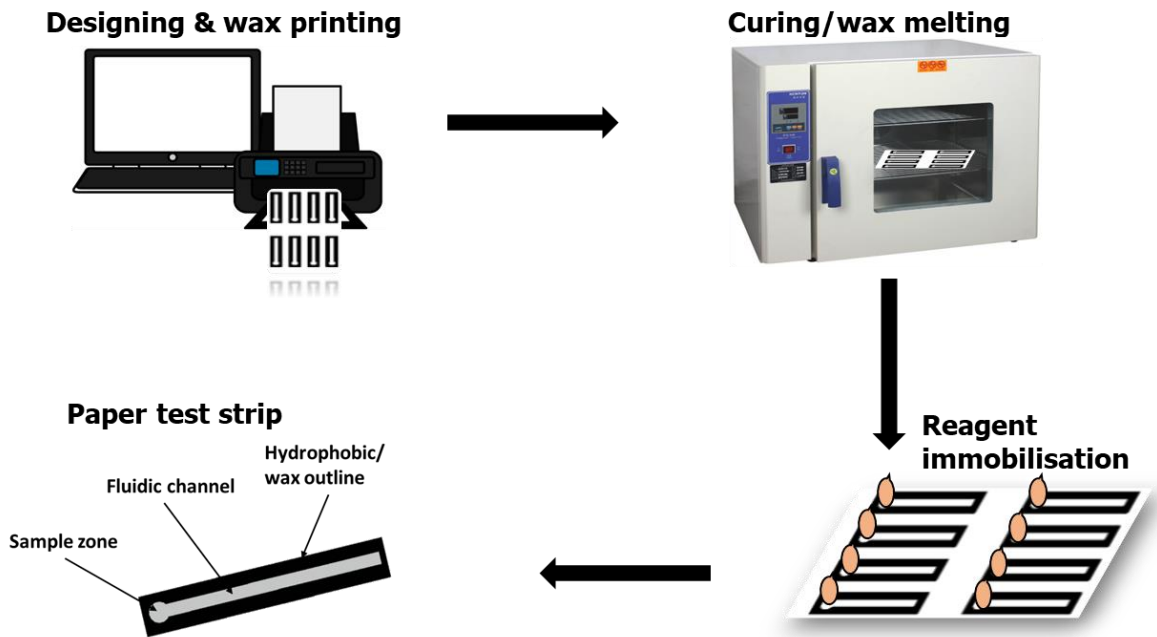
### **2.2.9 Scanning electron microscopy of lateral flow strips**

Two strips, one treated with DI water (50  $\mu$ L, control strip) and the other treated with ADP (500  $\mu$ M, 50  $\mu$ L, test strip) were tested with platelet samples ( $610 \times 10^9/L$ , 15  $\mu$ L), air dried, treated with methanol for 5 min, and allowed to dry again for one hour. Strips were then cut into sections, coated with gold using a sputter coater (Emscope SC500, Quorum Technologies Ltd) and then examined with a scanning electron microscope (Quanta 650 FEGSEM, FEI company). Sections of unmodified chromatography paper which were investigated as substrates in prothrombin assay development (Chapter 4) were also coated with gold and viewed with the electron microscope in a similar manner.

### **2.2.10 Fabrication of lateral flow test strips**

The test strips were designed using Microsoft PowerPoint. The strip designs generally consisted of a sample application zone, a microfluidic flow channel, and a waxy outer hydrophobic barrier. Strip designs varied in terms of length, width, and the presence of additional wax layers on the base of the strip. Specific designs employed are referred to in the relevant chapter.

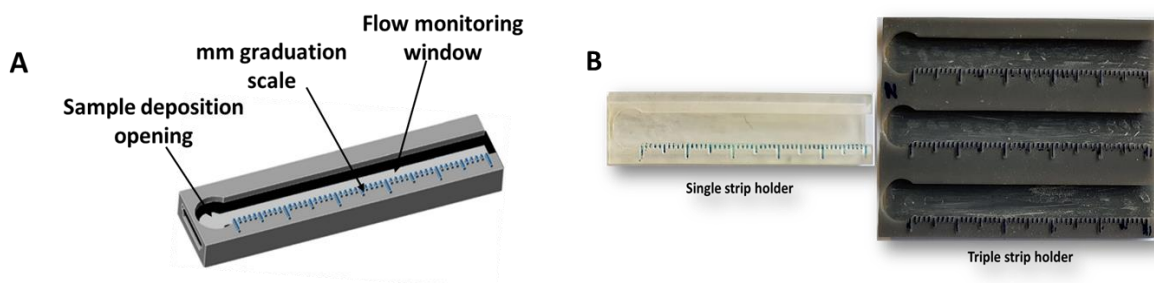
The designs were printed onto chromatography papers (Whatman No. 1, Whatman SG81 or Whatman 3MM) using a ColorQube 8570 wax printer (Xerox Corporation, Malaysia). To create a hydrophobic seal around the fluidic channels, the printed paper sheets were cured in an oven set at 100°C for 2 min. This allowed the wax to penetrate the paper to form a hydrophobic barrier (Martinez *et al.*, 2010). After curing, the sheets were cut into strips (Fig. 2.2).



**Fig. 2.2.** Workflow diagram showing the steps used for fabrication of paper-based lateral flow test strips. Strip designs were made using Microsoft PowerPoint, printed on chromatography papers which were cured in an oven set at 100°C for two minutes. After curing, the strips were modified with appropriate reagents, air dried and cut into shapes.

### 2.2.11 Fabrication of strip holders

Paper test strip holders, made of photopolymer resins, were designed using AutoCAD software and fabricated using 3D printing (Form 2 Desktop 3D printer, Formlabs). The strip holders were equipped with elevated rails to suspend the strips, an opening for sample deposition, a window for monitoring sample flow, and a millimetric graduation scale for reading sample travel distances. Both single (Fig. 2.3A) and triple strip holders (Fig. 2.3B) were fabricated and used.



**Fig. 2.3.** A) Diagram of a 3D printed single strip holder, showing the opening for sample deposition and fluid flow monitoring channel and the millimetre graduation scale B) images of single and triple strip holders.

### **2.2.12 General lateral flow assay development procedure**

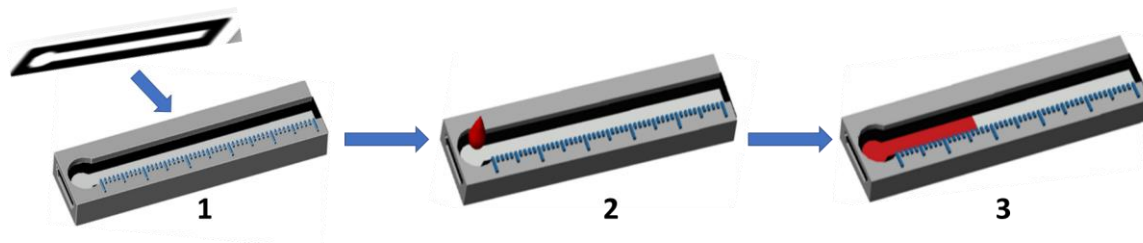
For the modification of strips with assay reagents, strips were typically placed on a metal rack and reagents were applied using a pipette. Strips were modified with a range of assay reagents and appropriate controls depending on the assay being developed, including thrombin for the fibrinogen assay (Chapter 3), thromboplastins and calcium chloride for the prothrombin assay (Chapter 4) and platelet agonists for the investigation of platelet aggregation (Chapter 5). Reagents were deposited in various locations on the strip, details of which are set out in the relevant sections. Following modification, strips were then allowed to air dry for up to 2 hrs.

Assay development was performed using a range of commercial plasma and platelet samples, along with appropriate controls. In the development of the fibrinogen assay (Chapter 3), Owren's buffer and serum were used as controls, while normal plasma, low fibrinogen plasmas and plasmas supplemented with fibrinogen were used as standards and samples. Routine control plasmas that differ in their PT values were used as standards with Owren's buffer and serum used as controls in the prothrombin assay development (Chapter 4). In the lateral flow platelet assay studies (Chapter 5), TBS, fibrinogen solution in TBS, and calibration plasma were used as control samples, while the standards and test samples were platelet suspensions prepared in each of these controls at different stages of the investigation. Following development, assays were further validated, either in artificially constructed commercial samples of unknown characteristics, or using clinical plasma samples (Chapter 4). In platelet assay studies (Chapter 5), performance testing was conducted using lyophilised platelets reconstituted in both buffer and plasma across a range of platelet counts, and in platelet samples treated with the platelet antagonist, aspirin. The specifics of these are set out in each chapter.

The measurement of the fluid dynamic processes of the various samples on the modified strips was performed by aligning the strips inside the strip holders and placing them on a dry heating block at 37°C. All assay materials were also equilibrated to 37°C for 5 min before use. Samples were applied to the strips at the sample zone and the flow of the sample along the strip recorded using video capture (Fig. 2.4). Videos were reviewed and the distances travelled by the fluid fronts were recorded to the nearest 0.5 mm at precise time points up to 300 s. Fluid fronts for the controls (i.e., water & buffer) were a bit difficult to read with naked eye but were clear from video frames.

The relationship between time and distance travelled by the fluid fronts were analysed. Experiments were typically performed in triplicates with determination of mean and standard deviation. The assays were optimised according to a number of parameters, such as the design and dimensions of the paper strips used, the type, volumes, concentrations, and deposition processes of reagents employed, as well as the types and volumes of samples used, and these are specifically detailed in the relevant chapters.

Where possible, assays were validated against a standard technique such as the Yumizen G200 coagulation analyser in the case of the fibrinogen and prothrombin assays, as well as against a hospital methodology in clinical samples, in the case of the prothrombin assay.



**Fig. 2.4.** Operational procedure for the paper-based lateral flow coagulation testing devices. 1) paper test strip was inserted into the strip holder, 2) sample applied to device sample zone, 3) distance travelled by sample recorded over five minutes.

### 2.2.13 Storage and stability studies of test strips

In strip stability and storage studies, prepared test strips were placed in folded protective papers, inserted into aluminium foil bags, vacuum sealed along with a sachet of silica gel desiccant, and stored at various temperatures (18 to 25°C [ambient], 2 to 6°C [fridge] and -15 to -18 °C [freezer]). The stored test strips were then tested weekly with normal samples to assess their functionality over time and determine the optimum temperature for storage. Freshly prepared test strips were also tested at different temperatures with normal samples to examine the effect of temperature on assay results.

### 2.2.14 Statistical and numerical analysis

Experiments were typically conducted in triplicates and mean values were expressed along with their standard deviations and relative standard deviations, where appropriate. Standard deviations were also used to graphically express error bars. For experimental



values determined using arithmetic operations such as addition and subtraction, errors were propagated using the formula:

$$\sigma_x = \sqrt{\sigma_a^2 + \sigma_b^2 + \sigma_c^2 + \sigma_d^2 + \dots} \quad (\text{Eq. 2.1})$$

Where  $\sigma_x$  is the propagated error,  $\sigma_a, \sigma_b, \sigma_c$  and  $\sigma_d$  are errors associated with individual values.

Assay performance was typically assessed using linear least squares regression analysis with the determination of regression coefficients and confidence intervals. Assay performance was also compared using Bland-Altman analysis (Giavarina, 2015).

Where appropriate, the confidence interval of the calibration curve was calculated using the formula:

$$CI = t * SE * \sqrt{\frac{\frac{1}{n} + (x - \bar{x})^2}{(n-1) * SV}} \quad (\text{Eq. 2.2})$$

Where:

CI = Confidence interval, t = t-value at 95% confidence level, SE = standard error, n = the number of calibration points, x = individual calibration points,  $\bar{x}$  = average of the calibration points, n – 1 = degree of freedom, and SV = sample variance.

Significance tests such as t-test and ANOVA were also conducted, where appropriate to indicate magnitude of the differences in response values between different treatments. Specifically, p-values at  $\alpha=0.05$  were used to indicate significance levels. For comparing slopes, standard errors of the slopes, values of the slopes, and sample size were used in ANOVA to generate the p-value. The standard errors of the slopes were calculated using the formula:

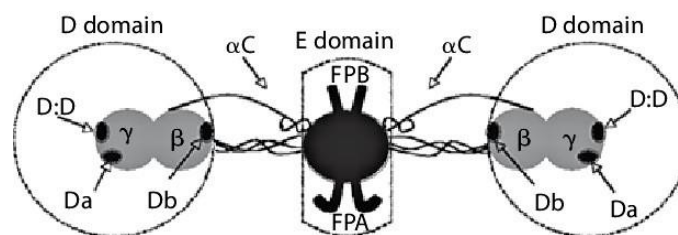
$$SE = \sqrt{\frac{1}{n-2} \times \frac{\sum(y_i - \hat{y}_i)^2}{\sum(x_i - \bar{x}_i)^2}} \quad (\text{Eq. 2.3})$$

Where SE = standard error, n = total sample size,  $y_i$  = actual response value,  $\hat{y}_i$  = predicted response value,  $x_i$  = actual predictor value,  $\bar{x}_i$  = mean predictor value.

### **3. DEVELOPMENT OF A PAPER-BASED LATERAL FLOW FIBRINOGEN ASSAY DEVICE**

### 3.1 Introduction

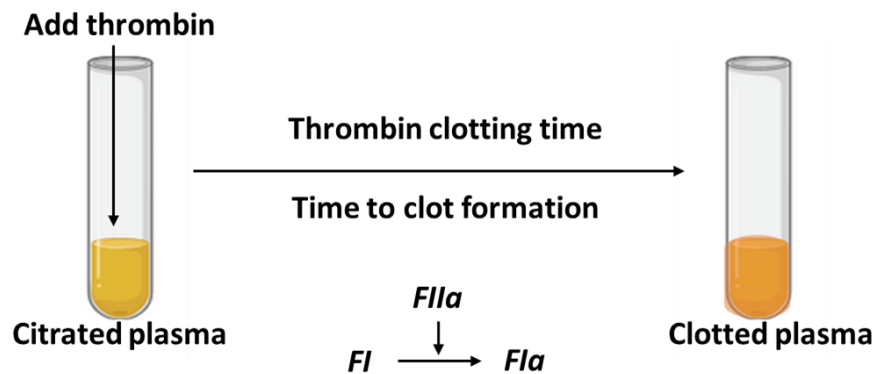
Fibrinogen is a 340 kDa glycoprotein synthesised in the liver by hepatocytes and secreted into circulation with a normal plasma concentration of 2 to 4 mg/mL. It consists of two chains each of three different polypeptides ( $2\alpha$ ,  $2\beta$ , and  $2\gamma$ ) linked together into a dimeric structure by disulphide bonds. The middle part, called the E-region contains the N- termini of all the six chains while the two ends contain the C-termini of  $\beta$  and  $\gamma$  chains (Undas and Ariëns, 2011) (Fig. 3.1). Fibrinogen plays a crucial role in the formation of the secondary haemostatic plug to permanently stop bleeding. It also plays an important role in the formation for the primary haemostatic plug in which it mediates platelet adhesion and aggregation at the site of injury. Fibrinogen abnormalities can lead to severe morbidity or even death. According to a study conducted by (Cortet *et al.*, 2012), the level of fibrinogen in blood at diagnosis correlates with haemorrhage and low level is associated with severity of post-partum haemorrhage (PPH). Afibrinogenaemia is linked with umbilical cord bleeding, muscle haematoma, oral cavity bleeding, and post-surgical bleeding. Hypofibrinogenaemia is often asymptomatic, but is linked to bleeding episodes in trauma, surgery, and concomitant coagulopathies. In women, hypofibrinogenaemia leads to complications during childbearing such as menorrhagia and recurrent placental abruption, while afibrinogenemia causes more severe forms of menorrhagia and peritoneal bleeding (Neerman-Arbez and Casini, 2018).



**Fig. 3.1.** Structure of fibrinogen showing D and E domains and three different polypeptide chains ( $2\alpha$ ,  $2\beta$ , and  $2\gamma$ ). The E domain contains the N- termini of all six polypeptide chains while each of the two D domains contains the C-termini of  $\beta$  and  $\gamma$  chains. Adopted from “Simulated point mutations in the A $\alpha$ -chain of human fibrinogen support a role of the  $\alpha$ C domain in the stabilization of fibrin gel” (Colafranceschi *et al.*, 2006).

Fibrinogen, being an essential molecule in haemostasis, is an important biomarker for evaluating haemostatic function. Measurement of fibrinogen in blood or plasma is, therefore, an important parameter for diagnosing bleeding and clotting disorders.

Thrombin clotting time (TCT) and Clauss fibrinogen assays are among the main recommended screening tests for measuring the level of functional fibrinogen in plasma. In the TCT (Fig. 3.2), exogenous thrombin is added to citrated plasma and the time it takes for initial appearance of a clot is measured. In the Clauss fibrinogen assay, the TCT of a range of fibrinogen standards is determined and the fibrinogen concentration of the unknown is determined from a calibration curve. TCT and Clauss assays are both laboratory-based and require at least thirty minutes turnround time.



**Fig. 3.2.** Schematic of the thrombin clotting time test showing conversion of fibrinogen (FI) to activated fibrinogen (FIIa) by thrombin (FIIa) and formation of fibrin clot.

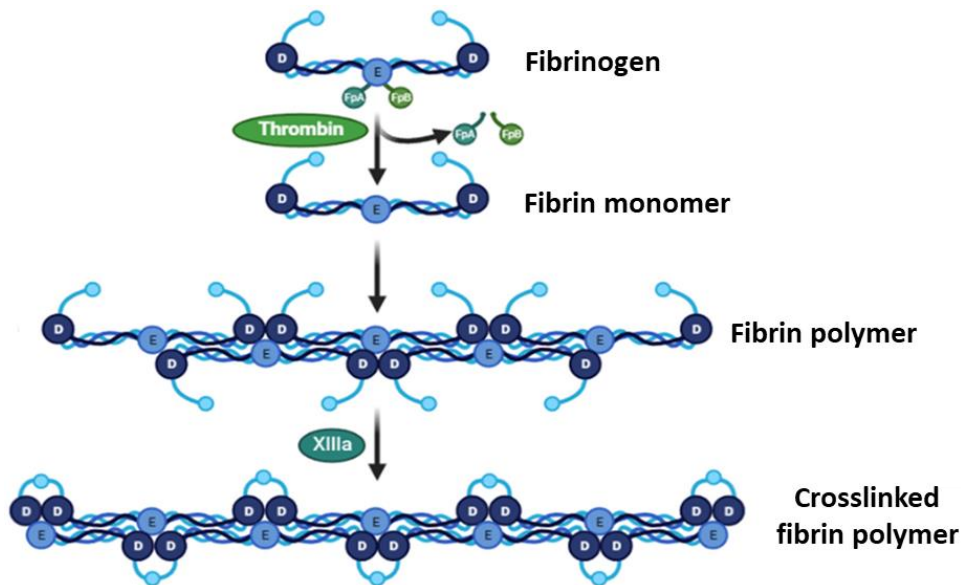
While PT and aPTT will be prolonged as a result of severe forms of fibrinogen deficiency, they are far less sensitive compared to TCT and Clauss (Verhovsek et al., 2008). The Clauss method has been integrated into many automated and semi-automated coagulation analysers that use photo-optical detection. PT-derived fibrinogen is also a common method used in many instruments. However, it is less accurate than the Clauss assay.

Clottable protein assays for fibrinogen determination are very accurate methods and are often used as reference methods for fibrinogen measurement. Here, thrombin is added to a plasma sample in the absence of calcium and the resulting clot is washed, dissolved in alkaline solution and its fibrinogen level determined using spectrophotometric measurement. Since the clot is almost pure fibrin, the protein concentration is approximately that of fibrinogen. Though very accurate, clottable protein methods are lab-based, time consuming, and technically difficult, they are therefore not suitable for routine coagulation screening much less for POC use (Ilan et al., 2003).

There are a number of immunological fibrinogen assays that utilise antigenic rather than functional fibrinogen measurements. These include ELISA, radial immunodiffusion, and electrophoretic techniques. Some of these methods such as ELISA are very accurate. However, they are again lab-based, require technical expertise, and take hours to complete (Ian *et al.*, 2003). Results from functional and antigenic measurements in combination can be used to distinguish hypofibrinogenaemia from dysfibrinogenaemia. However, individually, functional fibrinogen measurements are more clinically useful.

Thrombin is a potent coagulation factor that plays multiple roles in the blood clotting process including platelet activation and conversion of fibrinogen into fibrin. It is a proteolytic enzyme that is produced from its precursor, prothrombin by the action of a combination of enzymes and phospholipids called the prothrombinase complex. The inactive form, prothrombin is synthesised in the liver and secreted into circulation at a normal concentration of about 100 µg/mL. Thrombin itself exists in three forms,  $\alpha$ ,  $\beta$ , and  $\gamma$ , among which the  $\alpha$  is the form that is enzymatically active and physiologically functional, critical for haemostatic function.  $\alpha$ -thrombin, with a molecular weight of 37 kDa, consists of two polypeptide chains linked together by disulphide bonds (Aizawa *et al.*, 2008). In vivo, thrombin acts on fibrinogen by cleaving its fibrinopeptides A and B (FPA and FPB), releasing active fibrin monomers which polymerise and crosslink to form fibrin the clot (Fig. 3.3). As a result of its crucial and multiple roles in haemostatic function, thrombin is widely used in combination with collagen sponges and fibrinogen concentrates in many surgical procedures to reduce bleeding (Kumar and Chapman, 2007). Thrombin is also used as a reagent in many analytical methods designed for measuring functional fibrinogen in plasma including TCT and Clauss fibrinogen assay. While the catalytic pH range of thrombin is fairly wide (5 to 10), its optimal catalytic pH is 8.3 and it tends to precipitate at pH  $\leq$ 5 (Machovich, 1984)

Thrombin reagents for TCT and functional fibrinogen assays are typically derived from either bovine or human pooled plasma. They are prepared principally using two main approaches.



**Fig. 3.3.** Activation of fibrinogen and polymerization of fibrin monomers. The cleavage of the fibrinopeptides A and B (FPA and FPB) by thrombin produces activated fibrin monomers which polymerizes and form fibrin polymer fibres which are turned crosslinked by activated factor XIIIa (Rojas-Murillo et al., 2022).

In the first approach, prothrombin is extracted from plasma via cryoprecipitation, purified through several steps including ion-exchange chromatography, heparin affinity chromatography, and metal-affinity chromatography and then activated to thrombin by the addition of sodium citrate and incubation at an elevated temperature (Aizawa et al., 2008). In the second approach, plasma is triggered to clot by the addition of either thrombokinase or a thrombin reagent (Kumar and Chapman, 2007) and fibrin is removed from the resulting clot. The thrombin solution is then precipitated, purified, and dried. For coagulation tests, the thrombin produced is characterised, standardised, and lyophilised.

Another reagent sensitive to fibrinogen deficiency and dysfunction is the snake venom reptilase. This enzyme, which is known to cleave only FPA is less susceptible to the effect of heparin or FPB defects (Verhovsek et al., 2008). TCT and reptilase time in combination can distinguish quantitative fibrinogen deficiency from certain fibrinogen dysfunctions especially those related to FPB cleavage defect.

As mentioned above, many methods exist for determining fibrinogen in blood and plasma. However, most of these methods are lab-based, have long turnaround times, are relatively expensive, and/or are technically difficult to perform. These challenges

inspired the idea of developing low cost, fast and technically simple methods that can be performed by, or close to the patient's bedside and in communities that lack laboratories. Among the methods appropriate for this would be lateral and vertical flow fibrinogen assays that use low-cost materials such as paper as a substrate. One such approach employed a vertically suspended paper in a fluid reservoir and the concentration of fibrinogen was determined from the distance travelled up the strip by the sample (Bialkower *et al.*, 2019). This method was capable of measuring fibrinogen at the relevant clinical range, but the orientation of the device and the fluid reservoir made it impractical for easy portability and POC use. Another method used lateral flow in which the level of fibrinogen caused a decrease in paper permeability and therefore reduced sample travel distances (Bialkower *et al.*, 2020a). However, this method could only measure fibrinogen at low concentrations ( $\leq 1.6$  mg/mL). A similar method utilised the difference in hydrophobicity of paper exposed to samples to different fibrinogen concentrations which influenced the distance travelled by a dye along the paper strip (Bialkower *et al.*, 2020b). This method could also only measure fibrinogen at low concentrations ( $< 2$  mg/mL) and furthermore required multiple assay steps. Another method with a wide dynamic range (1.27 to 5.08 mg/mL) and high precision employed dielectrophoresis (Guan *et al.*, 2020). However, this method required complex electrophoretic instrumentation and would not be suitable for low resource and remote settings.

In this work, the aim was to develop a low-cost functional fibrinogen assay device using a paper-based lateral flow platform that would be robust, easy to operate and have wide clinically relevant dynamic range. Such a device might be more suitable for deployment in low resource areas. The device assay principle was based on the TCT with measurement converted to distance rather than time. In the TCT/Clauss assays, lower levels of, or defects in fibrinogen lead to prolonged clotting times. The conversion of fibrinogen into fibrin converts the liquid blood or plasma sample into a gel. If such a sample were moving via capillary action through, or across a substrate, the extent of formation of the gel would alter its fluid dynamic properties in a manner proportional to the concentration of fibrinogen, which has been demonstrated previously on polymeric substrates (Dudek *et al.*, 2010). This principle was applied in this work. However, it had to be demonstrated whether such an assay strategy could operate on a paper-based substrate.

## **3.2 Results and discussion**

### **3.2.1 Design of the paper-based lateral flow fibrinogen assay strip**

The initial investigations including studying the effect of thrombin clotting on sample flow rates and travel distance (Fig. 3.4) and investigation of the deposition of thrombin on paper strips (section 3.2.2) were conducted using strips with relatively large channels (5 x 80 mm) with no defined sample deposition locations. Samples could just be applied at either ends of the strips, and then monitored as they flowed toward the other end. Using this strip design, the appropriate reagent volume that would cover, but not over-saturate the paper test strips; and sample volume that would not overflow the fluidic channel (90 and 70  $\mu\text{L}$ , respectively) were first determined. Further developments of the assay were performed using strips with smaller channel dimensions (3 x 36 mm) and a circular sample deposition point (5 mm diameter) at one end. The smaller strips were used mainly to reduce reagent and sample consumption.

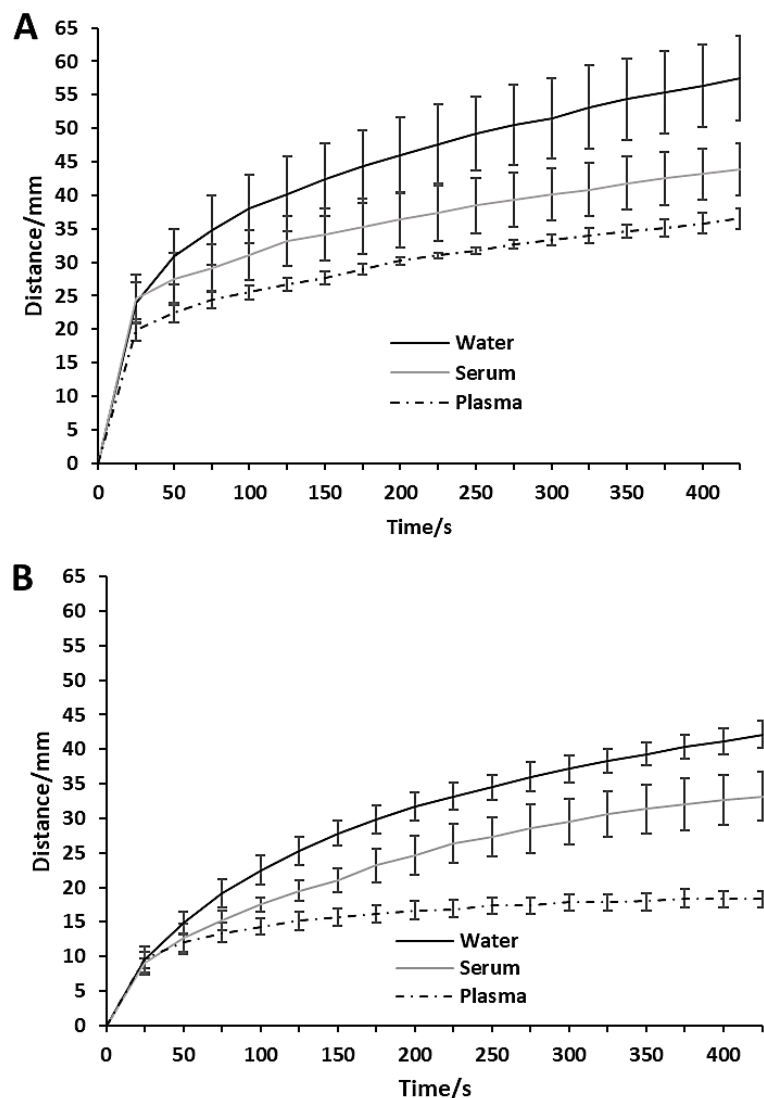
### **3.2.2 Assessing the effect of thrombin clotting on sample flow rate**

The flow rate and distance travelled by a sample in a lateral flow-based coagulation assay will be influenced not only by the coagulation rate, but also by the viscosity of the sample, the hydrophobicity and wettability of the substrate and the immobilised coagulation reagents on the test strips. To develop coagulation testing devices based on lateral flow principles and distance readout format, it is therefore essential to control the effect of all the other factors in order to establish and measure the effect of coagulation.

To isolate and quantify the effect of coagulation on sample flow rate and distance, it was necessary to perform appropriate sample and reagent controls to study viscosity, hydrophobicity, rehydration, and coagulation on the strip. This was performed using water, Owren's buffer, serum, and normal plasma as samples. For reagent controls, test strips were coated with either 50 NIH/mL thrombin or Owren's buffer by depositing the reagent in the middle of strip channels which then spread and cover the entire channel by capillary action. The flow rates of the various fluids on the control and test strips were compared and the effect of thrombin triggering clotting was calculated and quantified (n=3). As shown in Fig. 3.4A, on the strip modified with buffer, the flow rate of water was the highest, followed by that of serum, whilst that of plasma was the slowest. Since no clotting occurs in any of these, the differences in flow rate were predominantly due to differences in viscosity, with water being the least viscous



travelling fastest and plasma, the most viscous, travelling slowest. It could also be seen that sample flow rates were very fast within the first twenty seconds. This could be attributed to the sample deposition process which tended to initially force the sample to travel faster. On the thrombin-modified strip (Fig. 3.4B), the order of sample flow rate was the same, but all the samples travelled at slower rates than on the buffer-modified strip, suggesting that the presence of the thrombin reagent on the test strips generally reduced sample flow rate. This could be due to the fact that the thrombin reagent maybe more hydrophobic and requires rehydration, and may also reduce the porosity of the paper strip. However, the plasma sample in which clotting occurs, covered a much shorter distance than that of serum and water.



**Fig. 3.4.** Flow rates of 70  $\mu\text{L}$  water, serum or plasma samples on 5 x 80 mm paper strips modified with 90  $\mu\text{L}$  of (A) Owren's buffer, and (B) 50 NIH/mL thrombin. Reagents were deposited at the centre of the strip ( $n=3$ ).

The additional reduction in flow rate and distance (7.6 mm) covered by the plasma compared to that of serum was attributed to coagulation. Furthermore, while water, serum, and plasma continue to flow parallel on buffer modified strips, on the thrombin modified strips, only water and serum continued to flow parallel while the plasma did not, another indication of coagulation effect.

### **3.2.3 Investigation of the deposition of thrombin on paper strips**

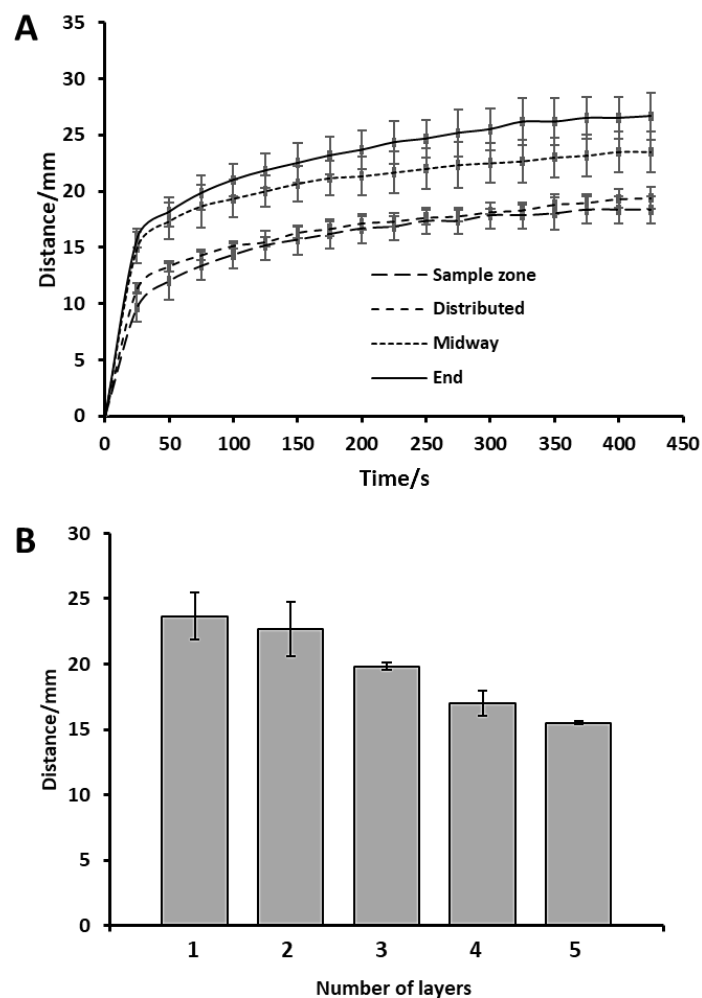
Different techniques such as spray coating, inkjet printing, drop casting and others have been used to deposit assay reagents on test strips (Akyazi *et al.*, 2018) and the technique used will affect the distribution of reagent on strips as well as the cost of the assay. The initial deposition technique explored here was drop casting, since it was simple to perform in the laboratory. When using drop casting, the quantity and distribution of reagent on the strip will depend on its volume and location of deposition, which will, in turn, affect the clotting rate and flow rate. To explore the impact of these parameters on assay behaviour further, the flow rate of normal plasma on strips modified by depositing thrombin at different locations on the strip using drop casting were compared. Solutions of thrombin were placed on strips in four configurations:

- a. Sample application zone (see Fig. 2.2)
- b. Distributed along the channel in 30  $\mu$ L volumes applied at 2 cm intervals
- c. Midway along the channel
- d. At the end of the channel

As shown in Fig. 3.5A, sample flow rate was lowest when the thrombin reagent was deposited at the sample application zone and highest when it was deposited at the end of the channel. The flow rate was midway between these two when the reagent was deposited midway along the channel, or in small volumes along the channel, with flow rate slower on the strips on which the reagent was distributed in small volumes. This suggested that the thrombin had maximum impact on fibrin formation when brought into contact with the sample as early as possible.

Sample flow behaviour was also assessed on test strips with thrombin deposited using inkjet printing. In this case, the channel dimensions were reduced from 5 x 80 mm to 3 x 36 mm and the reagent and sample volumes were reduced accordingly to 20  $\mu$ L and 27  $\mu$ L respectively to reduce reagent consumption and sample usage. A circular sample

zone of 5 mm was also introduced at the beginning of the fluidic channel to better accommodate application of the sample droplet (Fig. 2.2). Thrombin was printed on strips in layers of one to five ( $n=3$ ). The strips were printed at ambient temperature with the inkjet printer set at 40 V and the flow rate of the plasma sample (20  $\mu\text{L}$ ) on the strips recorded at 37°C. The distances covered by normal plasma samples on the strips after five min are shown in Fig. 3.5B. The number of layers of thrombin clearly affected the distance covered by plasma with more layers leading to shorter distances. Inkjet printing could be a means of potentially distributing thrombin evenly across the strips. However, the nozzles of the printer cartridge tended to be easily blocked/occluded by the reagent and so was not practical for initial assay development. The distance reductions achieved by the drop cast methodology were also comparable with ink jet printing. Further assay development was performed by depositing the reagent at the sample zone using the drop casting method.

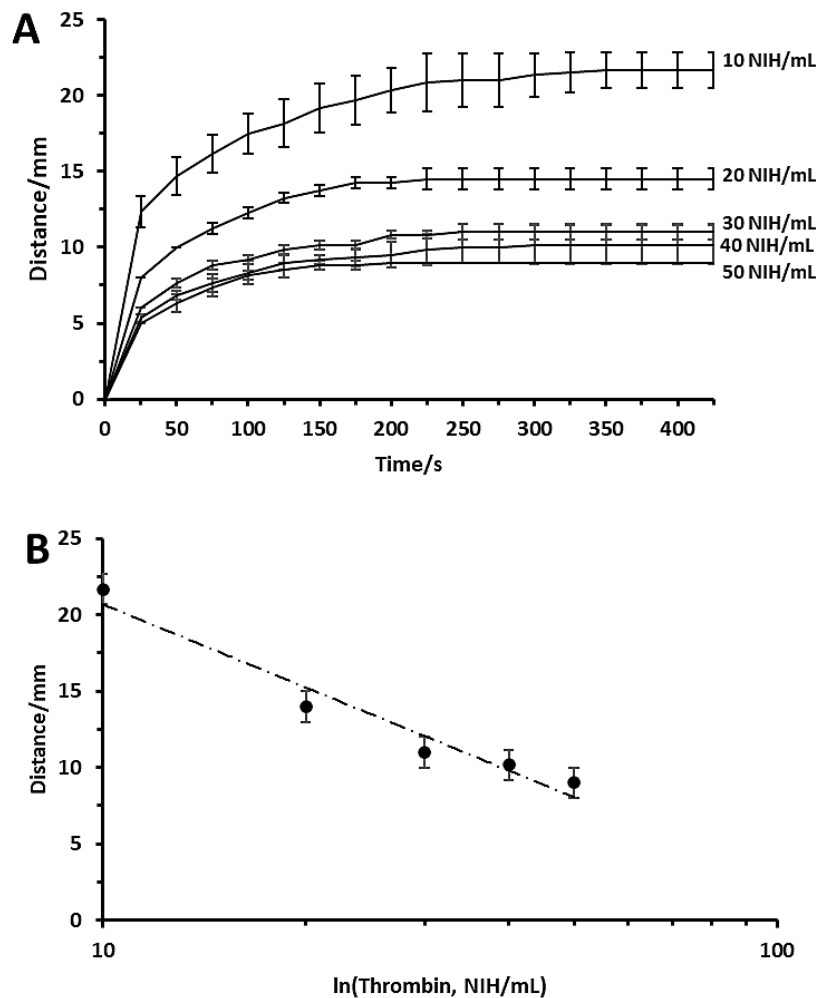


**Fig. 3.5.** Effect of thrombin reagent deposition on plasma sample flow rate. Deposition of 90  $\mu\text{L}$  50 NIH/mL thrombin: A) at different positions along the 5 x 80 mm strip fluidic channel ( $n=3$ ), B) using Inkjet printing with multiple depositions of reagent ( $n=3$ ).

### 3.2.4 Determination of the effect of thrombin activity on sample flow rate

As has been established, the flow rate of the plasma sample on the test strips is dependent on the rate of coagulation as well as the magnitude of flow inhibition caused by the immobilised reagent. Thrombin reagents are composed of thrombin which may differ in source (e.g., human or bovine), as well as stabilisers and other reagents, which may vary in their composition. These differences in composition could cause differences in hydrophobicity, rehydration, and sample retention. The ideal thrombin reagent for lateral flow fibrinogen measurements would be one with the least impact on sample flow because any effect that impedes sample flow besides clotting impairs analytical sensitivity and dynamic range. Two types of thrombin reagent were explored in this work which were a lyophilised thrombin from bovine plasma (T4648, Sigma-Aldrich) and a bovine thrombin from a Clauss fibrinogen assay kit (5556, Helena Biosciences). Following preliminary flow rate studies in a non-clotting control setting (data not shown), the Sigma-Aldrich thrombin retarded the plasma sample far more than the Helena Biosciences thrombin and hence the latter was chosen for further development of the assay. The thrombin from Sigma-Aldrich (T4648) was also found to take longer to dissolve than the one from Helena which could be due to purity difference, the one from Helena being purer.

Having selected an appropriate thrombin material, it was necessary to optimise thrombin activity and its effect on plasma sample flow behaviour across a range of fibrinogen concentrations. The strips used in thrombin optimization and later developments of the assay were conducted using strips with smaller channels (3 x 36 mm). The strips were modified with 27  $\mu$ L thrombin reagent from 10 to 50 NIH/mL and 20  $\mu$ L plasma samples were applied (n=3, Fig. 3.6A). Sample flow had typically ceased at approximately 300 s (5 min). The distance travelled in that time for 50 NIH/mL was 9.0  $\pm$ 0.0 mm while for 10 NIH/mL was 21.7  $\pm$ 1.2 mm, The response also appeared to be non-linear at higher thrombin activity, with only fractional decreases over 30 and 40 NIH/mL, suggesting that at 50 NIH/mL, the effect on clotting was close to maximum.



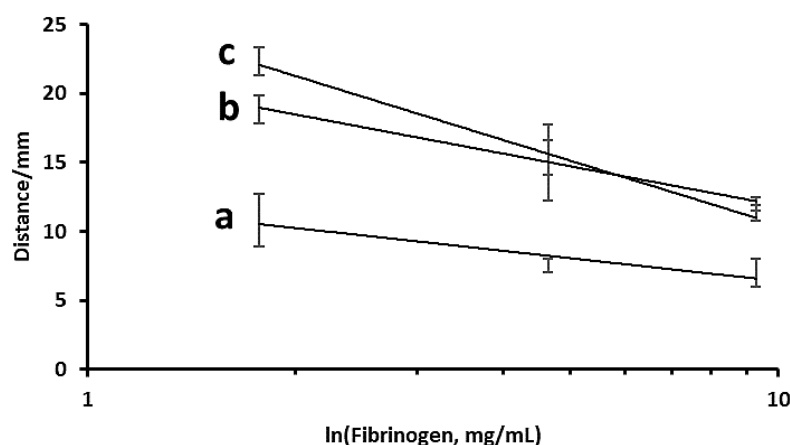
**Fig. 3.6.** (A) Flow rates of normal human plasma (20  $\mu$ L) on strips (3 x 36 mm) modified with 27  $\mu$ L thrombin at 10 to 50 NIH/mL. (B) Distance travelled by plasma samples after 300 s.

However, while the most rapid clotting rate might mean the fastest assay speed, it might not be optimal for other assay parameters such as dynamic range, sensitivity, linearity, and reproducibility. Normal human plasma has a fibrinogen concentration of approx. 2.8 mg/mL, which typically varies in the range of <1 to >5 mg/mL in hypo- and hyperfibrinogenaemic conditions, respectively (Besser and MacDonald, 2016; Machlus *et al.*, 2011). Optimization of thrombin activity was, therefore, critical to ensure that the assay can operate across this clinically relevant range. Optimisation of thrombin activity at a fibrinogen concentration of only 2.8 mg/mL might limit assay range, particularly at lower fibrinogen concentrations. Therefore, the impact of both thrombin activity and fibrinogen concentration on sample flow were investigated.

Three plasma fibrinogen concentrations of 1.77, 4.64, and 9.28 mg/mL (covering the entire clinically relevant range) were investigated with thrombin at 20 and 50 NIH/mL

deposited either midway in the channel, or at the sample application zone, as these had earlier been shown to be most effective (Section 3.2.2). The fibrinogen standards were prepared by dissolving lyophilised fibrinogen (F3879) in a low fibrinogen plasma (1.5 mg/mL). Optimum activity of thrombin was thought to lie between 20 and 50 NIH/mL). Lower activity (<20 NIH/mL) could render the assay less robust and precise while very high activity (>50 NIH/mL) could lead to a narrow linear range and less sensitivity.

As shown in Fig 3.7, the response to fibrinogen concentration was not linear as was found previously in a polymer-based lateral flow assay platform (Dudek et al., 2010). At 50 NIH/mL applied at the centre of the strip, this yielded a relatively low sensitivity/slope (-2.39 mm/mg/mL). Reducing the thrombin activity down to 20 NIH/mL when applied at the centre of the strip gave a steeper slope and better sensitivity (-4.09 mm/mg/mL). However, the slope was improved even further to -6.70 mm/mg/mL when the strips were coated by applying 20 NIH/mL of thrombin at the sample zone instead of midway along the channel. From an AVOVA, the three slopes were found to be significantly different ( $p < 0.001$ ) and that the graph generated from applying thrombin (20 NIH/mL) at the strip sample zone (Fig. 3.7 c) gave the steepest slope, and therefore the best sensitivity. This also gave the best correlation between distance and sample fibrinogen content ( $r = 0.9954$ ). Based on these findings, it was decided to apply the thrombin reagent at the sample zone.



**Fig. 3.7.** Distance travelled by 20  $\mu$ L plasma fibrinogen samples after 300 s on strips modified with 27  $\mu$ L thrombin a) at 50 NIH/mL applied mid-way along the channel ( $y = -2.385\ln(x) + 11.89$ ,  $r=0.953$ ); b) at 20 NIH/mL applied mid-way along the channel ( $y = -4.093\ln(x) + 21.30$ ,  $r=0.997$ ); c) at 20 NIH/mL applied at sample zone ( $y = -6.7\ln(x) + 25.90$ ,  $r=0.995$ ) ( $n=3$ ).

### 3.2.5 Optimization of thrombin activity and sample volume

Reduced activity of thrombin (20 NIH/mL) showed better sensitivity and correlation between sample fibrinogen concentration and distance travelled compared to higher thrombin activities (section 3.2.3), but thrombin activity had not been fully investigated. It was therefore necessary to further investigate this to establish the activity of thrombin at the 27  $\mu$ L reagent volume most suitable for the assay. The effect of thrombin activity on the assay performance was examined again using three fibrinogen standards (prepared as in section 3.2.3) of 1.47 (low), 3.70 (normal) and 6.36 (high) mg/mL and each of these was tested at thrombin activities of 20, 30, 40, and 50 NIH/mL with the reagent deposited at the sample zone of the strip (n=3). The analytical parameters are summarised in Table 3.1. The assay at 30 NIH/mL gave the overall best performance with the best combination of sensitivity, precision, and linearity, and so was adopted for further assay development. It may be that higher thrombin activities lead to faster coagulation rates, potentially higher precision, and shorter assay times, but at the expense of dynamic range and sensitivity. On the other hand, a lower thrombin activity could enhance sensitivity, but lead to lower precision and possibility longer assay time. 30 NIH/mL appeared to be the thrombin activity for best assay performance and was therefore used for further development of the assay.

**Table 3.1.** Analytical performance parameters for fibrinogen calibration assays across a range of thrombin concentrations. Assays based on 20  $\mu$ L fibrinogen standards of 1.47, 3.70 and 6.36 mg/mL and 27  $\mu$ L thrombin reagent and the slopes based on log concentrations.

Thrombin (NIH/mL)	Slope (mm/ln[mg/mL])	r	Mean SD
20	-3.398	0.971	1.69
30	-5.471	0.993	0.80
40	-1.800	0.997	2.17
50	-2.806	0.985	2.52

Another parameter that critically affects analytical performance is sample volume, influencing accuracy, sensitivity, precision, and in this particular assay, sample travel distance and assay time. Minimising the sample volume reduces the burden on patients at POC settings. However, reduced sample volume also decreases precision in the volume of sample delivered which influences accuracy. In this assay in particular, large sample volume encourages bulk flow across the strip rather than capillary action through it, which reduces the contact between fibrinogen in the sample and thrombin on

the strip surface, potentially reducing both precision and sensitivity. Sample volume was optimised in the range of 20 to 26  $\mu\text{L}$  using 27  $\mu\text{L}$  of 30 NIH/mL thrombin, with measurement using three fibrinogen standards (low, normal, and high), with the assay performance characteristics summarised in Table 3.2. A sample volume of 26  $\mu\text{L}$  gave the highest sensitivity (slope of -6.561), but poorest correlation ( $r=0.825$ ) and precision (3.09 mean SD), while 22  $\mu\text{L}$  gave better sensitivity than 20  $\mu\text{L}$  and 24  $\mu\text{L}$  volumes and had adequate correlation ( $r=0.977$ ) and precision (0.80 Mean SD). A sample volume of 22  $\mu\text{L}$  was chosen as optimal based on the best overall combination of regression coefficient, precision, and sensitivity. Precision was determined from the mean standard (mean SD) deviation of all the measurements made at each parameter value (e.g., 20, 22  $\mu\text{L}$  etc sample volume). The lower this value, the higher the precision.

**Table 3.2.** Analytical performance parameters for fibrinogen calibration assays across a range of sample volumes. Assays based on 30 NIH/mL thrombin and fibrinogen standards of 1.10, 2.84 and 5.68 mg/mL, ( $n=3$ ) and slopes based on log concentrations.

Sample volume ( $\mu\text{L}$ )	Slope (mm/ln[mg/mL])	r	Mean SD
20	-4.701	0.963	0.79
22	-5.373	0.977	0.80
24	-4.579	0.999	1.75
26	-6.561	0.825	3.09

### 3.2.6 Calibration of the paper-based lateral flow fibrinogen assay device

Having optimised key assay parameters such as strip design, sample volume, thrombin reagent, and reagent deposition point, it was necessary to undertake detailed calibration of the assay. Eight plasma fibrinogen standards across a concentration range of 0.87 to 7.4 mg/mL were prepared, measured using a reference coagulometer instrument (Yumizen G200) and tested on the device ( $n=3$ ) (Table 3.3). The data shows an average standard deviation and CV of 0.8 and 5.5%, respectively, all of which were below 10%, which indicated adequate precision. The data also shows that the sensitivity of the assay was greater at lower fibrinogen concentrations than at higher concentrations given that distance values were closer together for higher concentrations and further apart for lower concentrations. For instance, the sample distance for 0.78 and 1.17 mg/mL were 2.1 mm apart while for 5.68 and 7.40, the sample distances were 1.3 mm apart. This could be due to the fact that higher fibrinogen concentrations cause faster coagulation rates and shorter sample distance which forces distance values closer to each other,



while lower fibrinogen concentrations lead to slower coagulation rate with longer distances, making the distance values to spread out (Lo *et al.*, 2006).

**Table 3.3.** Calibration data of optimised fibrinogen assay device. 27  $\mu\text{L}$  reagent volume, 20  $\mu\text{L}$  sample volume and 5 min assay time ( $n=3$ ).

Fibrinogen concentration (mg/mL)	Sample distance (mm)			Mean	SD	CV (%)
	i	ii	iii			
0.87	21.5	20.0	19.5	20.3	1.0	5.1
1.17	18.0	20.0	16.5	18.2	1.8	9.7
2.13	16.0	15.5	15.5	15.7	0.3	1.8
2.83	14.0	13.0	13.0	13.3	0.6	4.3
3.46	13.0	12.0	12.5	12.5	0.5	4.0
3.82	11.5	11.0	12.5	11.7	0.8	6.5
5.68	11.5	11.0	10.0	10.8	0.8	7.1
7.40	9.0	9.5	10.0	9.5	0.5	5.3
<b>Mean</b>					<b>0.8</b>	<b>5.5</b>

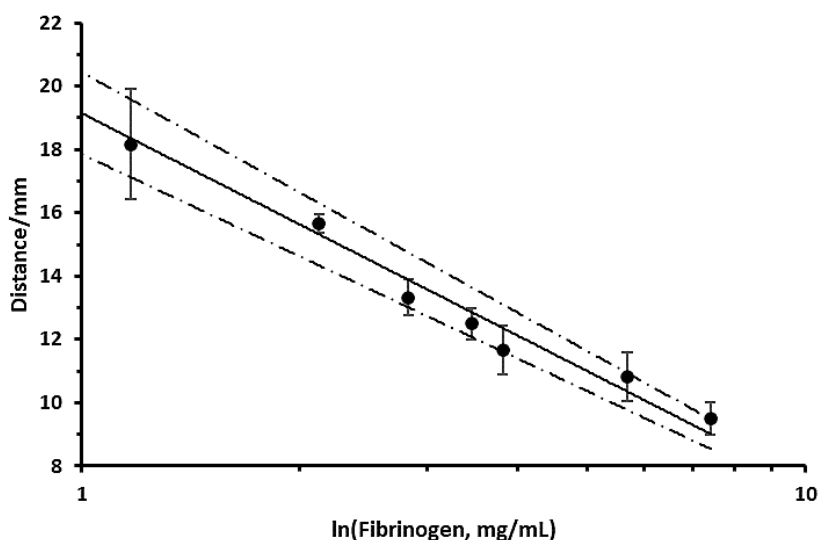
The relationship between the plasma fibrinogen concentration as determined by the Yumizen G200 and the performance of the assay device with confidence intervals are shown in Table 3.4 and Fig. 3.8. The response was curvilinear with an excellent fit to a semi-inverse logarithmic plot with a slope of -5.058 and  $r$  of 0.991. The minimum, mean, and maximum CVs of travel distance ( $n=3$ ) were 1.8, 5.5, and 9.7%, respectively (Table 3.3).

**Table 3.4.** Fibrinogen concentrations and their corresponding sample travel distances with 95% confidence interval. 27  $\mu\text{L}$  30 NIH/mL thrombin and 22  $\mu\text{L}$  sample ( $n=3$ ) used.

Fibrinogen concentration (mg/mL)	Distance (mm)	Confidence Interval (95%)	Lower confidence interval	Upper confidence interval
0.87	20.3	1.2	19.2	21.5
1.17	18.2	2.0	16.2	20.2
2.13	15.7	0.3	15.3	16.0
2.83	13.3	0.7	12.7	14.0
3.46	12.5	0.6	11.9	13.1
3.82	11.7	0.9	10.8	12.5
5.68	10.8	0.9	10.0	11.7
7.40	09.5	0.6	8.9	10.1

Using the regression expression  $y = -5.058\ln(x) + 19.143$  from the calibration curve (Fig. 3.8), the distance equivalence for specified fibrinogen concentrations in the range of 0.5 to 7 mg/mL was calculated and the results with their upper and lower 95% confidence limits are given in Table 3.5. The distance values from 16.0 to 11.5 mm were considered to indicate normal range (2 to 4 mg/mL fibrinogen). Distances below 11.5 mm indicate

hyperfibrinogenaemia while distance values above 16.5 mm show hypo-/dysfibrinogenaemia.



**Fig. 3.8.** Calibration curve of concentration of fibrinogen standards as determined by Yumizen G200 versus distance travelled after 300 s for the optimised paper-based fibrinogen assay. Assay based on deposition of 27  $\mu$ L 30 NIH/mL thrombin and 22  $\mu$ L sample ( $n=3$  repeats). Equation of the line,  $y = -5.058\ln(x) + 19.143$  ( $r = 0.991$ ). Dashed lines: 95% confidence.

**Table 3.5.** Fibrinogen concentrations and their corresponding calculated distance values. Normal range highlighted in grey.

Fibrinogen concentration (mg/mL)	Distance (mm)	95% confidence interval (mm)	Lower confidence limit (mm)	Upper confidence Limit (mm)
0.50	22.6	0.8	23.3	21.8
1.00	19.0	0.7	19.7	18.4
2.00	15.5	0.5	16.1	15.0
3.00	13.5	0.4	13.9	13.1
4.00	12.0	0.4	12.5	11.6
5.00	10.9	0.5	11.4	10.4
6.00	10.0	0.7	10.6	9.3
7.00	9.2	0.8	10.0	8.4

### 3.2.7 Validation of the paper-based lateral flow fibrinogen assay device

The assay was validated during the COVID-19 pandemic and there was no access to clinical samples for validation studies. Instead, ‘artificial’ samples constructed from commercial plasmas and lyophilised fibrinogen were developed to validate the assay. The samples were prepared by mixing low and normal fibrinogen plasmas as well as

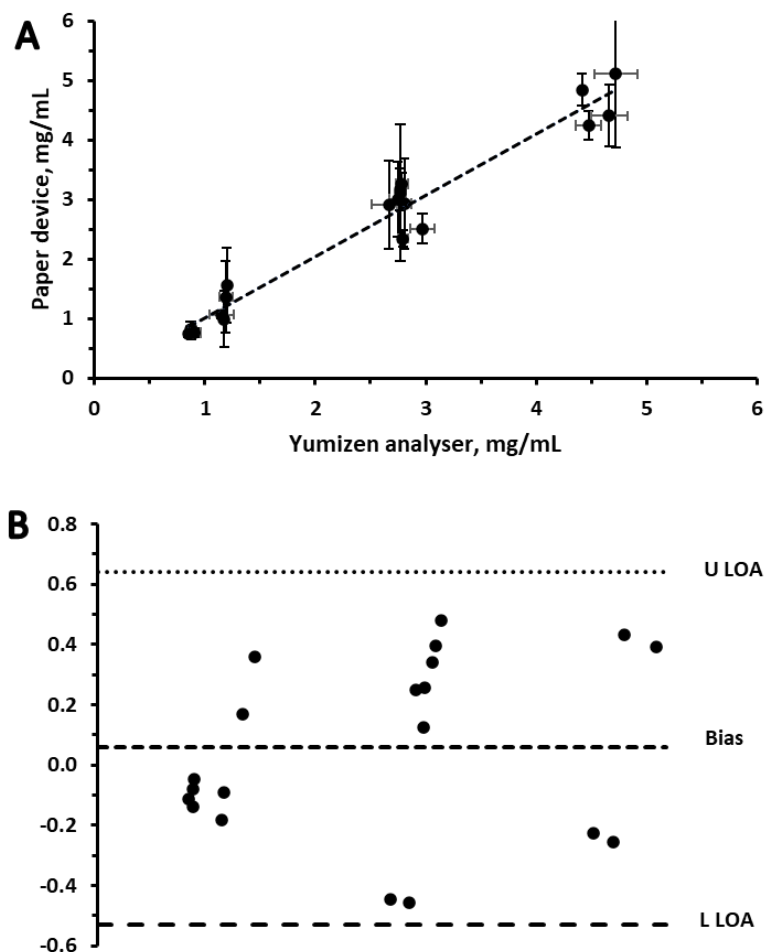
supplementing plasmas with lyophilised fibrinogen to create unknowns with fibrinogen concentrations in the regions of low (0.8 to 1.2 mg/mL), normal (2 to 3 mg/mL), and high ( $\geq 4$  mg/mL). In total, 20 samples were prepared and tested in triplicates on the device and on the Yumizen G200 coagulometer. The measured distance values from the device were converted into their fibrinogen concentration equivalents in mg/mL (Table 3.6) using the calibration expression ( $y = -5.058\ln(x) + 19.143$ ) and compared with the results from the Yumizen analyser using linear least squares regression (Fig. 3.9A) and Bland-Altman analysis (Fig. 3.9B).

**Table 3.6.** Tabulation of fibrinogen concentrations in mg/mL calculated from travel distances on assay strips based on the regression equation (Fig. 3.7) and corresponding results from Yumizen G200.

Sample	Distance (mm)	Developed Assay		Yumizen G200	
		Fibrinogen concentration (mg/mL)	SD	Fibrinogen concentration (mg/mL)	SD
1	13.83	2.93	0.76	2.81	0.07
2	13.17	3.26	0.18	2.78	0.06
3	13.67	3.00	0.64	2.75	0.08
4	13.83	2.92	0.74	2.67	0.16
5	14.83	2.35	0.14	2.79	0.05
6	14.50	2.51	0.25	2.97	0.11
7	13.67	3.11	1.14	2.77	0.04
8	13.33	3.17	0.35	2.77	0.04
9	18.00	1.36	0.60	1.19	0.06
10	19.67	1.00	0.47	1.18	0.04
11	17.17	1.56	0.64	1.20	0.01
12	18.83	1.06	0.06	1.15	0.11
13	20.17	0.82	0.12	0.87	0.02
14	20.33	0.80	0.16	0.88	0.04
15	20.50	0.77	0.08	0.91	0.05
16	20.67	0.74	0.04	0.85	0.04
17	11.00	5.11	1.24	4.72	0.19
18	11.17	4.85	0.27	4.41	0.01
19	11.83	4.25	0.25	4.47	0.11
20	11.67	4.40	0.52	4.66	0.17
<b>Mean</b>			0.43		0.07

Looking at the data in Table 3.6, it can be seen that the developed assay had a mean SD of 0.43, which was less precise than the reference method which had a mean SD of 0.07. This variability of the assay could be due to the non-uniform nature of the paper substrate used with uneven distribution of paper fibres and varying porosity. However, with replicate measurements, the device had a satisfactory agreement, adequate for the determination of the bleeding tendency of patients.

With a slope of 1.03, and a very small offset of 0.02 mg/mL, the assay showed an excellent agreement with the reference method (Fig. 3.9A). The assay also had good linearity across the entire clinically relevant range and a very good correlation coefficient of  $r=0.979$ . It had a wide dynamic range (0.5 to 7 mg/mL) and an adequate agreement with the well-established routine reference method, as indicated in the Bland-Altman plot (Fig. 3.9B), making the performance of this device acceptable. It was capable of making reliable measurements of fibrinogen at concentrations across the full range found in human plasma and thus suitable for both hyper- and hypofibrinogenaemic conditions, in contrast to the very narrow assay ranges of other recent works (Bialkower, et al., 2020). Furthermore, this method is simple, robust, and single step, making it more user friendly and less prone to errors and interferences. It is also compact, portable, and instrument-free which makes it highly suited to point-of-care application.

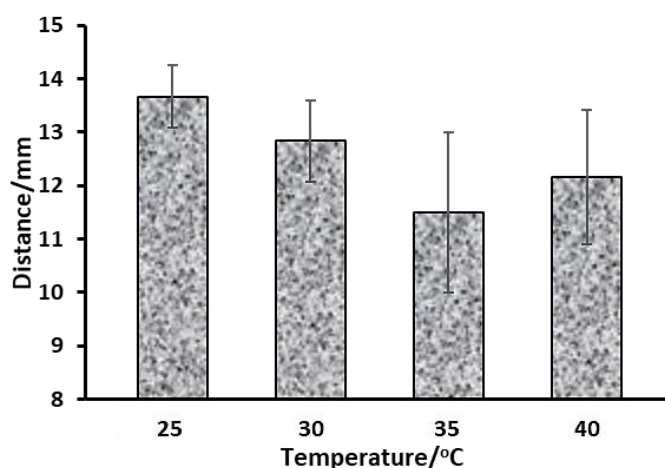


**Fig. 3.9.** Validation of the paper-based fibrinogen assay device in artificial plasma samples. (A) Correlation between paper-based device and Yumizen G200 fibrinogen assay reference method. Slope 1.03, intercept of 0.02 and  $r$  of 0.979 (20 samples, 3 repeats). (B) Bland-Altman shows that all of the data points fall within the range between the upper limit of agreement (U LOA) and the Lower limit of agreement (L LOA), signifying adequate agreement between the two methods.

### **3.2.8 Investigation of the effect of temperature on device storage and operational stability**

For devices intended for low resource environments, the test strips should be less prone to variations in environmental conditions such as humidity and temperature during operation. Furthermore, for affordable usage, mass production and storage, the test strips should have long storage working lives. The type of packaging and storage used also add cost and complexity to the fabrication process of devices. It was therefore necessary to examine the operational robustness of the device and the most ideal cost-effective option for storage of the test cartridges.

To test the operational stability of the device with reference to variations in ambient temperature, test strips were prepared and evaluated with normal plasma at a range of temperatures (25 to 40°C) likely to be encountered in remote tropical areas. As shown in Fig. 3.10, although not statistically significant ( $p=0.169$ ), the sample travel distance appeared to decrease with increasing temperature from 25 to 35°C, consistent with the dominant effect of enzymatic activity in speeding up clotting rate over the effect of reducing viscosity which promotes faster and longer flow distances. However, a larger sample set would be required to confirm this. An increased travel distance was registered at 40°C which could be caused by reduced enzymatic activity due to too high temperature coupled with further decrease in sample viscosity. This finding suggested that the assay results would be influenced by variations in temperature. To overcome this defect, different measurement scales could be developed and used for different temperatures. Also, patient plasmas could be run alongside normal ones with known fibrinogens levels and distance ratios used to work out the fibrinogen level in the unknowns. The latter could be used to get around the effect of humidity as well.



**Fig. 3.10.** Effect of operating temperature on assay results showing the distance travelled by normal plasma on test strips at different temperatures. 27  $\mu\text{L}$  of 30 NIH/mL thrombin and 22  $\mu\text{L}$  sample volume ( $n = 3$ ) and assay time of 300 s.

To assess the effect of storage conditions on working life, test strips were placed in folded paper sheets and sealed under vacuum in aluminium pouches along with a sachet of desiccant and stored at different temperatures for four weeks. At the end of each week, strips were removed and tested with normal plasma for performance. As shown in Table 3.7, sample distance on strips stored in the fridge and freezer remained within the acceptable performance range ( $13.17 \pm 0.76$ ) for 0 to 21 days ( $p=0.590$  and  $0.877$ , respectively). The results on day 21 for both the fridge and freezer also maintained acceptable precision (CV = 0.0% and 5.8%, respectively). However, on day 28 for the fridge and freezer, although not significantly different from day zero ( $p=0.380$ , and  $0.497$ , respectively), these had reduced precision (CV=20.8%, and 23.2%, respectively). The apparently increased variability at day 28 could be due to thrombin on strips losing its activity and were less reliable. Further work to stabilise these reagents would be critical for the deployment of these devices in the field.

**Table 3.7.** Effect of storage conditions on clotting properties of paper-based fibrinogen assay strips ( $n=3$ ).

Storage conditions	Distance travelled by normal plasma (mm) after number of days storage				
	Day 0	Day 7	Day 14	Day 21	Day 28
Freezer (-15 to -18°C)		$12.83 \pm 0.76$	$13.00 \pm 1.00$	$12.67 \pm 0.58$	$14.67 \pm 3.40$
Fridge (4 to 6°C)	$13.17 \pm$	$13.50 \pm 1.50$	$12.50 \pm 0.50$	$13.00 \pm 0.00$	$15.00 \pm 3.12$
Ambient (18 to 23°C)	0.76	$13.00 \pm 0.00$	$11.83 \pm 1.76$	$11.17 \pm 0.76$	$11.67 \pm 1.04$
Oven (37°C)		$10.83 \pm 0.58$	$12.67 \pm 0.29$	$12.33 \pm 1.04$	$10.67 \pm 0.76$

As for the strips stored under ambient conditions (18 to 23°C), the sample distance was within the working range after the first week and appeared reduced in the following weeks. This may have been due to the increased desiccation of those strips, making them more hydrophobic. The travel distances on strips stored at elevated temperature (37°C) varied considerably and were generally below the working reference range which could also be attributed to increased drying. However, it is safe to say that if the test strips are packaged and stored in a fridge or freezer ( $\leq 6^{\circ}\text{C}$ ), they could remain viable for 21 days without further stabilisation, comparatively longer than that reported by Magdalene *et al* (2010).

In summary, a compact, paper-based lateral flow device that can reliably measure fibrinogen concentration in human plasma within five minutes was developed in this work. It comprises a disposable paper-based assay strip with immobilised thrombin reagent and a reusable plastic holder. The device uses a simple distance readout format, requires no instrumentation, and correlates adequately well with a routine laboratory coagulometer ( $r=0.979$ ). A number of similar devices have been reported in literature but each of those devices either have a narrow dynamic range (Bialkower *et al.*, 2020), are not compact/portable (Bialkower *et al.*, 2019), require complex fabrication and instrumentation methodology (Dudek *et al.*, 2011b; Guan *et al.*, 2020) or use non-biodegradable materials (i.e. polymer) as substrates (Dudek *et al.*, 2010) and so are not ideal for use in resource scarce and emergency settings. The device developed in this work, however, is low-cost, compact/portable, instrument free, easy to operate, environmentally friendly, adequately reliable and have a wide dynamic range (0.5 to 7.0 mg/mL) that covers the entire range of clinically relevant fibrinogen concentrations in human plasma. It is therefore environmentally friendly and comparatively more suitable for POC fibrinogen measurements in low-income and emergency situations.

### **3.3 Conclusion**

A paper-based lateral flow assay device was developed for the measurement of fibrinogen in blood plasma. The device was fabricated using a chromatography paper as a substrate, wax printing to define strip geometries and 3D printing to fabricate strip holders. The paper test strips were modified with thrombin which was brought into contact with a deposited plasma sample, inducing fibrin clot formation and altering the sample flow rate and the distance travelled by the sample in a manner relative to the sample fibrinogen concentration. The distance travelled by the sample was inversely

related to fibrinogen concentration. The device could be conveniently read visually using a millimetre graduation scale after five minutes following sample application. It was capable of measuring fibrinogen in a concentration range of 0.5 to 7.0 mg/mL with a strong correlation ( $r = 0.979$ ) with a routine laboratory coagulometer. The test strips, when packaged with a desiccant in aluminium foil pouches and stored in a fridge or freezer, remained stable and functional for 21 days. The device was low cost and simple to operate and therefore ideal for measuring fibrinogen in low resource and emergency settings. However, assay results could be influenced by humidity and temperature variations. This could be overcome by using different temperature reading scales or running patient plasmas with normal plasmas and calculating the unknown from distance ratios.

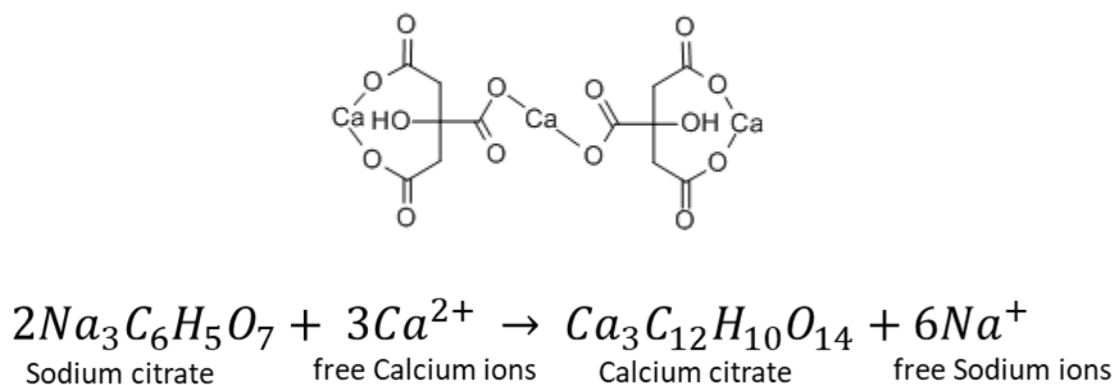


#### **4. DEVELOPMENT OF A PAPER-BASED LATERAL FLOW PROTHROMBIN ASSAY DEVICE**

## 4.1 Introduction

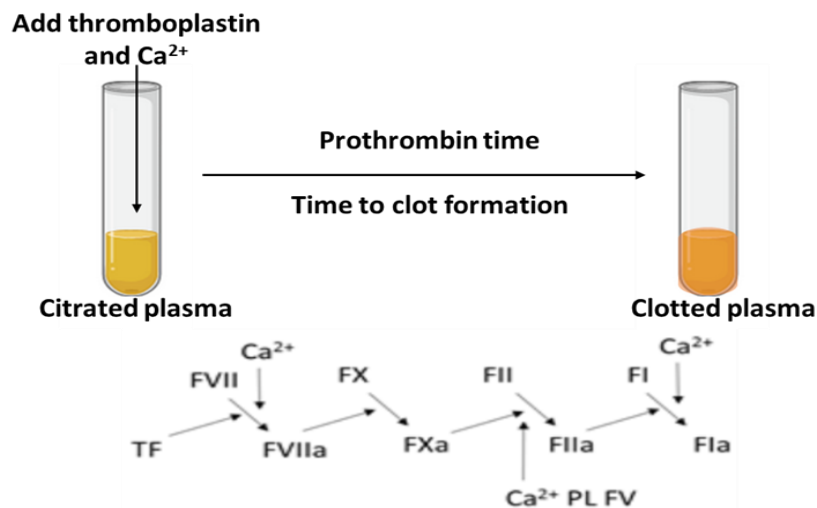
Prothrombin Time (PT) is a routine screening test for evaluating the activity of the extrinsic and common coagulation pathways. It is used for detecting congenital and acquired deficiencies of coagulation factors in the extrinsic and common pathways and, along with its standardised format, the International Normalised Ratio (INR), it has become an essential test in diagnosing bleeding and clotting disorders (Dorgalaleh *et al.*, 2021; Kitchen *et al.*, 2018). Among other things, PT is requested for assessing unexplained bleeding, (Winter *et al.*, 2017), induction and monitoring oral anticoagulant therapies using vitamin K antagonists (Shih *et al.*, 2012; Levy *et al.*, 2014), monitoring pre-, peri-, and post-operative coagulation status of patients (Guler *et al.*, 2018), checking liver function in coagulation factor synthesis (Levy *et al.*, 2014) and diagnosing DIC and detecting antiphospholipid antibodies. With its many applications, PT has become a routine and frequently ordered test in hospitals, clinics, and GP offices.

For laboratory-based PT analysis, the blood sample is collected in a tube containing sodium citrate which removes free calcium ions from solution via chelation and renders the sample anticoagulated (Fig. 4.1). The anticoagulated sample is then centrifuged, typically at 1600 x g for 15 minutes to remove cellular components and produce platelet poor plasma (PPP) (Dashkevich *et al.*, 2014).



**Fig. 4.1.** The structure of sodium citrate and its reaction with calcium. Calcium becomes bound to the sodium citrate and is unavailable to act as a cofactor in coagulation.

As shown in Fig. 4.2, PT generally involves adding a thromboplastin reagent along with calcium to citrated plasma or whole blood and measuring the time it takes for initial detection of the fibrin clot. Conventionally, this is performed either manually using test tubes with visual detection of the onset of clot formation, or instrumentally in which clot formation causes changes in light transmission or light scattering (Rifai, 2018).



**Fig. 4.2.** Schematic of prothrombin time test showing a series of enzymatic reactions initiated by addition of thromboplastin and calcium and leading to conversion of fibrinogen (FI) to fibrin (FIa) which polymerises to form a clot.

Thromboplastin is typically a mixture of tissue factor, which initiates the clotting process via the extrinsic pathway, and phospholipids which provide a pro-coagulant surface for clotting factor binding. They may be supplied as either a liquid or a lyophilised solid. They may also contain calcium, or this may be provided separately. Thromboplastin reagents are produced from human or animal tissue extracts e.g., rabbit brain or human placenta, or via production of recombinant human tissue factor (RHTF) and synthetic phospholipids (Smith *et al.*, 2006; Smith and Morrissey, 2004).

Due to variations in the sensitivity of individual reagents, a calibration system was developed in which each thromboplastin reagent was assigned an international sensitivity index (ISI) value with respect to the international WHO reference called the International Reference Preparation (IRP) which has an ISI value of 1.0. The ISI value is a measure of sensitivity of a particular thromboplastin reagent to changes in the level of Vitamin K-dependent clotting factors, the higher the value the less sensitive the reagent. The reagents with recombinant thromboplastins i.e., those using RHTF and synthetic phospholipids generally tend to have low ISI values (i.e. close to 1.0) and are considered most ideal for conventional PT assays (Smith and Morrissey, 2004). Thromboplastins from crude extracts of human and animal origin tend to have slightly higher ISI values partly because they are less pure. According to a study by Smith *et al.* (2006), the sensitivity of a particular thromboplastin reagent tends to be influenced by its phospholipids and sodium chloride content. Furthermore, thromboplastins of similar

ISI values show differences in their sensitivity towards each of the concerned clotting factors. It is also known that reagent sensitivity is influenced by the type of coagulometer or testing method used (Lee *et al.*, 2014).

There are many different PT assay methods which can be categorised into manual, instrumental/automated, and POC methods. Manual and automated methods are conducted in research and clinical laboratories, while POC methods are designed for near patient and community-based settings. In a manual method, a mixture of thromboplastin and excess calcium ions is added to a PPP sample at 37°C and the time interval between addition of reagent and onset of clot formation is measured. This method, although not very costly, requires skill and laboratory infrastructure. The method is also fairly accurate and precise for PT values within the normal range, but precision decreases significantly as PT values increase which is due to the difficulty in precisely visualising the onset of clot formation. Automated laboratory instruments use the same principle, but the onset of clot formation, which is optically or electrochemically detected and digitally read, is typically more convenient, accurate and precise than the manual method. However, automated laboratory methods are more costly and also require expertise and infrastructure. Clearly, manual and automated laboratory instrumental methods are adequate and excellent for inpatient care, but are not suitable for community-based care especially for remote and low-income areas (Hood and Eby, 2008). The need for monitoring at primary care and in community and home-based settings has necessitated the development of POC PT assay devices. Current POC devices that perform clotting time tests including the PT are: CoaguCheck® XS (Roche Diagnostics Cooperation), which uses electrochemical detection, CoagMax (Microvisk Ltd), which uses elasto-mechanical detection, and Hemochron Signature (Werfen), which uses cessation of blood flow in a micro-channel for detection. These devices are mainly semi-automated and depending on the detection method, they use disposable cartridges or test strips that contain electrodes, or magnetic particles and reagents. Most of these devices exhibit good performance and adequate reliability. However, their instrumental complexity and relative cost limit their use, particularly in developing countries (Yang *et al.*, 2004).

Coagulation assay methods based on microfluidic platforms using detection techniques such as impedance (Ramaswamy *et al.*, 2013; Anubhuti and Shantanu, 2020), frequency shift in quartz crystal microbalance (Andersson *et al.*, 2005a), fluorescence

(Andersson et al., 2005b; Dudek *et al.*, 2011), and centrifugal force (Lin *et al.*, 2014); have also emerged in a bid to develop novel simplified PT assays. Most of these methods also lack compactness, which is a necessary requirement for POC testing. Coagulation testing devices that use polymeric substrates and distance-based detection techniques have also been developed in a bid to simplify the PT test. Such devices require either pumps (Guler *et al.*, 2018) or micropillars (Dudek *et al.*, 2011) to induce sample flow along the fluidic channel, of which the former introduces instrumental complexity. Devices based on polymeric substrates are also not environmentally sustainable, and with approaches based on paper rapidly increasing in interest due to their low cost, simplicity, and sustainability (Li and Steckl, 2019), polymer-based substrates are no longer an attractive solution.

In this study, the aim was to develop a passive, cellulose paper-based prothrombin assay in which capillary action within the paper would drive the flow of the sample which would come into contact with a deposited thromboplastin reagent to induce coagulation. The distance travelled by the sample would be the measured signal which would be determined visually. The assay was expected to be simple and user friendly, have a short turnaround time, and be economically and environmentally sustainable and most importantly suitable for remote and low-income areas.

The first task undertaken was assessment and identification of the effect of thromboplastin triggered clotting on sample flow rate and travel distance. This was conducted by testing plasma, serum, and buffer samples on test and controls strips and studying their flow behaviours. The identified effect i.e., reduction in sample flow rate and distance travelled due to clotting, was enhanced by assessing and optimizing different assay parameters such as thromboplastin type and amount, paper type, strips geometry, and sample volume. The device was then calibrated using plasmas of different PT values to establish the distance equivalent of different PT values in seconds after which it was validated against an established hospital PT method with both artificially constructed and real patient plasma of wide range PT values. It showed a satisfactory correlation with the hospital method for plasma samples with PT values within the range of 9.8 to 40.0 s.

## 4.2 Results and discussion

### 4.2.1 Investigation of paper substrates for lateral flow prothrombin assay

In the development of the paper-based fibrinogen assay (Chapter 3), only Whatman No. 1 chromatography paper was investigated as a substrate. However, the fibrinogen assay comprised a very short reaction sequence requiring just two enzymes (thrombin and fibrinogen monomers) and essentially just two reaction steps (i.e., action of thrombin on fibrinogen and polymerisation of the resulting fibrin monomers). Exogenous thrombin deposited on the test strips converted fibrinogen into its monomers which polymerised and formed a clot. Having only a few reaction steps made it more efficient and potentially more robust. A prothrombin assay, on the other hand, involves many coagulation factors and a longer sequence of reactions and the principal factor, thrombin, has to be generated from those reactions before it converts fibrinogen into fibrin. The rate of clot formation is, therefore, likely to be slower, which will result in different lateral flow assay dynamics. Papers with different pore sizes and thicknesses might be more optimal for use in the prothrombin assay.

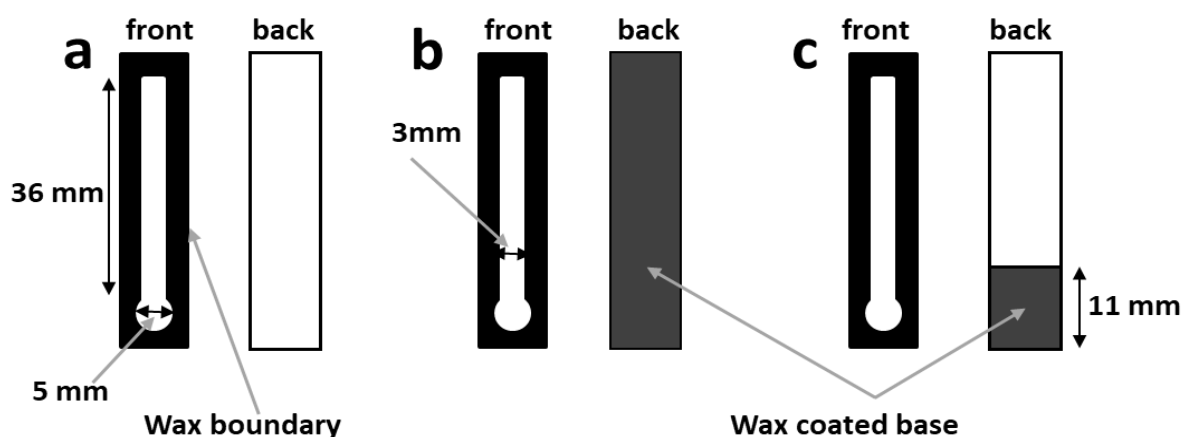
Different grades of paper vary in their properties such as chemistry (e.g., cellulose versus nitrocellulose), thickness, pore size and linear water flow rate, all of which could potentially influence the suitability for fabrication of test strips and the performance of any assay. In addition to the Whatman No. 1 chromatography paper already used, two other cellulose-based papers (Whatman SG81 and Whatman 3MM) were investigated in the development of the prothrombin assay (Fig. 4.3). Whatman No. 1 has a very smooth surface, a thickness of 0.18 mm, 11  $\mu\text{m}$  pore size and 130 mm/30 min water flow rate and is the most widely used in assays and chromatographic separations (Manisha *et al.*, 2018). In this work, the Whatman No. 1 chromatography was also found to be easy to use in fabricating assay strips via wax printing and curing. The 3MM paper has a greater thickness (0.34 mm), slightly larger pore size (12  $\mu\text{m}$ ), but has a water flow rate similar to that of No. 1 paper (130 mm/30 min) (Mahmud *et al.*, 2018). However, this paper was more difficult to print due its increased thickness i.e., it jammed the printer and also did not allow the wax layer to penetrate the full thickness of the paper to bring about a complete hydrophobic seal, and which allowed reagents and plasma samples to escape through the wax boundary (data not shown). It was clearly not suitable as an assay substrate. Whatman SG81 is composed of both cellulose and large pore silica particles. It has a large empty pore size, a thickness of 0.27 mm, and linear water flow rate of 110 mm/30 min (Primpray *et al.*, 2019). It has been mainly used for chromatographic separations and enzyme assays. While it was easy to print strip

designs using the wax printer, it did not allow the wax to penetrate during curing and so, again, did not allow the formation of hydrophobic boundaries (data not shown). Of the three, Whatman No. 1 paper remained the most suitable and so was selected and used in the development of the prothrombin assay. For future work, papers slightly thicker than Whatman No 1 but thinner than the 3MM paper such as Whatman No 4 or DE 81 with more uniform pore size distribution could be assessed for assay precision and sensitivity.



**Fig. 4.3.** Scanning electron micrographs of chromatography papers (x 500, 2.00 kV) A) Whatman No. 1, B) Whatman SG81, C) Whatman 3MM.

The initial strip design used in the prothrombin assay development was the smaller strip type used in the optimization and validation of the paper-based lateral flow fibrinogen assay device (Chapter 3). The strip had a sample zone of 5 mm diameter and a 3 x 36 mm analytical channel on the front surface (Fig 4.4A). However, as explained in section 4.2.4, other strip designs were later investigated and a more suited design (Fig 4.4C) was chosen.

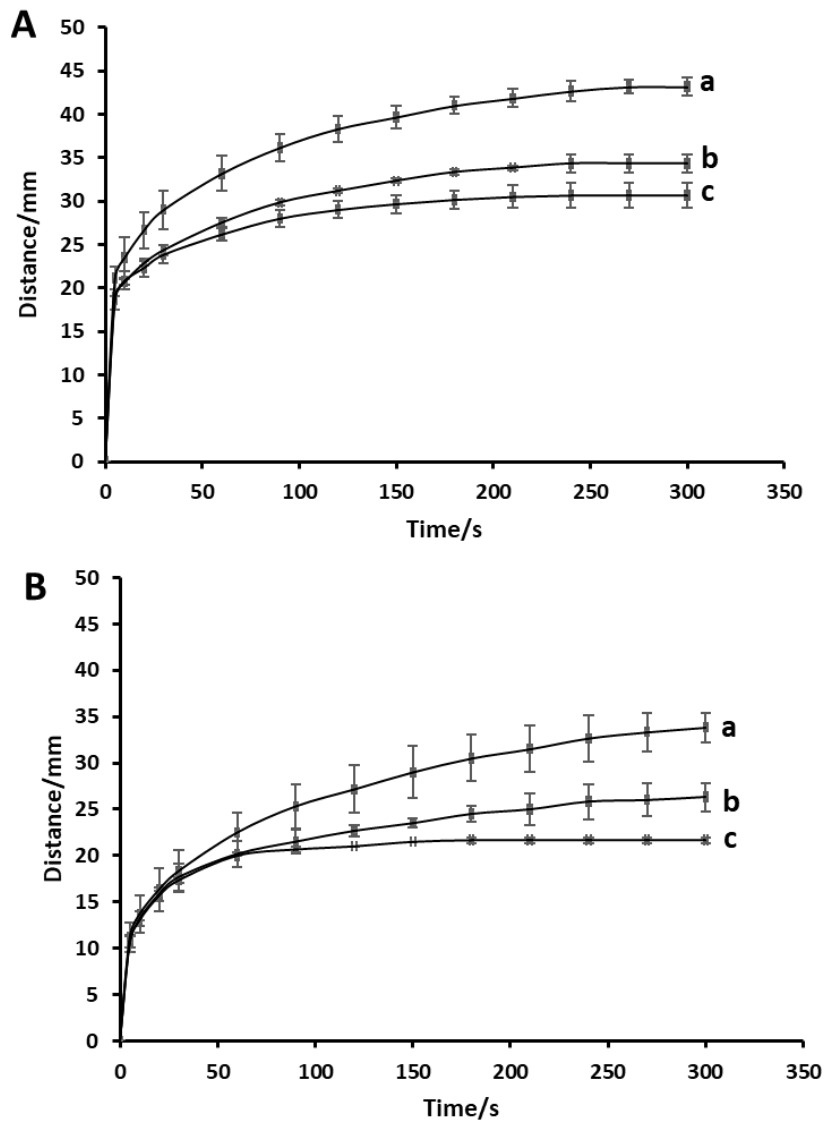


**Fig. 4.4.** Assay strip design configurations explored to improve sample behaviour. a) None coated base, b) Fully coated base, c) Base partially coated in sample zone.

#### **4.2.2 Investigation of sample flow rates on thromboplastin-modified substrates**

The principle of the classical PT assay is to measure the time taken for a blood plasma sample to produce a fibrin clot via the extrinsic coagulation pathway. However, the rate of clot formation could, in principle, be determined by the flow rate and distance travelled by a plasma sample in a capillary flow-based configuration, with the rate of coagulation correlating with the flow rate and distance travelled by the sample. However, there are other factors which may affect the flow rate, among which the hydrophobicity and rehydration of the paper substrate and any deposited reagents are important as was the case in the fibrinogen assay development (Chapter 3). The thrombin modified strips influenced the flow rate of the control samples (water and serum) more than the buffer modified (Fig 4.5). The aim here was to identify and quantify the effect of thromboplastin activation of coagulation on sample movement and then to enhance this effect to allow samples across a range of prothrombin times to be determined with respect to the distances travelled by the sample. The effect of clotting on sample flow rate and distance was investigated by performing a series of experiments involving a combination of test and control strips with normal plasma and non-coagulating control samples such as serum and Owren's buffer. The control strips (modified with 30  $\mu$ L Owren's buffer) and test strips (modified with 30  $\mu$ L PT-Reco 10) were both tested with the three sample types in triplicate and their average flow rates and sample distances compared (n=3) (Fig. 4.5).





**Fig. 4.5.** Flow dynamics on 3 x 36 mm strips modified with 30  $\mu$ L of A) Owren's buffer, or B) PT Reco 10 deposited in the sample application zone, with 22  $\mu$ L samples of a) Owren's buffer, b) serum, or c) normal plasma ( $n=3$ ). Strips with no coating on the back surface were used (Fig 4.4a).

This initial reagent and sample volumes (30 and 20  $\mu$ L) were based on the optimisation in Chapter 3. The optimal reagent and sample volume were believed to be close to the optimal values in the fibrinogen assay development (27 and 22  $\mu$ L, respectively).

The flow rates and distances travelled by all three sample types were greater on control strips modified with buffer than on strips modified with PT Reco 10 reagent, indicating modification of the strip with PT Reco 10 inhibited flow compared to the buffer due to hydrophobicity and rehydration of the reagent by the sample. The flow rates and distances travelled by the three sample types relative to one another was attributable to

differences in their viscosities. On control strips, the buffer sample having the lowest viscosity covered the longest distance (43.17 mm), followed by serum (34.33 mm) and plasma, the most viscous, covered the least distance (30.67 mm). On the test strips, the three samples also exhibited the same order in flow rates. However, they all covered shorter distances compared to that of the control strips. This was most likely due to flow inhibition caused by the prothrombin reagent present on the surface of the test strip rather than any clotting effect. Looking at the distances travelled by serum and plasma in the presence and absence of reagent, the gap was 4.8 mm on the test strips ( $p=0.002$ ) and 3.7 mm on the control strips ( $p=0.012$ ). Although the gap appeared larger on the test strips compared to that on control strips, at this sample size and with additional error propagation this was not statistically significant ( $p=0.542$ ). While it might be expected that clotting would occur on the test strips, and that any differences between the gaps might be attributable to clotting, further investigation was required to demonstrate if the effect was real and could be enhanced to a statistically significant level where it could be sensitive enough to perform a prothrombin assay. As was the case in the fibrinogen assay development (Chapter 3), sample flow had not changed after 300 s, and so the assay time chosen for the PT assay was again 300 s.

#### **4.2.3 Optimization of thromboplastin and sample volume**

Thromboplastin reagents are typically designed for use in solution in which their optimal concentrations and amount have been determined with respect to the volume of plasma sample employed. For instance, in the case of PT Reco 10, the reagent and sample are mixed in a 2:1 volume ratio. Such volumes and quantities may not be optimal in a lateral flow configuration, and hence there was a need to study and determine the appropriate amounts of sample and reagent for this scenario. In lateral flow coagulation assays, the reagent is typically distributed and dried on the strip surface where it comes in contact with, rehydrates, and mixes with the sample as the latter travels down the strip channel. In such a configuration, a larger sample volume will encourage bulk flow in which a portion could escape the reagent by travelling along, rather than within the strip, while smaller sample volumes may clot more quickly and cover only very short distances which would significantly limit the assay dynamic range and sensitivity again as was the case in the fibrinogen assay development. However, the optimization of both reagent and sample volumes in the lateral flow format, in both cases, is limited by the amount of fluid the test strips can absorb. In the case of the reagent, the maximum amount was the volume that would not over-saturate the strip on a single deposition. With regards

to the sample, it was the maximum volume that would not overflow the fluidic channel. Within these constraints, both the reagent and sample can be adjusted to levels more suited to the lateral flow format.

Based on the initial volumes of reagent and sample used in the lateral flow assay format, these were further studied in the ranges of 30 to 60  $\mu\text{L}$  and 12 to 22  $\mu\text{L}$ , respectively, by measuring travel distances of three plasma standards on the test strips. The plasma standards, Normal (N), Abnormal (A) and Severe Abnormal (SA) had corresponding PT values of 9, 17 and 34 s, respectively. The distance difference between N and SA at 300 s was considered a measure of the dynamic range (Table 4.1).

**Table 4.1.** Distance travelled after 300 s by Normal (N), Abnormal (A) and Severe Abnormal (SA) control plasmas for strips modified with PT Reco 10 ( $n=3$ ). Reagent volume was optimised with 22  $\mu\text{L}$  sample, while sample volume was optimised with 30  $\mu\text{L}$  reagent.

Plasma (PT)	Distance travelled by plasma after 300 s (mm)							
	Reagent volume with 22 $\mu\text{L}$ sample				Sample volume with 30 $\mu\text{L}$ reagent			
	60 $\mu\text{L}$	50 $\mu\text{L}$	40 $\mu\text{L}$	30 $\mu\text{L}$	22 $\mu\text{L}$	18 $\mu\text{L}$	15 $\mu\text{L}$	12 $\mu\text{L}$
N (9 s)	23.3 $\pm$ 1.3	24.3 $\pm$ 1.2	20.7 $\pm$ 1.2	22.2 $\pm$ 1.0	23.7 $\pm$ 1.2	18.8 $\pm$ 1.6	14.0 $\pm$ 0.9	9.2 $\pm$ 1.0
A (17 s)	24.3 $\pm$ 1.9	22.5 $\pm$ 0.9	22.2 $\pm$ 0.6	21.3 $\pm$ 0.3	22.5 $\pm$ 0.9	20.8 $\pm$ 1.5	17.2 $\pm$ 1.5	10.3 $\pm$ 1.9
SA (34 s)	24.0 $\pm$ 2.1	25.0 $\pm$ 1.0	21.7 $\pm$ 0.8	24.0 $\pm$ 0.0	25.0 $\pm$ 1.0	21.7 $\pm$ 0.3	18.7 $\pm$ 1.2	11.3 $\pm$ 1.3
<b>Dynamic range (mm)</b>	0.7 $\pm$ 2.5	0.7 $\pm$ 1.6	1.0 $\pm$ 1.4	1.8 $\pm$ 1.0	1.3 $\pm$ 1.6	2.8 $\pm$ 1.6	4.7 $\pm$ 1.5	2.2 $\pm$ 1.6

While not statistically significant ( $p=0.115$ ), the combination of reagent and sample volumes of 30 and 15  $\mu\text{L}$ , respectively, gave the widest dynamic range (4.7 mm) and so these were selected for further development of the assay. Increasing the volume and therefore the amount of reagent beyond 30  $\mu\text{L}$  did not appear to improve sensitivity. This suggested that at 30  $\mu\text{L}$ , a sufficient amount of the reagent was deposited on the strips which did not elicit too rapid a rate of clotting which would potentially narrow the assay dynamic range, but also not too slow to result in portions of the sample to escape coagulation, leading to less precise results. Likewise, too large a sample volume i.e., above 15  $\mu\text{L}$ , did not improve the assay sensitivity and in addition it could have potentially reduced precision due to the fact that the further the sample travels the larger the tendency for variability between travel distances of individual repeats. This is in turn due to the fact that large sample volumes encourage bulk flow which drastically reduces the sample/reagent contact and reaction, which reduces assay robustness and leads to reduced precision. On the other hand, a sample volume which if small tends to introduce larger errors in sampling, which reduces precision in results. Furthermore, very small

sample volumes may result in reduced clot formation which would lead to less coagulation effect and narrow the dynamic range and reduce sensitivity.

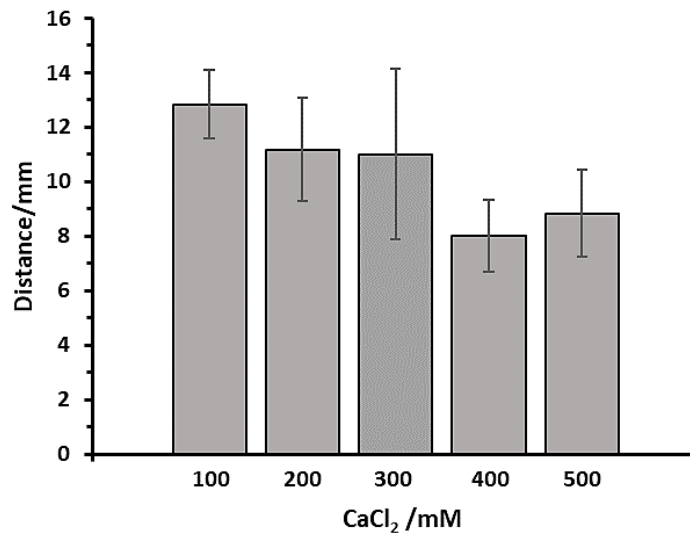
#### **4.2.4 Optimization of strip format and calcium chloride deposition**

Blood samples for coagulation testing are typically collected in a 9:1 v/v ratio with 109 mM trisodium citrate to chelate and remove free calcium from the sample to prevent clotting before testing. During coagulation testing, calcium is added back in the form of  $\text{CaCl}_2$  (25 mM) in order to allow clotting to take place so that the sample's ability to clot can be measured.  $\text{CaCl}_2$  may be either part of the reagent formulation or added separately during testing. In many thromboplastin reagents including PT Reco 10, calcium is part of the reagent at an appropriate concentration for when reagent and sample are combined in a 2:1 v/v ratio. In conventional PT assays, the reagent and sample are reacted in bulk solution. However, in a lateral flow clotting assay format, the reagent and sample combine in a gradual, progressive manner while the sample traverses the fluidic channel via capillary action. This gradual interaction may result in the less-than-optimal level of calcium coming into contact with the sample, and hence there was a need to investigate and determine the optimum calcium required for the lateral flow prothrombin assay format.

A previous study sought to study the effect of clotting rate on travel distance on lateral flow assay strips (Han *et al.*, 2014). In this work, 15  $\mu\text{L}$  calcium chloride in the range of 100 to 500 mM was added to strips and it showed that sample flow rate was reduced with increasing calcium concentration, meaning, clotting rate increased with calcium concentration. However, this study used whole blood rather than plasma, which contains red blood cells and platelets, and which could greatly impact the sample flow behaviour. However, their results suggested that the optimum calcium concentration for lateral flow coagulation measurement could lie in the range of 100 and 500 mM.

The impact of calcium concentration on coagulation rate was initially investigated using 15  $\mu\text{L}$  of normal plasma and 50  $\mu\text{L}$  of PT Reco 10 as the full optimization of reagent and sample volumes in Section 4.2.3 had not yet been completed. Here, 30  $\mu\text{L}$  of calcium at 100 to 500 mM was first deposited on the strips at the sample zone and, after drying, 50  $\mu\text{L}$  PT Reco 10 reagent was deposited. This equated to 3 to 15  $\mu\text{moles}$  of calcium. As shown in Fig. 4.6, plasma distance decreased with calcium concentration up to 400 mM (12  $\mu\text{moles}$ ) and then began to increase. 400 mM calcium concentration appeared

to give the fastest clotting rate and so led to the shortest travel distance ( $p=0.076$ ). There was, however, no statistically significant difference between the travel distances for 400 and 500 mM calcium concentrations ( $p=0.263$ ). Nonetheless, 400 mM was chosen to be the optimum calcium concentration.



**Fig. 4.6.** Effect of calcium concentration on plasma distance after 300 s on lateral flow strips. 50  $\mu$ L reagent volume, 30  $\mu$ L calcium chloride volume and 15  $\mu$ L sample volume ( $n=3$ ,  $p=0.076$ ).

The amount of calcium chloride used was again investigated, this time based on the optimised values of sample and reagent volumes (15 and 30  $\mu$ L respectively, Table 4.1) as set out above. In conjunction with this, a number of alternative assay strip design formats were investigated to improve sample flow, particularly to prevent the sample forming a droplet beneath the paper. Three designs were explored (Fig. 4.4) with configuration 4.4B appearing to allow the best control of sample flow and also prevent droplet formation beneath the strip (data not shown). This might also reduce the effect of sample evaporation since it reduces the exposure of the sample to the air. Wax based test strips were hence prepared according to the three designs shown. Strips were modified with the addition of a range of volumes of 400 mM calcium chloride, followed by deposition of 30  $\mu$ L PT Reco 10. Both calcium and the thromboplastin reagent were deposited at the sample zone of the strips. Normal and Severe Abnormal plasma samples (15  $\mu$ L) were added to the strips and the difference in sample distance between the two sample types expressed as the dynamic range.

As shown in Table 4.2, strip design Fig. 4.4B modified with 2 x 2.5  $\mu$ L calcium chloride solution gave an improved dynamic range of 6.0 mm. However, test strips with the wax

base at the sample zone alone (Fig. 4.4C) and supplemented in the same manner gave a slightly improved dynamic range (6.2 mm). This indicated that applying 2.5  $\mu\text{L}$  of calcium (400 mM) twice at the sample point, gave the optimal amount and location for the calcium. This could be because adding two layers may cause the calcium to become redistributed in gradients throughout the strip which may improve optimal mass interactions and lead to more efficient clotting. It could also mean that less calcium applied at the sample zone promotes clotting more than inhibit sample flow. The data also showed that strips with a wax base at the sample zone (Fig. 4.4C) was the preferred of the three strip formats investigated. The presence of a wax base layer at the sample zone increased the hydrophobicity on the underside of the strips which appeared to slow down the initial rapid flow of the sample upon its deposition and may have allowed greater interaction of the sample and reagents before permitting the sample to traverse the strip. In addition, strips with the fully wax base (Fig. 4.4B) tended to excessively restrict sample flow, while the original strips without a base (Fig. 4.4A) allowed the most rapid flow of the sample which could potentially reduce effectiveness of clotting reaction and lead to less robustness and precision. Therefore, the strip format Fig. 4.4C in combination with 2.5  $\mu\text{L}$  of 400 mM calcium chloride deposited twice that the sample zone was used for further development of the assay.

**Table 4.2.** *The effect of strip configuration and volume of 400 mM calcium chloride deposited on the assay dynamic range, as determined by the difference in distance travelled by Normal and Severe Abnormal samples in 300 s.*

Strip configuration	CaCl <sub>2</sub> (400 mM) volume ( $\mu\text{L}$ )	Dynamic range (mm)
Fig. 4.6b	4.5	3.50
	3.5	4.50
	2.5	5.50
	1.5	2.33
	2.5 x 2	6.00
Fig. 4.6c	2.5 x 2	6.17

#### 4.2.5 Investigation of the effect of thromboplastin reagent type

Thromboplastin reagents differ in source, preparation and composition and so differ in their sensitivity (Smith and Morrissey, 2004) and potentially will differ in their effect on the flow and coagulation kinetics of plasma samples on lateral flow assay strips. While PT Reco 10 had been used in the initial investigation and had already proven to work in the lateral flow prothrombin assay, it might not be the most ideal reagent for this assay format and hence the need to examine other thromboplastin reagents. Several

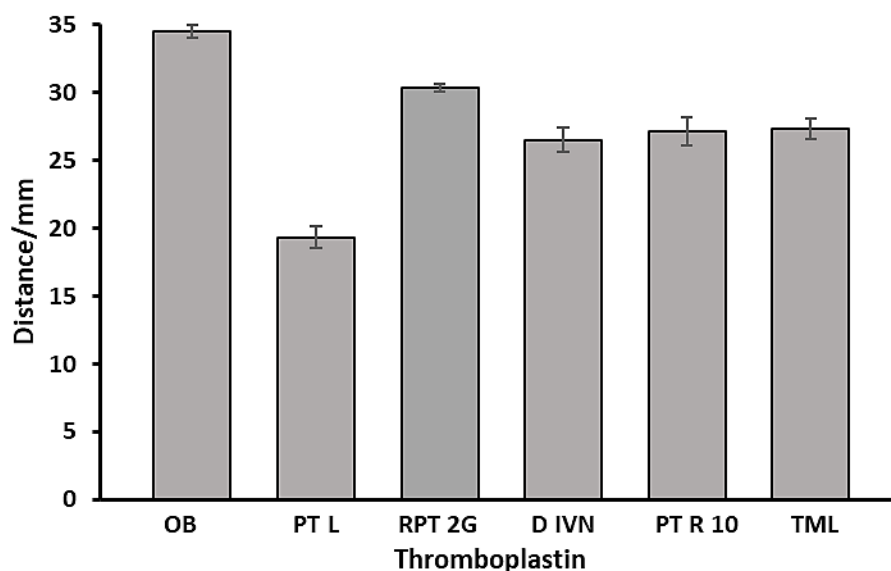
thromboplastin reagents, including PT Reco 10 were further assessed for application in this assay, with their corresponding sources and composition shown in Table 4.3.

**Table 4.3.** Properties of thromboplastin reagents investigated in this study.

Reagent type	Source	Composition	Format	Company
Thromboplastin L	Rabbit brain	Rabbit brain extract, saline, Ca <sup>2+</sup> , P, S	Liquid	Helena Bioscience
PT Reco 10	Recombinant	RHTF, Pls, S	Lyophilised + diluent containing Ca, NaN <sub>3</sub> ,	Horiba Medical
RecombiPlasTin 2G	Recombinant	RHTF, Pls, B, P, S	Lyophilised + diluent containing Ca <sup>2+</sup>	Instrumentation Laboratory
Dade ® Innovin	Recombinant	RHTF, Pls, Ca <sup>2+</sup> , B, S	Lyophilised, reconstituted with DW	Siemens
Thromborel ® S	Human placenta	HTF, Pls, CaCl <sub>2</sub> , S †	Lyophilised, reconstituted with DW	Siemens

† *Thromborel stabilizers: gentamicin (0.1 g/L), 5-chloro-2-methyl-4-isothiazol-3-one, and 2-methyl-4-isothiazol-3-one (<15 mg/L), RHTF = Recombinant human tissue factor, HTF = Human tissue factor, P = preservatives, S = stabilizers, B = Buffer, DW = Distilled water*

In the strip-based prothrombin assay, sensitivity tends to be reflected in the dynamic range, which is, in turn a function of both reagent potency and composition. In principle, the optimum thromboplastin reagent would be the one that has the greatest potency in triggering coagulation and has the least impact in obstructing sample flow. The reagents were initially assessed for their effect on the flow properties of an Owren's buffer sample. The distance travelled by the buffer in 300 s on strips modified with 30 µL of reagent are shown in Fig. 4.7. It seems the materials from animal sources have a lot of poorly soluble materials, while the synthetic ones have less of an issue in this regard. All the thromboplastin reagents obstructed the free flow of the buffer to some extent compared to a strip modified with buffer alone (34.5 mm). With the shortest sample distance (19.3 mm,  $p < 0.05$ ), compared to the of the rest of the PT reagents investigated, Thromboplastin L had the most obstructive effect on the buffer, which could be due to the fact that it originated from rabbit brain and could contain lots of insoluble impurities. Based on this data, Thromboplastin L could be considered the least ideal reagent for lateral flow prothrombin assay. RecombiPlasTin 2G had the least impact on the flow kinetics of the buffer, while Thromborel S (27.3 mm), PT Reco 10 (27.2 mm) and Dade Innovin (26.5 mm) were all similar in distance ( $p = 0.523$ ), suggesting they may all contain less insoluble impurities that could deter sample flow.



**Fig. 4.7.** Distance travelled by 15  $\mu$ L Owren's buffer after 300 s on strips modified with 30  $\mu$ L of different thromboplastin reagents: Owren's buffer (OB); Thromboplastin L (PT L); RecombiPlasTin 2G (RPT 2G); Dade Innovin (D IVN); PT Reco 10 (PT R 10); Thromborel S (TML) ( $p < 0.05$ ).

The thromboplastin reagents were further compared for their performance using the Yumizen G200 commercial coagulometer using normal, abnormal, and Factor VII-deficient plasma samples (Table 4.4). It should be noted that particular instruments are optimised to operate with particular reagents, and, in the case of the Yumizen G200, this is designed to operate with PT Reco 10. Any comparisons should be conscious of this fact. As expected, potentially due to their purity and potency, the recombinant thromboplastins: PT Reco 10 and Dade Innovin produced relatively low PT values for the normal control plasma of 8.9 s and 9.3 s, respectively. The RecombiPlasTin 2G, though expected to give a comparatively low PT value in normal plasma based on its origin as a recombinant type of thromboplastin, gave a slightly higher PT value of 11.1 s. This reagent could be less pure, more sensitive to factor levels, or contains more phosphatidylserine, a component that makes PT reagents less potent. The reagents based on tissue extracts such as Thromboplastin L and Thromborel S, both gave relatively long PT values for normal plasma of 13.0 s and 11.9 s, respectively. Among all of the reagents, Thromborel S gave the widest gap in PT values between normal and abnormal plasmas (16.8 s) followed by RecombiPlasTin 2G (12.8 s) and then Innovin (12.0 s). Thromboplastin L gave a gap of 10.6 s, while PT Reco 10 gave the least gap (8.2 s). This gap may potentially equate with the level of sensitivity that might be achieved in the lateral flow assay, but it is limited given that the abnormal plasma has small PT value and a plasma with a larger or no PT value at all like severe abnormal or deficient plasma is required for determining the dynamic range that caters for plasmas



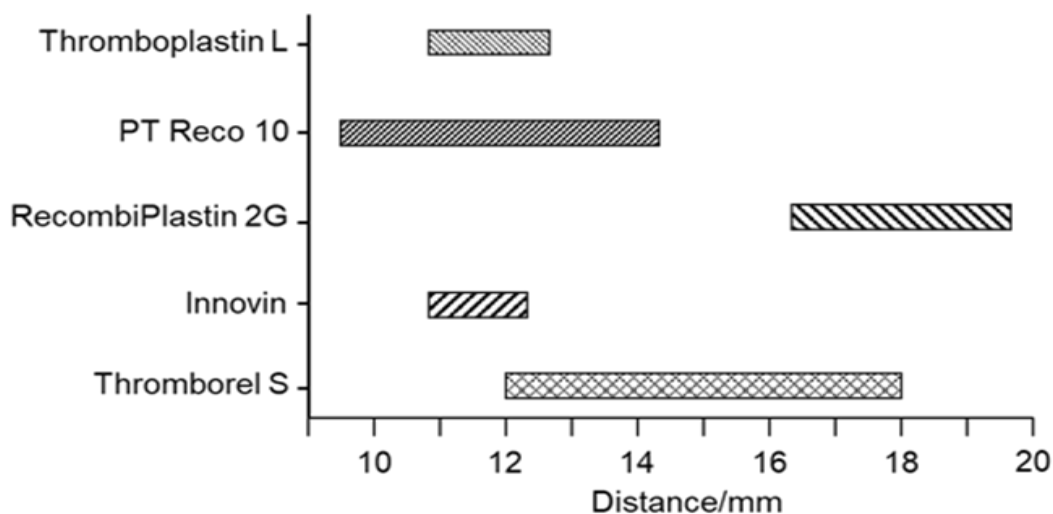
with wider range of PT values. With respect to the Factor-VII deficient plasma, all the PT reagents except the Thromborel S, did not return a clotting value. Factor-VII deficient plasma should result in a non-clotting response, and so the clotting value it produced with the Thromborel S reagent could be due a presence of an artifact within the reagent mixture that caused the plasma to clot, or an artefact of measurement on this instrument, for which the reagent was not designed. In short, based on the combined effects of potency and least impact on free sample flow, PT Reco 10 and Innovin appeared to be the competing candidates.

**Table 4.4.** PT and INR values for Normal, Abnormal and FVII-deficient (FVIID) plasmas measured using different thromboplastin reagents with Yumizen G 200, and their corresponding distances and dynamic ranges on assay test strips modified with 30  $\mu$ L of reagent.

Plasma sample	PT (s) and INR									
	Thromboplastin L		PT Reco 10		RecombiPlasTin 2G		Innovin		Thromborel S	
	PT	INR	PT	INR	PT	INR	PT	INR	PT	INR
Normal	13.0	1.34	8.9	0.93	11.1	1.15	9.3	0.97	11.9	1.23
Abnormal	23.6	2.39	17.1	1.75	23.9	2.42	21.3	2.16	28.7	2.89
FVIID	>200	>200	>200	>200	>200	>200	>200	>200	56.7	5.6
<b>Assay test strips, distance travelled (mm)</b>										
Normal	10.83		9.50		16.33		10.83		12.00	
Abnormal	11.50		11.33		18.00		11.17		16.67	
FVIID	12.67		14.33		19.67		12.33		18.00	
Dynamic range	1.8		4.8		3.3		1.5		6.0	

For the strip assay, using the optimised calcium chloride (400 mM, 2.5  $\mu$ L x 2), reagent (30  $\mu$ L), and sample (15  $\mu$ L) volumes, the five thromboplastin reagents were examined for the overall dynamic range achievable using normal, abnormal, and Factor VII-deficient control plasmas (Table 4.4). In this case, the five reagents were assessed in terms of the gap in distance between the normal clotting plasma and the non-clotting Factor-VII deficient plasma. With respect to the non-clotting plasma whose travel distance was mainly dictated by the reagent's physical properties, Thromboplastin L and Dade Innovin had a strong impact in limiting the flow of the FVIID plasmas, which would significantly limit the achievable dynamic range. The PT Reco 10 had an intermediate impact, while Thromborel S and RecombiPlasTin 2G had very minimal impacts and thus allowed the furthest travel of the non-clotting plasma, with RecombiPlasTin 2G exhibiting the largest distances. However, RecombiPlasTin 2G did little to bring about the early arrest of flow in the normal clotting plasma, thus exhibiting a narrow dynamic

range (3.3 mm). Although the PT Reco 10 showed the largest impact in limiting the flow of the normal plasma, Thromborel S elicited the widest dynamic range (6.6 mm) in the strip assay even though it did show clotting in the Factor-VII deficient plasma with the Yumizen G200 analyser. Innovin, unexpectedly exhibited the least dynamic range (1.5 mm) followed by Thromboplastin L (1.8 mm) while PT Reco 10 gave the second widest (4.8 mm). A graphical representation of the dynamic ranges elicited by the various thromboplastin reagents in the strip assay is shown in Fig. 4.8. Thromborel S, with a wider dynamic range over that of PT Reco 10, was chosen for further development of the strip PT assay. It was interesting to see that Thromborel S emerged the best, even though it is a tissue extract. This could be because it is refined and formulated which probably removed most of the impurities commonly found in tissue extracts. The sample and reagent volumes were re-optimised for use with respect to Thromborel S. However, the maximum dynamic range remained 6.0 mm with the previously determined optimum values of these parameters of 15 and 30  $\mu\text{L}$ , respectively, and which were employed for further assay development.



**Fig. 4.8.** The distance ranges determined by the difference in distance travelled by 15  $\mu\text{L}$  of a normal control versus a Factor VII-deficient plasma on assay strips modified with 30  $\mu\text{L}$  different thromboplastin reagents.

#### 4.2.6 Determination of optimised lateral flow prothrombin assay in calibration plasmas

Following optimisation of the assay device parameters of paper type (Whatman No. 1), strip configuration (Fig. 4.4C), reagent type (Thromborel S), reagent volume (30  $\mu$ L), calcium chloride concentration and volume (2 x 2.5  $\mu$ L 400 mM), reagent deposition parameters and sample volume (15  $\mu$ L), the analytical performance of the assay was determined in normal, abnormal, and severe abnormal control plasma standards. The control plasmas used in the development of the assay differ in the levels of clotting factors they contain so that they can simulate a range of clotting times (Diagnostics Reagents Ltd., 2022). Normal plasma is a lyophilised platelet poor plasma containing the clotting factors at normal level. The abnormal and severe abnormal control plasmas are lyophilised platelet poor plasmas with artificially depleted levels of clotting factors. Abnormal plasma contains less while severe abnormal plasma contains even lesser level of clotting factors than normal plasma. In addition to these plasma standards, factor-deficient plasmas are also available. For example, Factor-VII deficient plasma is an immunodepleted platelet poor plasma that contains the clotting factors at normal level except for Factor-VII which is at low or undetected level and would be insensitive to tissue factor activation. These plasmas are commercial formulations which also contain stabilisers and preservatives which may differ between plasma types. The different preparation procedures, composition and factor levels could potentially influence plasma viscosity and hence result in inconsistencies in the distances travelled by the samples that was not due to coagulation, but due to differences in viscosity.

Prior to final analytical characterisation and validation of the assay, it was necessary to determine that the plasma controls did not cause significant non-clotting variations by assessing their behaviour on test strips modified with thromboplastin and controls which were modified with Owren's buffer only. As indicated in Table 4.5, the plasmas did not significantly differ in distance on the control strips ( $p=0.707$ ), being between 21.0 and 22.8 mm while they differ very significantly on the test strips ( $p=0.003$ ), increasing in distance from 12.3 mm (normal plasma) to 18 mm (severe abnormal plasma). The minor differences in distance on the control strips did not show any pattern, meaning it was due to random variations in sample flow pattern. Since it contains a lesser amount of coagulation factors, severe abnormal plasma might be expected to be less viscous than both normal and abnormal plasma, and therefore should cover a longer distance than the other two on control strips. Instead, it travelled similar if not a shorter distance (21.0

mm) than both the normal and abnormal plasmas (21.2 and 22.8 mm, respectively). Furthermore, the differences in distance on the control strip compared to those on the test strip, decrease proportionally from normal to severe abnormal, strongly suggesting that the plasma samples were suitable for assay characterisation.

**Table 4.5.** Distances travelled after 300 s by 15  $\mu$ L plasma samples on control (modified with 30  $\mu$ L Owren's buffer) and test (modified with 30  $\mu$ L Thromborel S). N = Normal, A = Abnormal, SA = Severe abnormal, FVIIID = Factor-VII deficient.

Plasma	Control strips (mm)	Test strips (mm)	Difference (mm)	PT (s)
N	21.2	12.3	-8.9	11
A	22.8	16.3	-6.5	19.4
SA	21.0	18.0	-3.0	35.7
FVIIID	21.5	18.0	-3.5	> 120

Having confirmed the suitability of the plasma controls, the analytical performance of the optimised assay was determined (n=4 repeats). As can be seen in Table 4.6, the CV was 5.27% for normal plasma and rising to 9.35% for severe abnormal. It is well-established that increase in mean clotting time is also accompanied by increased variability (Sunnersjö *et al.*, 2023). A 95% confidence interval of 0.65 mm was also determined for the normal plasma, rising to 1.65 mm in the severe abnormal.

**Table 4.6.** Distances of 15  $\mu$ L normal, abnormal, and severe abnormal control plasma samples after 5 min on strips optimised with 30  $\mu$ L Thromborel S, and 2 x 2.5  $\mu$ L 400 mM  $CaCl_2$  (n=4, p=0.003).

Plasma	Mean distance (mm)	SD (mm)	CV (%)	95% CI
Normal	12.3	0.6	5.27	0.63
Abnormal	16.3	1.0	6.41	1.02
Severe abnormal	18.0	1.7	9.35	1.65

Based on mean distance, 95 % CI, and PT values and their ranges, the relationship between lateral flow prothrombin assay distance and PT values were determined (Table 4.7). The normal plasma with a PT range of 8.5 to 14 s had a corresponding distance range of 10 to 14 mm, abnormal plasma with 15.0 to 30.0 s, has a distance range of 14.5 to 17.5 s, while severe abnormal plasma with PT values >30 s had travel distances  $\geq$ 16.0 s. Hypercoagulable plasmas (Low) would have distances <10 mm and PT <8.5 s, those with between 10 and 14 mm are normal while those with distances  $\geq$ 14 mm would be abnormal or prolonged.

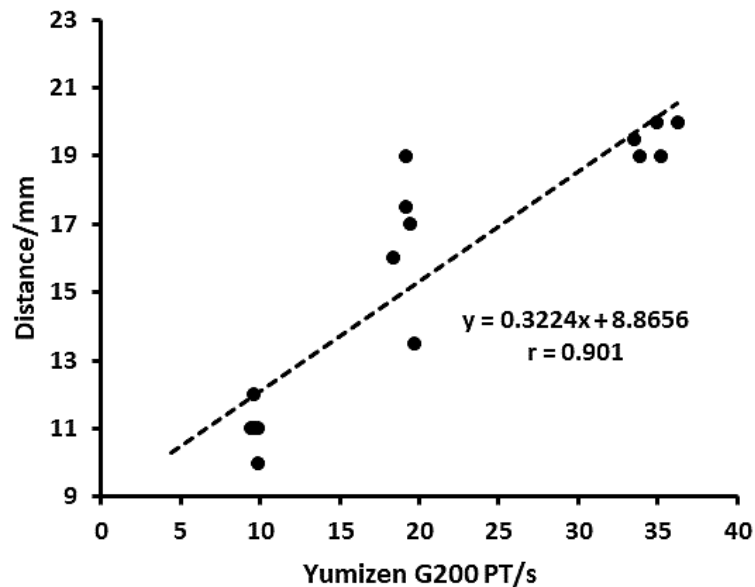
**Table 4.7.** Comparison of lateral flow prothrombin assay distance ranges and PT values across a range of clotting times.

<b>Plasma</b>	<b>Distance range (mm)</b>	<b>PT (s)</b>
Low	<10.0	<8.5
Normal	10.0 - 14.0	8.5 – 14.0
Abnormal	14.5 - 17.5	15.0 – 30.0
Severe Abnormal	≥16.0	>30.0

Again, it is important to note that these distance ranges are subject to operational conditions, mainly temperature and humidity as well as batch of paper substrate used. Each batch of Whatman chr no 1 paper used as substrate would require calibration.

#### **4.2.7 Validation of the paper-based lateral flow prothrombin assay device**

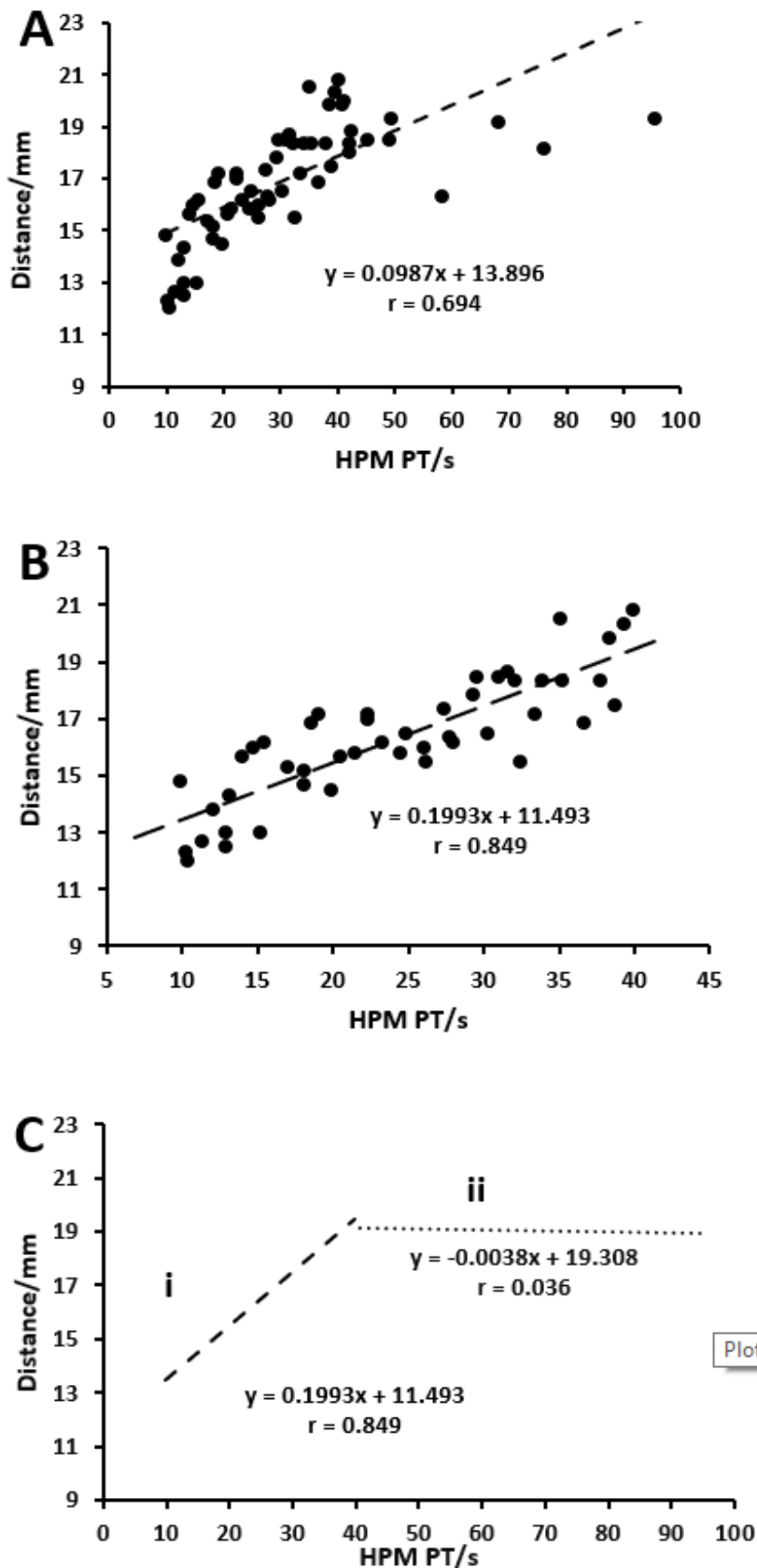
The paper-based lateral flow prothrombin assay device was initially evaluated against the Yumizen G200 analyser using artificially constructed commercial plasmas samples. Fifteen lyophilised artificial control plasma samples with varying clotting capacities were reconstituted and tested using the paper-based strip assay. The travel distances of the plasmas were compared with their corresponding PT values (9.8 to 36.0 s) as determined with the Yumizen G200. As shown in Fig. 4.9, there was a good correlation ( $r=0.901$ ) between the developed assay and the reference Yumizen method with linear expression of  $y = 0.3224x + 8.866$ . Furthermore, all of the normal plasma samples had mean travel distances that fell within the normal distance range (9.5 to 14 mm), and those of the abnormal plasma samples fell above the normal distance range (>14 mm). However, there was a considerable variation in the distance values for the plasmas with moderately prolonged (17 to 20 s) PT values. This could be because the coagulation rate is not fast enough to give more precise results and also not slow enough to be impacted more by environmental conditions such as humidity which tend to normalise the travel distance of severely abnormal plasmas.



**Fig. 4.9.** Validation of the paper-based lateral flow device for PT assay using artificial plasma samples ( $n=3$  repeats) with PT values 9.8 to 36 s, comparing results from the paper device (mm) and Prothrombin Time (s) from the Yumizen G200 analyser.

The device was further validated against a routine hospital method using clinical plasma samples. Sixty patient plasma samples, with a wide range of PT clotting values (9.8 to 95.4 s) were taken at Southmead Hospital, North Bristol NHS Trust and tested with the device ( $n=3$  repeats) and the measured distances compared with their corresponding hospital determined PT values (Fig. 4.10A). The entire data set gave a linear regression expression of  $y = 0.0987x + 13.896$  and a correlation coefficient of  $r = 0.694$ . This low regression value could be because the travel distance of plasmas with very large PT values tends to be impacted more and somehow normalised by humidity/sample evaporation.

Further analysis of the data (Fig. 4.10B) revealed that the developed assay correlated well for PT values at 40 s and below. For these plasma samples, the paper-strip assay showed improved correlation ( $r=0.849$ ) between plasma distance on test strips and the PT values from the hospital method. For plasmas with PT values above 40 s (Fig. 4.10C, ii), there was no statistically significant correlation ( $r=0.036$ ) with the hospital method. This could be because for plasmas with significantly prolonged PT values, the effect of ambient environmental conditions such as temperature and humidity were greater on travel distance. It could instead be because while the hospital-based PT method has no upper limit of measurement, the lateral flow assay is limited by the overall sample volume and the maximum distance it may travel along the strip.



**Fig. 4.10.** Validation of the paper-based lateral flow device for PT assay using clinical plasma samples, comparison between paper-based device and the hospital method ( $n=3$  repeats) for A) plasmas with PT values 9.8 to 95.4 s. B) plasmas with PT values  $\leq 40$  s ( $n=3$ ). D) (i) PT values  $\leq 40$  seconds and (ii) PT values  $\geq 40$  s.

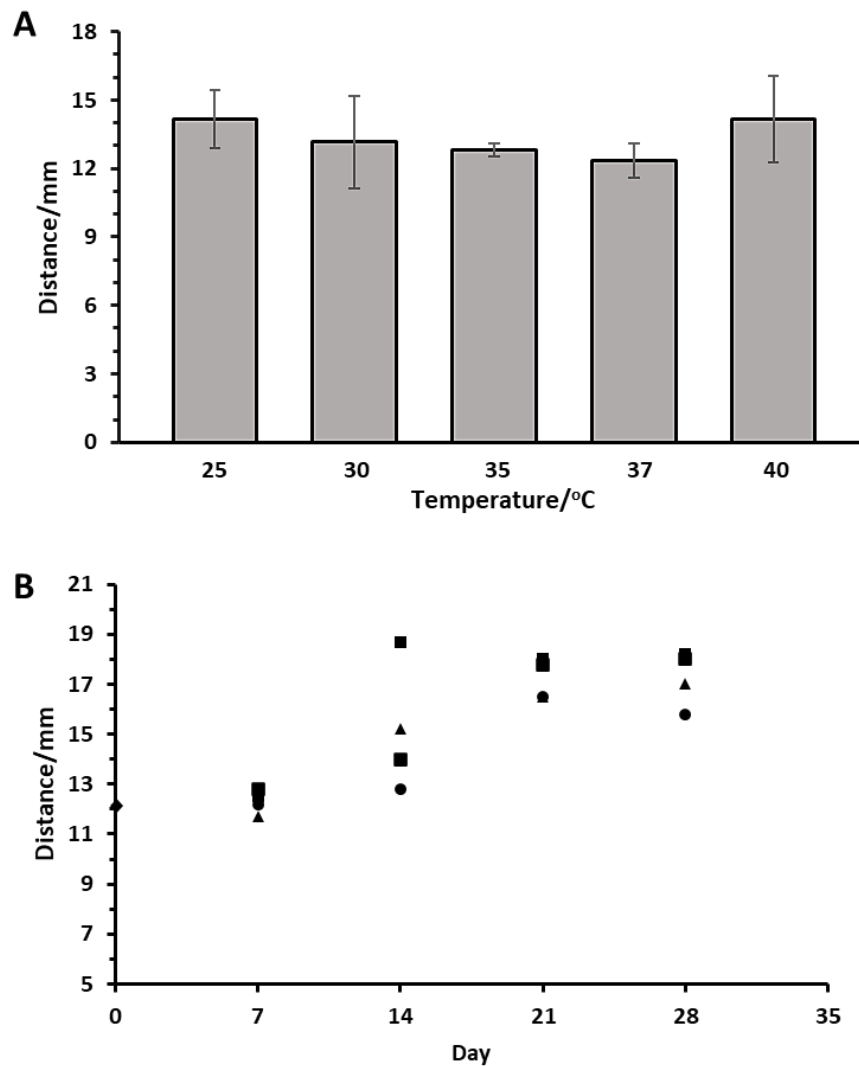
Considering the data for both artificial and patient samples, the distances for over 90% of all of the normal plasmas fell within the normal range (9.5 to 14.0 s) and over 98% of those of the abnormal plasmas fell above the normal range (>14.0 s). This signified a satisfactory performance of the strip assay in distinguishing normal plasmas from abnormal ones based on their thromboplastin-triggered clotting abilities.

#### **4.2.8 Investigation of the storage and operational stability of the prothrombin assay device**

The prothrombin assay involves a series of enzymatic reactions triggered by tissue factor which leads to the formation of the fibrin clot. The rate of these enzymatic reactions is directly related to the rate of clot formation, which in turn is directly related to the increase in plasma viscosity due to clotting. Viscosity and enzyme reaction rates which determine assay behaviour are both a function of temperature. While the assays are developed and performed at 37°C, which is optimum for coagulation, actual environmental operational conditions may vary if deployed in the field. Furthermore, temperature may affect the stability and long-term viability of the tissue factor and phospholipids. Hence it was necessary to assess the operational stability of the assay device with respect to temperature and the viable life of the assay strips based on storage conditions.

With regards to operational stability, the device was tested with normal plasma at various temperatures, 25 to 40°C and the mean travel distances assessed with respect to the normal operational range (10 to 14 mm, 37°C). As shown in Fig. 4.11A, while there were no significant differences in distance with respect to temperature at this sample size ( $p=0.448$ ), the apparent trend was consistent with enzyme reaction kinetics with an optimum at 37°C (Jeppesen *et al.*, 2016), i.e., decreases from 25 to 37°C and then increased at 40°C which could be attributed to increased and decreased reaction rates, respectively. The optimal temperature was 37°C and beyond that, enzyme-catalysed reactions tend to slow down which slows the clotting rate, leading to a longer distance.





**Fig. 4.11.** Effects of operational and storage temperature on assay device behaviour. Distances of normal control plasma at 300 s with operation of the optimised assay at: (A) different temperatures, and (B) at 37°C following storage at -20°C (circle), 6°C (ex-sign), ambient (triangle) and 37°C (square) for up to 28 days (n=3).

A similar trend was observed in the case of the fibrinogen assay (Section 3.2.7), although the prothrombin assay has a longer chain of enzymatic reactions than the fibrinogen assay, which is predominantly dependent on thrombin activity. These variations in assay behaviour due to temperature could be addressed by using multiple temperature-dependent graduation ranges, or simultaneously running known and unknown plasma controls in a multiple assay format as calibrators.

In the investigation of storage and active life of the assay strips, the strips were covered with folded papers, vacuum sealed with a sachet of desiccant and stored under various conditions of freezer (-20°C), fridge (4 to 6°C), ambient (18 to 23°C) and elevated temperature (37°C). After every week for four weeks, strips from each storage condition were removed and tested with normal plasma for their response (Fig. 4.11B). On the

seventh day, all the strips appeared to have remained active and produced results that fell within the reference range and did not differ significantly in distance from fresh strips ( $12.3 \pm 0.8$ ,  $p=0.945$ ). On the fourteenth day, only strips stored in the fridge and freezer remained viable and did not differ in distance from fresh strips ( $p=0.616$ ), with strips from other storage conditions deviating from the reference range and distance on fresh strips ( $p=0.020$ ), with the magnitude of deviation proportional to storage temperature. On days 21 and 28, strips from all of the storage conditions were essentially no longer functional i.e., they all differ in distance from fresh strips ( $p=0.041$ ) and also fall outside the reference range (10 to 14 mm). This indicated that the most appropriate storage temperature evaluated was 6°C or below and if stored under those temperatures, the strips could remain active for two weeks. However, for longer storage, additional development would be required to prevent loss of reagent activity over time and will relate to the stability of both tissue factor and phospholipids. There are approaches that could be used to improve the stability of dried assay reagents (Rechner, 2009) which could be used to address the long-term storage issue. Individual, or combinations of excipients such as dextran trehalose, polyethylene glycol (Kumar *et al.*, 2020), could be either added to assay reagents directly before deposition on test strips or to the test strips before drying and storage. Also, the test strips could be freeze-dried, stored at low temperatures, and tested for stability over weeks or months.

Compared to POC coagulation testing devices on the market such as CoaguCheck® XS (Roche Diagnostics Cooperation), CoagMax (Microvisk Ltd), and Hemochron Signature (Werfen), the method developed in this work was less precise but far cheaper as it requires low-cost materials and fabrication techniques, no power or instrument-based detection/readout with low reagent and sample volume needed in testing. Compared to polymer-based lateral flow coagulation testing devices in the literature (Dudek *et al.*, 2010; Dudek, *et al.*, 2011), this device is much more environmentally friendly as it uses biodegradable disposable cellulose-based strips. For the paper-based devices developed previously, (Anubhuti and Shantanu, 2020; Guler *et al.*, 2018; Hegener *et al.*, 2017), the device developed in this work was more compact and, because it did not require power or instrumentation, should be better suited to POC testing in low resource settings.

### 4.3 Conclusion

A paper-based lateral flow prothrombin assay device employing a visual distance-based readout format was developed in this work. The device showed a good correlation with a reference Yumizen G200 method ( $r=0.901$ ) for artificial plasma samples; and a routine hospital method ( $r=0.849$ ) for clinical plasma samples with PT values  $\leq 40.0$  s. However, the device could not produce exact precise PT values, but, with replicate measurements ( $n=3$ ), it could successfully distinguish plasmas with normal PT values from those with abnormal PT values based on their travel distances on test strips. Moreover, the assay used minimal sample and reagent volumes with disposable and sustainable paper test substrates, thus it is potentially low cost, more environmentally friendly, and less demanding on patients than many established prothrombin assays. Furthermore, it has a short turnaround time (5 min) and was easy to operate, making it potentially suitable for point-of-care use. When packaged with a desiccant, vacuum sealed and stored at  $\leq 6^{\circ}\text{C}$ , the test strips could remain active for two weeks, and, with further development, may make it field deployable.

The assay results, however, are susceptible to fluctuations in operational conditions such as temperature and humidity. This could be addressed using multiple temperature dependent reading scales or testing known samples alongside unknown samples and determining the unknown value from the ratio of travel distances. The durability of the assay strips can also be extended via dry enzyme assay reagent stability techniques. The device may not give accurate results for plasmas with very low or very high viscosities.

## **5. INVESTIGATION OF PLATELET AGGREGATION ON PAPER-BASED LATERAL FLOW STRIPS**

## 5.1 Introduction

Platelets are anucleate cytoplasmic fractions that play a central role in normal haemostasis. They adhere to exposed subendothelial tissue at an injured site via their surface receptors GP I<sub>B</sub>/IX, and via  $\alpha$ 1 $\beta$ 2 and GPVI with the help of vWF. The activated platelets then release ADP and thromboxane A<sub>2</sub> which further enable more platelets to be recruited and aggregated at the site via the GPIIb/IIIa receptors, mediated by fibrinogen. The aggregated platelets form a primary haemostatic plug, slow down bleeding to reduce blood loss and also provide a procoagulant surface for the formation and deposition of fibrin clot to effectively stop bleeding. Platelets also contain coagulation factors which they release to promote secondary haemostasis; as well as platelet derived growth factor (PDGF) which stimulates wound healing (Hoffbrand and Steensma, 2019).

Defects in platelet function usually stem from problems with platelet receptors which lead to the impairment of adhesion, or in the release reaction which causes impaired aggregation. Quantitative platelet disorders include low platelet count (thrombocytopenia) or high platelet count (thrombocytosis). Each of these disorders may result in either haemorrhage or pathologic thrombosis, respectively. Platelet function tests are used to evaluate the capacity of platelets to function adequately in terms of adhesion, aggregation, release-reaction, and wound occlusion. They are used to detect platelet dysfunction, monitor anti-platelet therapies, manage preoperative haemostasis and in platelet banking for making concentrates and for transfusion (Paniglia *et al.*, 2015). The bleeding time test was the first test to assess the ability of platelets to form the primary haemostatic plug in response to injury by measuring the time it takes for a skin puncture to stop bleeding. Others such as light transmission aggregometry measure the ability of platelets to aggregate in response to exposure to agonists such as ADP, arachidonic acid, epinephrine, and collagen. Other methods such as flow cytometry assess platelet function by measuring certain substances e.g., nucleotides released by functional platelets (Paniglia *et al.*, 2015) as well as platelet GP number and dysfunction.

A number of platelet function tests are currently in existence such as PFA-100/200, Impact, Thromboelastography, VerifyNow, Multiplate and Microparticles (Choi *et al.*, 2014). However, almost none of these are particularly ideal for low resource areas which lack lab facilities, expertise, and affordability. The bleeding time is simple and inexpensive, but it is considered invasive, less effective, and difficult to standardise. The

advanced, and more effective methods are expensive and technically demanding and so are less affordable and sustainable in resource constrained areas. The aim of this study was to explore the behaviour of activated platelets in influencing fluid flow mechanisms in paper-based lateral flow platforms with a view to setting a foundation for developing simple, low-cost platelet function tests suitable for low-resource regions. Changes detected in fluidic flow due to the behaviour of activated platelets might form the basis of tests for detecting qualitative or quantitative platelet dysfunction.

As has been illustrated in Chapters 3 and 4, coagulation assays that involve the flow of a sample in a paper-based lateral flow strip have utilised passive movement of fluid by capillary action from the sample zone to the analytical/detection zone. The sample fluid wets and flows over a network of cellulose fibres, through its microporous network along a fluidic channel to a point determined mainly by the properties of the paper strip, immobilised reagent on the strip, inherent properties of the sample, and the sample volume. In assays of platelet aggregometry, the process of aggregation is brought about by the addition of an agonist reagent. It could be hypothesised that platelets in a plasma sample exposed to agonists deposited on a paper strip would become activated, adhere, and aggregate in the paper matrix which would influence fluid flow in a way that could translate into a reduction in the flow rate of the sample, and that the magnitude of reduction in flow rate would be an indication of platelet function or platelet count. The main challenge here was the very small volume fraction of platelets (<0.25%) in the sample (Pogorzelska *et al.*, 2020) which might make it difficult for platelet adhesion/aggregation to significantly influence the sample flow behaviour.

To test this idea, the study involved investigating fluidic flow behaviour on agonist-modified paper strips to identify the effect of platelet aggregation, to enhance this effect by optimising the type and amount of agonist, sample matrix/media, and sample volume and then testing performance in detecting platelet dysfunction simulated by the use of an anti-platelet agent.

The paper strips used in this investigation were similar to that used in the prothrombin assay development (Chapter 4, Fig. 4.4C). They had a sample deposition point (5 mm diameter) and a fluidic flow/analytical channel (3 x 40 mm) with a wax outer boundary on the front surface and wax base covering the sample deposition zone on the back surface. However, the analytical channel of the strips used here was slightly longer than that of those used in the prothrombin assay development. This was because the platelet suspensions in TBS used as samples in the initial investigations were less viscous and

tended to flow faster and cover longer distances than the plasma samples used in prothrombin assay development. The back surface of the strips was coated with wax in a similar manner to the prothrombin assay to reduce the initial rapid flow caused by the sample deposition process.

The agonists investigated here as potential platelet function assay reagents included epinephrine, adenosine diphosphate (ADP), collagen, and arachidonic acid. Each of these agonists can effectively activate platelets. However, they differ in structure, molecular weight, mode of action, potency, and other properties relevant to performance of this assay, particularly hydrophobicity, which might affect their suitability for use in this assay.

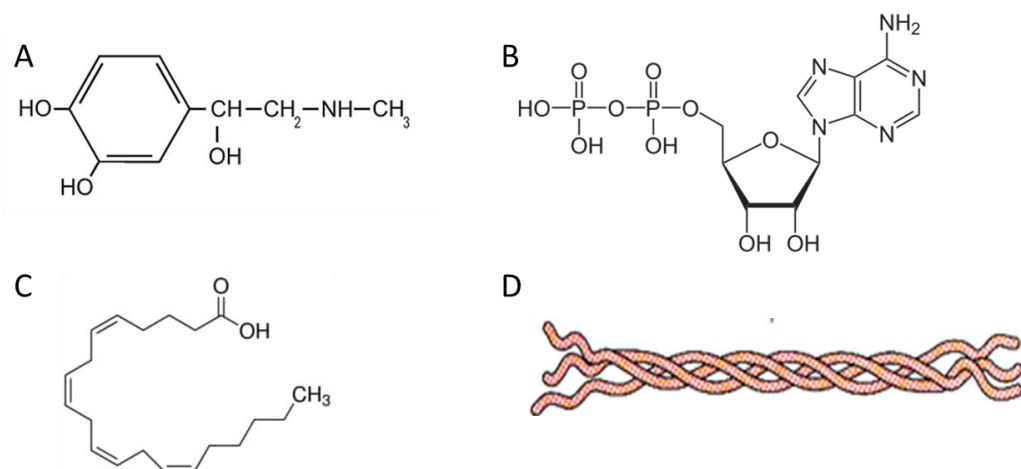
Epinephrine, also known as adrenalin, is an organic compound comprising a catechol ring and a two-carbon chain that bears a hydroxyl group and a secondary amine with a methyl group (Fig. 5.1A). It is a white microcrystalline solid with a chemical formula of  $C_9H_{13}NO_3$  and molecular mass of 183.20. It is a hormone and neurotransmitter produced by adrenal glands with many biological functions including platelet activation. Epinephrine is not actually considered a direct platelet activator or aggregating agent, but rather it potentiates the actions of the other agonists in secretion, aggregation, and fibrinogen binding, etc. It does this by interacting with  $\alpha_2$ -adrenergic receptors which potentiate the aggregatory responses induced by the other aggregating agents (Lanza *et al.*, 1988).

ADP is an organic compound composed of an adenine ring, a ribose sugar, and two phosphate groups. The adenine ring is connected to the ribose sugar molecule which is connected to the phosphate groups (Fig. 5.1B). It has a molecular mass of 427.201 and a chemical formula of  $C_{10}H_{15}N_5O_{10}P_2$ . It is slightly soluble in water and organic solvents such as DMSO and methanol and has many biologically active properties including production of adenosine triphosphate (ATP) and activation of platelets. ADP is mainly produced from dense granules of activated platelets and acts to activate and recruit more platelets to aggregate at the wound site. It activates platelets by binding to platelet receptors (P2Y1, P2Y12, and P2X1) which induces shape change, aggregation, and production of thromboxane  $A_2$  (another platelet agonist). Shape changes in platelets expose fibrinogen receptors (GP IIb/IIIa) on platelets surface, enabling aggregation and adhesion with the help fibrinogen acting a bridge (Jin *et al.*, 2002).

Collagen is a structural protein composed of three polypeptide chains each of which contains a series of three amino acid sequences that begins with glycine. It forms a

major component of the extracellular matrix, with flexible mechanical properties for handling stresses and binding sites for cell interactions. There are about twenty-eight different types of collagen in humans which include type I, type II and so on among which, type I and III are the most relevant given that they are the major constituent the extracellular matrix of blood vessels (Nieswandt and Watson, 2003). In the context of haemostasis, collagen acts both as a substrate for platelet adhesion and as a platelet activator. In vivo, upon exposure, platelets adhere to collagen via integrin  $\alpha 2\beta 1$  receptors, allowing the platelets to interact with the low affinity GPVI on collagen which then activates the platelets. GPVI-platelet interaction causes biochemical reactions which activate phospholipase  $Cy2$  and subsequently, production of 1,2-diacylglycerol, and calcium from dense granules. Calcium and 1,2-diacylglycerol are mediators in platelet activation responses including shape change, secretion, and aggregation. Collagen induced platelet activation is also believed to proceed via its production of thromboxane  $A_2$  (Roberts *et al.*, 2004).

Arachidonic acid is an  $\omega$ -6 polyunsaturated fatty acid with a chemical formula  $C_{20}H_{32}O_2$  and a molecular mass 307.467. As shown in Fig. 5.1C, it has a carboxylic acid group and a twenty carbon long chain with double bonds at positions 5, 8, 11, and 14. It is found incorporated in phospholipids in cell membranes and lipid bodies of immune cells. Through sequential oxygenation, arachidonic acid is converted into thromboxane  $A_2$  by cyclooxygenase-1 and thromboxane  $A_2$  synthase. Thromboxane  $A_2$  is a potent platelet activator that acts by interacting with and activating its receptor on platelets, which induces shape changes and release reactions and eventually recruitment and aggregation of more platelets (Jin *et al.*, 2002).



**Fig. 5.1.** Molecular structure of the agonists, A) epinephrine, B) adenosine diphosphate, C) arachidonic acid, D) schematic of triple helix of collagen fibre.



Each of these platelet agonists discussed and used in this study are used in other methods for clinically testing platelet function, or in research to study platelet behaviour and mechanism of activation in response to them. Other platelet activators not used in the study include thrombin and ristocetin. Thrombin is a very potent platelet activator, but it would also cause fibrin clot formation which would make it difficult to isolate and quantify the effect of platelet aggregation. Ristocetin could potentially be used but has to be used along with vWF.

Different buffers and media are used in platelet function tests. The media that will most closely mimic the natural physiological environment of platelets would be plasma and the most appropriate sample would be a platelet rich plasma. However, in platelet function testing, the plasma or some of its components are not compatible with the detection method. This makes it necessary for the platelets to be extracted from the plasma, washed, and then resuspended in a more compatible media. The buffers often used as platelet suspension media include TBS, and PBS. Also, the most appropriate sample for investigating platelet behaviour would be fresh PRP. However, due to the associated challenges of collecting fresh PRP, commercial lyophilised platelets were used to research their behaviour on the strips, initially resuspended in buffer and then progressively using commercial platelet poor calibration plasma as the resuspension medium to better mimic the behaviour of real samples.

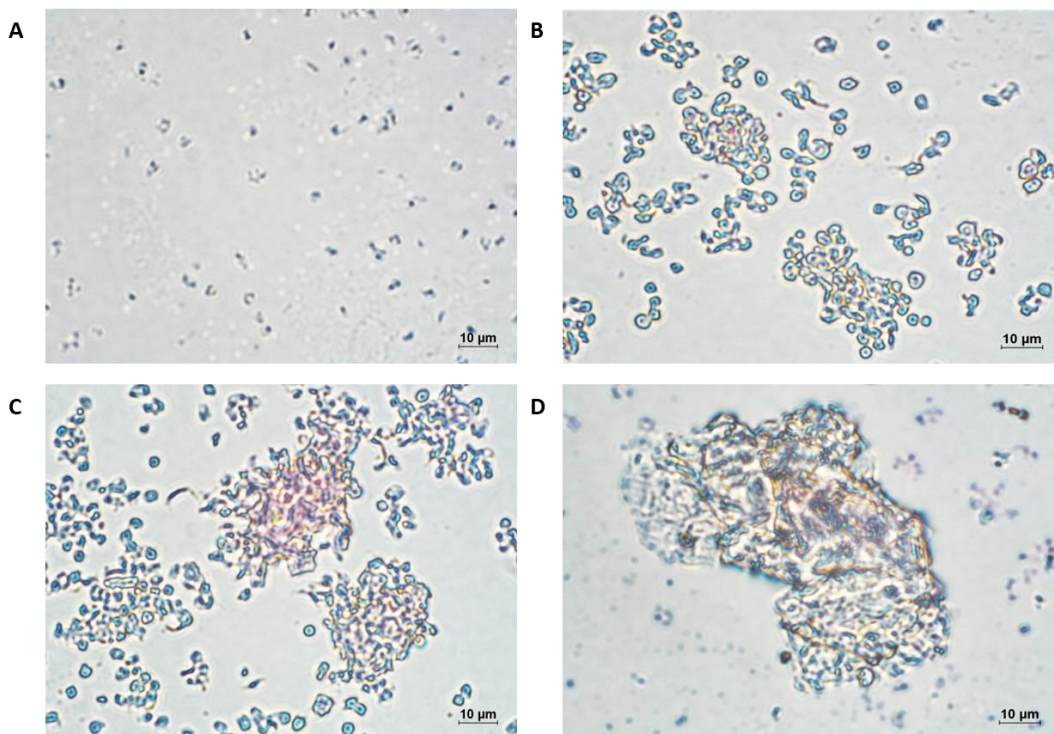
The potential for platelet suspensions to become activated in the presence of agonists was explored, optimised according to a range of test parameters and quantified with respect to changes in flow rate. A measure of the contribution of platelet aggregation as opposed to other effects such as viscosity differences and strip wetting effects was developed, which was referred to as the Aggregation Effect.

The validity of the concept of the Aggregation Effect was tested both quantitatively with respect to platelet count, and qualitatively with respect to platelet function, when inhibited using aspirin. Initial evidence suggests that, while the contribution to aggregation is small, it demonstrates a potential foundation for measuring platelet aggregation using paper-based devices.

## 5.2 Results and discussion

### 5.2.1 Study of lyophilised platelet viability using staining and light microscopy

Investigation of platelet behaviours on lateral flow paper strip could be conducted using any viable platelet samples including lyophilised and fresh PRP. For early exploration, it was decided to use lyophilised platelets since they are more readily available and do not require blood donors, sample collection and processing, which could delay progress. Commercial lyophilised platelet samples were reconstituted according to manufacturer's instruction and used in this study. Consequently, it was necessary to test and confirm that these platelets were in fact active and functional and were capable of activation and aggregation responses to the addition of agonists. Aliquots of 450  $\mu\text{L}$  lyophilised platelets reconstituted in TBS ( $586 \times 10^9/\text{mL}$ ) were treated with 50  $\mu\text{L}$  of agonists ADP (200  $\mu\text{M}$ ), epinephrin (3 mM), collagen (100  $\mu\text{g}/\text{mL}$ ) or TBS and incubated at 37°C for 3 min. Smears of the platelet samples were prepared on glass slides, fixed with methanol, and stained with eosin. After thorough air drying, the glass slides were evaluated for platelet aggregation using a light microscope. As shown in Fig. 5.3, platelet aggregation could be seen in all the treated samples and for all the agonists used, thus confirming that the platelets were functional. Little if any aggregation was seen on the control which could be due to sample agitation during sample preparation and straining.



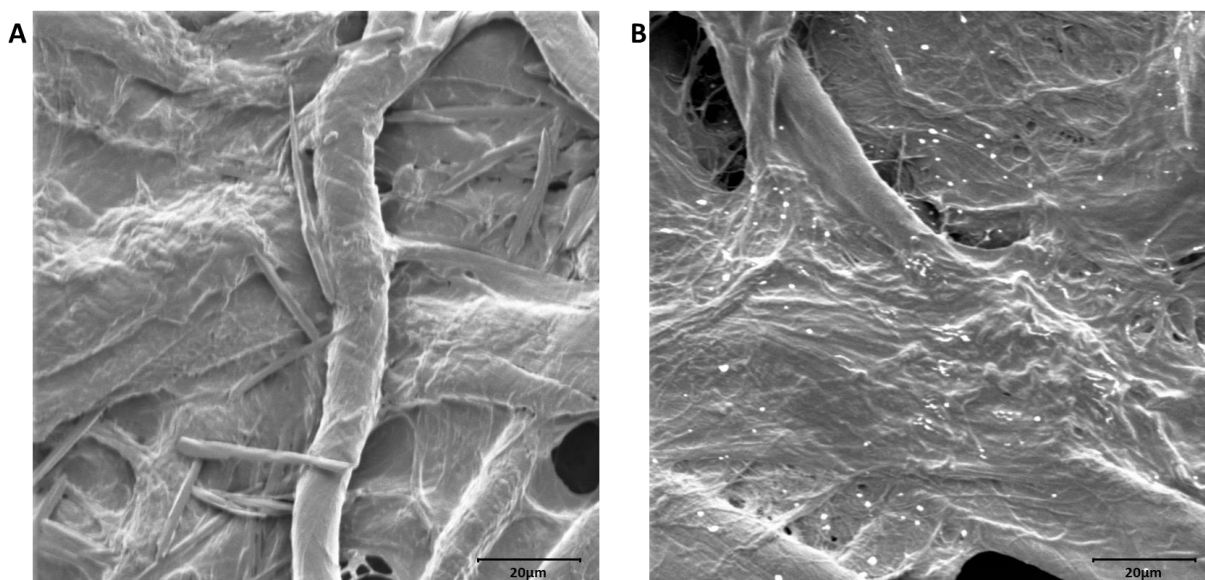
**Fig. 5.3.** Aggregation of platelets on glass slides. 450  $\mu\text{L}$  of lyophilised platelets reconstituted in TBS buffer to about  $586 \times 10^9/\text{mL}$  and treated with 50  $\mu\text{L}$  of A) no agonist, B) 3 mM epinephrine, C) 200  $\mu\text{M}$  ADP, D) 100  $\mu\text{g}/\text{mL}$  collagen. Magnification  $\times 1,000$ .

### **5.2.2 Study of platelet adhesion and aggregation on test strips using light and electron microscopy**

As explained in Section 5.2.1 and shown in Fig. 5.3, the viability and functionality of the commercial lyophilised platelets in response to agonists was tested and confirmed. However, the mere viability of the platelets could not serve as evidence that the platelets would adhere and aggregate on assay strips and influence sample flow dynamics. Visual qualitative evidence showing aggregated platelets on strip surfaces would be more convincing evidence that the observed changes in sample flow were in fact due to aggregation effects.

An attempt was made to study platelet aggregation in situ on the paper substrates (Fig. 4.4C) using eosin staining and light microscopy in a manner similar to that shown in Section 5.2.1. However, the paper fibres also became stained along with the platelets, which could not then be seen in contrast to the background. Scanning electron microscopy (SEM) was then employed.

The test and control strips with dried platelet samples on the surface, were fixed with methanol, coated with gold, and viewed using SEM. Fig. 5.4 shows images of paper strips exposed to 15  $\mu\text{L}$ ,  $610 \times 10^9/\text{L}$  of platelets without exposure to agonist (Fig. 5.4A) and following exposure to 50  $\mu\text{L}$  of 500  $\mu\text{M}$  ADP (Fig. 5.4B). As can be seen, there appeared to be no adhesion of platelets to the surface of the control strip, while platelets could be seen adhered to the strips exposed to agonist. While platelets do appear to be adhering, there is little evidence of significant aggregation and the platelets do appear to be quite dispersed, and that one might speculate that such a dispersed arrangement of platelets might have little impact on sample flow. However, the SEM images are only able to observe the surface of the paper, and there might be more significant aggregates within the porous structure of the paper that cannot be seen using SEM. Using SEM to look deeper into the porous structure of the paper could reveal such information. However, this was not attempted here due to time constraints and feasibility issues.

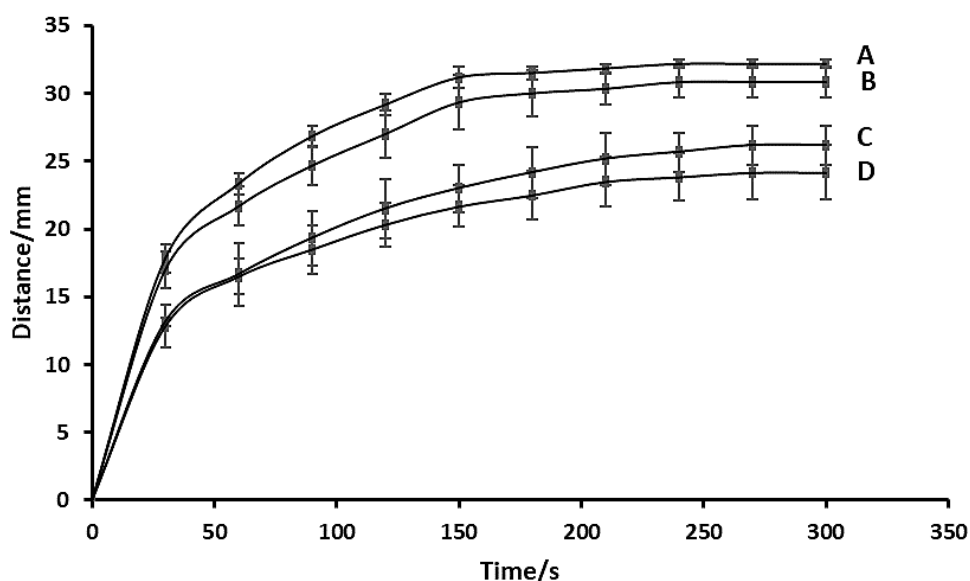


**Fig. 5.4.** Scanning electron micrographs of paper strips tested with 15 $\mu$ L platelet suspensions ( $610 \times 10^9/L$ ). Paper strips modified with 50  $\mu$ L A) TBS; B) 500  $\mu$ M ADP. Magnification  $\times 1,000$ , 2.00 keV.

### 5.2.3 Assessment of the effect of platelet aggregation on sample flow rate


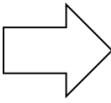



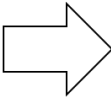
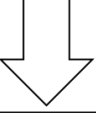
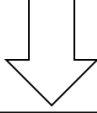

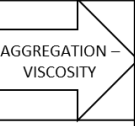
In a paper-based lateral flow platform, adhesion and aggregation of activated platelets might, in principle inhibit free sample flow and consequently lead to reduced flow rate and distance travelled. That a reduction in sample flow rate can be induced by platelet adhesion and aggregation is the hypothesis being investigated here. However, there are other factors that might also influence sample flow rate. Principal among these is the viscosity of the platelet sample and the wettability of the modified paper strips. It was therefore necessary to first of all isolate and quantify, at a fundamental level, the changes in flow rate caused by adhesion and aggregation of platelets on paper test strips, as well as changes caused by the deposition of agonist reagents. This was investigated by performing appropriate controls, comparing flow rates, and determining the effect due to platelet adhesion and aggregation. Negative control samples (TBS, 15  $\mu$ L) and positive control samples (platelet suspension in TBS,  $304 \times 10^9/L$ , 15  $\mu$ L), were tested on control strips (modified with TBS, 50  $\mu$ L) and test strips modified with epinephrine (3 mM, 50  $\mu$ L) and the sample flow rates were recorded over five minutes (Fig. 5.5). While platelet assays may ultimately be performed in plasma samples in which appropriate controls for viscosity would be PPP, in this instance in which lyophilised platelet suspensions were used, TBS buffer which was used to resuspend the platelets was employed as the control for viscosity and zero platelet count. Just a point of note that, although adhesion and aggregation are two distinct processes in

platelet activation, both are assumed to occur together, and so, for simplicity, these combined processes will just be referred to as aggregation from this point forward.



**Fig. 5.5.** Flow rates of platelet suspension ( $304 \times 10^9/L$ ,  $15 \mu L$ ) and control samples (TBS,  $15 \mu L$ ) on TBS ( $50 \mu L$ ) and epinephrine ( $3 \text{ mM}$ ,  $50 \mu L$ ) modified strips in five minutes. A) TBS on TBS modified strips, B) TBS on epinephrine modified strips, C) Platelets on TBS modified strips, D) Platelet on epinephrine modified strips ( $n=3$ ).

It can be seen that, in all cases, samples had ceased flowing after 5 min, and so the data analysis was based on the distances travelled by the samples at this time. The TBS samples had faster flow rates on the TBS-modified (Fig. 5.5A,  $32.2 \pm 0.3 \text{ mm}$ ) than the platelet samples (Fig. 5.5C,  $26.2 \pm 1.4 \text{ mm}$ ,  $p < 0.01$ ) and this difference was presumed to be due to the difference in viscosity between the TBS and the platelet suspension. However, the difference in flow rates of TBS and platelets samples on strips modified with epinephrine (Fig. 5.5B,  $30.8 \pm 1.2 \text{ mm}$  and Fig. 5.5D,  $24.2 \pm 2.0 \text{ mm}$ , respectively) were presumed to be due to contributions from both aggregation and viscosity ( $p < 0.01$ ). The difference in flow rate between the TBS samples on the TBS-modified strips and on the epinephrine-modified strips was  $1.4 \pm 0.8 \text{ mm}$  ( $p = 0.120$ ) and was believed to be principally due to the hydrophobicity and wetting of the deposited agonist, while the difference in flow rates between platelet samples on TBS-modified strips and epinephrine-modified strips was  $2.0 \pm 1.7 \text{ mm}$  ( $p = 0.230$ ) and was believed to be due to both wetting as well as aggregation of the platelets on the epinephrine strips. These relationships have been expressed graphically in Fig. 5.6.

		STRIP MODIFICATION			WETTING EFFECT	
		TBS		EPI		
<b>SAMPLE</b>	TBS	<b>A</b>		<b>B</b>		<b>A-B</b>
		32.2		30.8		1.4
						
	PLATELETS	<b>C</b>		<b>D</b>		<b>C-D</b>
26.2		24.2		2.0		
						
<b>VISCOSITY EFFECT</b>		<b>A-C</b>		<b>B-D</b>		(B-D)-(A-C) (C-D)-(A-B)
		6.0		6.6		0.6

**Fig. 5.6.** Illustration of the distance travelled (mm) at 5 minutes by samples of TBS or platelet suspensions on strips modified with TBS buffer or epinephrine (EPI). The figure also illustrates the various contributions to these values by differences in sample viscosity, strip wetting and aggregation and determine the net contribution to aggregation when these contributions have been removed ( $p>0.05$ ).

In instances where there was a contribution to the difference in flow rate due to sample viscosity (A-C, or B-D), this will, in future be referred to as a “Viscosity Effect”, and where there was a contribution to the difference in flow rate due to the deposition of agonist (A-B or C-D), this will be referred to as a “Wetting Effect”. In the cases where there is a presumption that platelets may also be activated and aggregated in the presence of epinephrine (Fig. 5.5D), these values will have contributions from both aggregation and viscosity (B-D) or aggregation and wetting (C-D).

The effect of aggregation was extracted from the effects associated with sample viscosity:

$$\text{Sample viscosity (A-C): } 32.2 - 26.2 = 6.0 \pm 1.4 \text{ mm}$$

$$\text{Aggregation and viscosity (B-D): } = 30.8 - 24.2 = 6.6 \pm 2.3 \text{ mm}$$

$$\text{Aggregation (- viscosity): (B-D) - (A-C): } 6.6 - 6.0 = 0.6 \pm 2.7 \text{ mm}$$

In this instance, the contribution to the differences in distance due to flow rate was found to be  $0.6 \pm 2.7$  mm.

The effect of aggregation was also determined by extracting the contribution of strip wetting:

$$\text{Strip wetting (A-B): } 32.2 - 30.8 = 1.4 \pm 1.2 \text{ mm}$$

$$\text{Aggregation and wetting (C-D): } 26.2 - 24.2 = 2.0 \pm 2.4 \text{ mm}$$

$$\text{Aggregation (- wetting): (C-D) - (A-B) = } 0.6 \pm 2.7 \text{ mm}$$

In this instance, the contribution to the differences in distance due to flow rate was again found to be  $0.6 \pm 2.7$  mm (450% CV).

Based on these findings, a parameter termed the "Aggregation Effect" (AE) was established to account for the contribution to changes in sample flow rate due to platelet aggregation by elimination of contributions from Viscosity Effects or Wetting Effects. This was determined using the following formulae:

$$AE = (B-D) - (A-C) \quad (\text{Eq. 5.1})$$

$$AE = (C-D) - (A-B) \quad (\text{Eq. 5.2})$$

Where AE is the Aggregation Effect, (A-C) is the sample viscosity, (A-B) is strip wetting, (C-D) is aggregation and wetting and (B-D) aggregation and viscosity.

Since it would appear that the differences in flow rates due to sample viscosity and strip wetting were comparable regardless of the type of sample used, it might be assumed that there were no non-linear contributions from either sample type or strip modification on changes to flow rate. The differences due to strip wetting were also found not to be statistically significant. In addition, since all strips would ultimately be modified in the same manner, any differences in flow rates due to strip wetting (for epinephrine at least) should be minimal, or absent, and so can be disregarded. However, it had to be determined whether this was also the case for other agonists.

In either case, the contribution to the distance travelled by the sample that was thought to be due to platelet aggregation was small (0.6 mm) with a very large standard deviation (2.7 mm, 450% CV, n=3). This very large variance is due, in part, to the propagation of errors which results from the subtraction of these four elements from one another, which

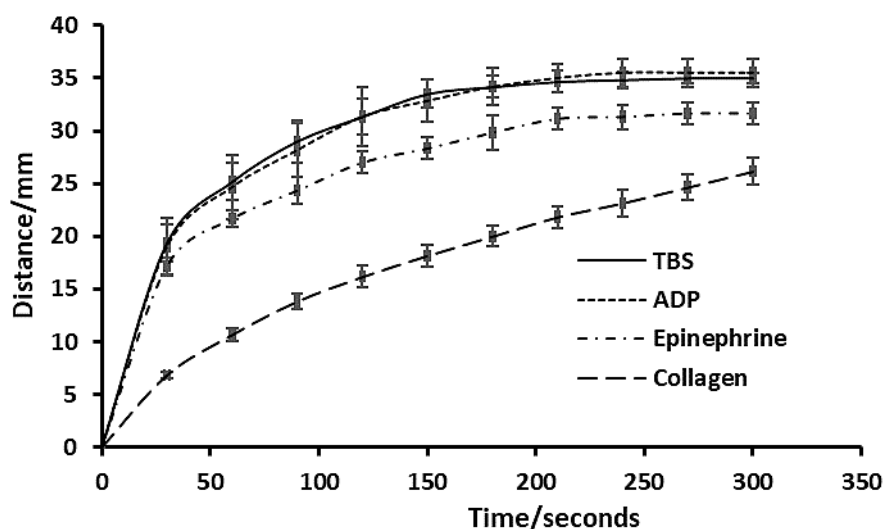
causes an accumulation of error according to the sum of the root mean squares of their individual variances (Section 2.2.14). Further development was required to determine whether this was a small, but real effect, or was just due to random error. In addition, to be of any measurement value, the contribution from aggregation on flow rate would have to be enhanced further to overcome issues of variance.

#### **5.2.4 Investigation of agonist on strip-based aggregation**

In the initial evaluation of strip-based aggregation in section 5.2.3, only epinephrine was investigated as an agonist. However, due to differences in their mode of action and potency in activating platelets, as well as the differences in impact on flow rates due to wetting and rehydration, other agonists might prove more effective in this scenario. In addition to epinephrine, three agonists (ADP, collagen, and arachidonic acid) were investigated for their ability to induce aggregation on the strips.

Initially, the effect of the deposited agonists on the flow rate of TBS buffer (15  $\mu$ L) on the strips over five minutes was assessed (Fig. 5.7). At this stage, the agonists were studied at the concentrations prescribed by the manufacturer for use in platelet aggregometry, being 200  $\mu$ M (85.4  $\mu$ g/mL), 3 mM (183.2  $\mu$ g/mL) and approx. 0.3  $\mu$ M (100  $\mu$ g/mL) and 15.3 mM (5 mg/mL) for ADP, epinephrine, collagen and arachidonic acid, respectively. While arachidonic acid was also investigated, due to its lipophilic and surfactant properties, it was capable of passing through the hydrophobic wax boundary and so was not suitable for further investigation. Flow rates were greatest on ADP-modified strips (35.3  $\pm$ 1.3 mm), followed by that of epinephrine (31.7  $\pm$ 1.0 mm), and then that of collagen (26.2  $\pm$ 1.3 mm). This may be due to a combination of concentration and hydrophobicity. ADP and epinephrine are both small, water-soluble molecules, with ADP having a higher solubility (85 mg/mL at 25°C) than epinephrine (44 mg/mL, at 25°C). Collagen, on the other hand is only poorly soluble in water, which means it would be much more difficult to rehydrate in the sample media than either ADP or epinephrine, making the paper strips significantly more hydrophobic and so significantly retarding sample flow. It can also be seen that the flow rate of TBS was similar if not identical for TBS and ADP modified strips, signifying that there was not significant difference in wetting effect between the two strips.



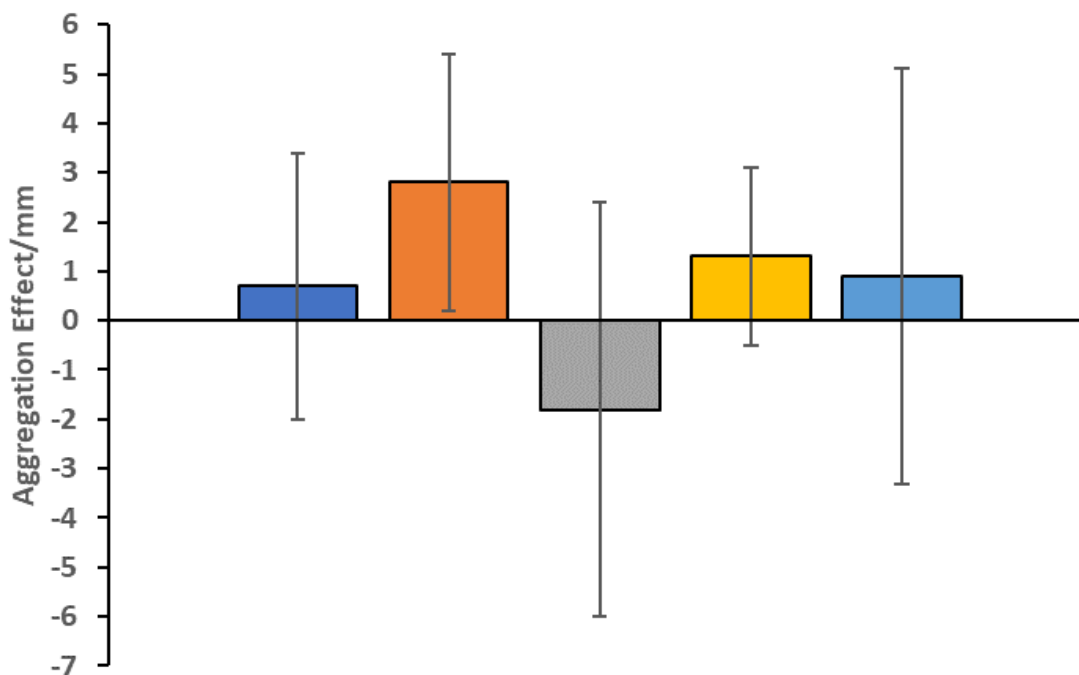


**Fig. 5.7.** Flow rates of 15  $\mu\text{L}$  TBS on strips modified with 50  $\mu\text{L}$  TBS buffer, 200  $\mu\text{M}$  ADP, 3  $\text{mM}$  epinephrine, or 100  $\mu\text{g}/\text{mL}$  collagen ( $n=3$ ).

Using the approach described in section 5.2.3, the agonists ADP, collagen and epinephrine were studied further for their potential to bring about platelet aggregation on the strips, as well as 50:50 v/v combinations of ADP:collagen, and epinephrine:collagen (Fig. 5.8). Collagen being a platelet adhesion agent has been used in combination with epinephrine or ADP in platelet tests such as PFA 100/200 to detect different platelet function abnormalities (Shirlyn, 2010). The Aggregation Effect was calculated for all combinations using both formulae for AE (Eqs. 5.1 and 5.2). However, these were the same in all cases, and appeared to show that the method chosen to determine the Aggregation Effect did not have any impact on the result. Based on this, calculations were made using Eq. 5.1, as in any assay methodology, the agonist would likely remain constant in all cases.

ADP alone gave the largest Aggregation Effect and the best standard deviation ( $2.8 \pm 2.6$  mm, 93% CV), followed by the epinephrine:collagen mixture ( $1.3 \pm 1.8$  mm, 138% CV), ADP:collagen ( $0.9 \pm 4.2$  mm 467% CV), epinephrine alone ( $0.6 \pm 2.7$  mm, 450% CV) and lastly, collagen alone ( $-1.8 \pm 4.2$  mm, 233% CV). It should be noted that the difference in Aggregation Effect among the reagents was not significant ( $p=0.560$ ) at this stage probably due to accumulation errors involved in the determination of Aggregation Effect. The largest positive effect given by ADP could be explained by the fact that ADP is a potent direct platelet activator, unlike the other agonists. In addition, it also had the least effect on flow rate (Fig. 5.6). This suggested ADP was the preferred choice for further exploration of platelet behaviours on lateral flow strips. Its direct

platelet activation and high potency makes it of potential use at relatively low concentrations, which would minimise wetting effects. As explained in Section 5.1, epinephrine is an indirect platelet activator (Lanza *et al*, 1988) similar to collagen which might result in slower platelet activation kinetics than ADP. Collagen had such a significant impact on sample flow that it may be more likely to mask the effects of aggregation and contribute to the variability in sample flow.



**Fig. 5.8.** Aggregation Effect of platelets on agonist-modified paper-based lateral flow strips. Epinephrine (Epi) (■), ADP (■), collagen (Col) (■), Epi:Col (■) and ADP:Col (■) ( $n=3$ ,  $p=0.560$ ).

While the optimum Aggregation Effect achieved with ADP at 200  $\mu$ M was found to be 2.8 mm, this was still small and had a standard deviation of 2.6 mm, again caused by inherent strip variability and the significant propagation of errors which accumulate during calculation of the Aggregation Effect, eliminating any statistically significant differences. However, it was still believed that, while statistical significance was not yet established ( $p=0.560$ ) due to these errors, that these could be further minimised to identify a real effect due to aggregation.

### **5.2.5 Investigation of the enhancement of aggregation using fibrinogen**

Fibrinogen plays a crucial role in platelet adhesion and aggregation during primary haemostasis by enabling platelets to bind to the injured vessel wall and to other platelets via the glycoprotein IIb/IIIa receptor complex. Low fibrinogen concentration has been linked to reduced and unstable platelet plug formation (Mikhailidis *et al.*, 1985), and fibrinogen is essentially a cofactor in platelet aggregation. However, the platelet suspensions used in this study were prepared from lyophilised platelets using TBS. These platelet suspensions were low in fibrinogen and this low fibrinogen level could reduce the level of aggregation of the platelets. Therefore, supplementing the platelet samples with fibrinogen could potentially improve the effect. In addition, while the platelet suspensions were within the normal range of platelet count ( $304 \times 10^9/L$ ), increasing the platelet count might provide a more obvious demonstration of an Aggregation Effect on the paper strips. These two parameters were assessed together by preparing and testing a concentrated platelet suspension ( $607 \times 10^9/L$ ) prepared in TBS containing fibrinogen at 2.1 mg/mL. Samples were then deposited on TBS and ADP-modified strips ( $n=3$ ). In this case the change in sample flow attributable to aggregation rose from  $2.8 \pm 2.6$  mm (93% CV) to  $3.4 \pm 2.3$  mm (68% CV). Using this new data, the  $p$ -value from ANOVA showed an improvement from 0.560 to 0.448. While the gain in Aggregation Effect of 0.6 mm was still relatively small, there was an improvement in precision as the magnitude of the contribution to flow rate due to aggregation becomes proportionally greater than effects due to inherent strip variability. It was hence decided to supplement platelet samples with fibrinogen at approx. 2.1 mg/mL in future investigations.

### **5.2.6 Optimisation of ADP concentration**

While the observed change in flow attributable to aggregation of  $3.4 \pm 2.3$  mm of a sample with a platelet count of  $\sim 600 \times 10^9/mL$  was still relatively small and lacking sufficient precision, this was based on a single concentration of ADP which is recommended for bulk aggregation of platelets (200  $\mu M$ ), rather than in a lateral flow configuration. A different concentration of ADP might be more optimal for the activation and aggregation of platelets in this format, although increases in the concentration of agonist might cause some change in the wetting dynamics of the strips. An optimum ADP concentration might, therefore, have improved platelet activation, but have no significant additional Wetting Effect. To explore and optimise the effect of ADP, strips were modified with 50  $\mu L$  ADP at a range of concentrations from 100 to 700  $\mu M$  and investigated for their Aggregation Effect calculated using platelet samples ( $607 \times 10^9/L$ )

in 2.1 mg/mL fibrinogen in TBS, and control samples of fibrinogen in TBS (n=3). The sample viscosity (A-C) was determined on unmodified strips from the two sample types. The control sample value was  $28.0 \pm 0.5$  mm, while the platelet sample was  $25.7 \pm 0.8$ , yielding a sample viscosity contribution of  $2.3 \pm 0.9$  mm. This was then subtracted from the differences in distance values of the two sample types on strips modified with different ADP concentrations (Table 5.1).

**Table 5.1.** Determination of the Aggregation Effect of platelets in response to different concentrations of ADP. Samples (15  $\mu$ L) composed of 2.1 mg/mL fibrinogen in TBS containing no platelets (Control sample, B) or platelets at  $607 \times 10^9/L$  (Platelet sample, D) were applied to unmodified strips, or strips modified with 50  $\mu$ L ADP (n=3). The sample viscosity was calculated from the difference travelled on the unmodified strips by the two samples (A-C,  $28.0 \pm 0.5 - 25.7 \pm 0.8 = 2.3 \pm 0.9$  mm) which was subtracted from the difference travelled by Control sample (B) and the Platelet sample (D), according to Eq. 5.1. ( $p=0.123$ )

ADP ( $\mu$ M)	Platelet sample (D) (mm)	Control sample (B) (mm)	Aggregation Effect (mm)	SD (mm)	CV (%)
100	$23.8 \pm 0.3$	$27.5 \pm 1.0$	1.4	1.3	93
300	$21.8 \pm 0.8$	$26.6 \pm 0.6$	2.5	1.3	52
500	$21.0 \pm 0.5$	$27.7 \pm 0.8$	4.4	1.2	27
700	$19.7 \pm 1.0$	$25.3 \pm 0.8$	3.3	1.6	48

As indicated in Table 5.1, the sample distance decreased with increasing ADP concentration for both test (with platelets) and control (TBS) samples. In the control samples, this effect was due entirely to a strip wetting effect from the increased ADP loading on the strip, while on the platelet samples, this was due to both wetting and aggregation. The Aggregation Effect appeared to increase, though not at a significance level ( $p=0.123$ ), with ADP concentrations from 100 to 500  $\mu$ M and then declined slightly at 700  $\mu$ M. The aggregation effect at 500  $\mu$ M was larger than that at 100  $\mu$ M ( $p=0.043$ ) but not significantly larger than those at 300  $\mu$ M ( $p=0.136$ ) and 700  $\mu$ M ( $p=0.395$ ). However, at 500  $\mu$ M an Aggregation Effect of  $4.4 \pm 1.2$  mm (27% CV) achieved, showed further improvement in precision and in reaching a value that suggested a genuine and quantifiable effect.

### 5.2.7 Experimental and mathematical reduction of errors in Aggregation Effect

While the optimisation of the measurement approach by using fibrinogen, and then through optimisation of agonist type and concentration had resulted in gradual improvements in the precision of the Aggregation Effect, the employment of four terms in the calculation would lead to an inherently high error value due to the propagation of errors. Elimination of some of these terms from the calculation would improve its

precision. Experiments had shown that, for epinephrine and ADP at least, the effect of wetting was negligible ( $p=0.120$ ) and constant if all samples were applied to agonist-modified strips. If one assumes this to be the case, then, for a given sample type, one can say that, in Eq. 5.1  $A \approx B$ , and one can then substitute B for A, which allows elimination of one of the terms:

$$(B - D) - (B - C)$$

If the equation is solved further as follows:

$$= B - D - (B - C)$$

$$= B - D - B + C$$

$$= C - D \quad \text{Eq. 5.3}$$

This result is logical both mathematically and experimentally, as, if we see in Fig. 5.6, the difference between C and D is due to aggregation and wetting, and where the difference due to wetting is negligible and can be eliminated, then we can neglect both A and B. Thus, we can legitimately eliminate both of the two terms, A and B from the experiment and calculation, and also reduce the error propagation as now only two terms are required. If the values of Aggregation Effect shown in Table 5.1 are recalculated using only the terms C and D (Eq. 5.3), the resulting new values and errors could be determined (Table 5.2). Firstly, there was a general increase in the magnitude of the Aggregation Effect, as both the values of A and B were no longer subtracted from the difference between C and D.

**Table 5.2.** Determination of the Aggregation Effect of platelets in response to different concentrations of ADP. Samples (15  $\mu\text{L}$ ) composed of 2.1 mg/mL fibrinogen in TBS containing platelets at  $607 \times 10^9/\text{L}$  were applied to unmodified strips (Platelet control, C), or strips modified with 50  $\mu\text{L}$  ADP ( $n=3$ ) (Platelet test, D). The difference travelled by C and D were determined according to Eq. 5.3. ( $p=0.008$ )

ADP ( $\mu\text{M}$ )	Platelet control (C) (mm)	Platelet test (D) (mm)	Aggregation Effect (mm)	SD (mm)	CV (%)
100	25.7 $\pm$ 0.8	23.8 $\pm$ 0.3	1.9	0.85	45
300	25.7 $\pm$ 0.8	21.8 $\pm$ 0.8	3.9	1.13	29
500	25.7 $\pm$ 0.8	21.0 $\pm$ 0.5	4.7	0.9	19
700	25.7 $\pm$ 0.8	19.7 $\pm$ 1.0	6.0	1.2	48

In addition, there was a significant improvement in the precision, with the Aggregation Effect at 500  $\mu\text{M}$  achieving an CV of <20%, which demonstrates significant precision and confidence in the result since the p-values rose from 0.123 (Table 5.1) to 0.008

(Table 5.2). In this case however, 700  $\mu\text{M}$  ADP resulted in the greatest Aggregation Effect, although 500  $\mu\text{M}$  resulted in the greatest precision.

### 5.2.8 Investigation of the plasma sample matrix on the Aggregation Effect

While platelet suspensions in TBS buffer solutions, even with fibrinogen, may provide a model sample matrix for preliminary evaluation of the fluid dynamic properties of samples containing platelets on paper strips in response to agonists, such a sample would not be representative of the physiological situation, as these would be composed of whole blood, or plasma. It was therefore necessary to evaluate platelet sample behaviour on the strips in a more physiologically relevant matrix which was composed of plasma. In this regard, lyophilised calibration plasma reconstituted with TBS was, in turn used to prepare lyophilised platelets for measurement of the Aggregation Effect. The effect of ADP concentration on the Aggregation Effect was again investigated using this as the sample matrix. However, the platelet poor calibration plasma was itself found to have a platelet count of  $101 \times 10^9/\text{L}$ , and so platelet counts were based on the contribution from the plasma and the lyophilised platelets, on the assumption that all platelets were activating and aggregating in a comparable manner. Platelet samples were again applied to strips that were now unmodified (Platelet control) or modified with 50  $\mu\text{L}$  ADP (Platelet test), and the difference of the distance travelled by the two samples determined as the Aggregation Effect (Table 5.3).

**Table 5.3.** Sample distances at five min of platelet suspensions ( $607 \times 10^9/\text{L}$ ) in calibration plasma on unmodified strips (Platelet control) or strips modified with 50  $\mu\text{L}$  ADP Platelet test ( $n=3$ ,  $p=0.038$ ).

ADP ( $\mu\text{M}$ )	Platelet control (mm)	Platelet test (mm)	Aggregation Effect (mm)	SD (mm)	CV (%)
100	19.5 $\pm$ 0.5	18.7 $\pm$ 1.3	0.8	1.4	174
300	19.5 $\pm$ 0.5	18.8 $\pm$ 0.8	0.7	0.9	135
500	19.5 $\pm$ 0.5	14.5 $\pm$ 2.6	5.0	2.6	53
700	19.5 $\pm$ 0.5	15.2 $\pm$ 1.9	4.3	2.0	46

When plasma was used as the sample matrix, overall precision, though still significant (Table 5.3,  $p=0.038$ ), was reduced when compared with platelet suspensions in buffer (Table 5.2,  $p=0.008$ ). The elevated viscosity of the sample matrix reduced the total distance travelled on both modified and unmodified strips, leading to an inherently poorer 'signal to background' ratio and reduced precision. However, though not statistically significant ( $p=0.730$ ), the Aggregation Effect appeared to be greater at 500  $\mu\text{M}$  than at 700  $\mu\text{M}$  and in plasma rather than in buffer (5.0 mm), although ADP at 700

$\mu\text{M}$  appeared to give a better CV. While precision was reduced in the plasma matrix, it was decided to continue to explore the performance of the system since it would be necessary to use this in any future analysis of real samples.

### 5.2.9 Optimization of sample volume

Sample volume, since it also influences sample distance, could be optimized to enhance the Aggregation Effect. Using strips modified with 50  $\mu\text{L}$  of 500  $\mu\text{M}$  ADP, the sample volume was optimised by testing the platelet and control samples at various sample volumes. As shown in Table 5.4, Aggregation Effect appeared to increase with sample volume from 1.7  $\pm$ 0.9 mm (12  $\mu\text{L}$  sample) to 4.0  $\pm$ 1.6 mm (15  $\mu\text{L}$  sample) but then decreased to 2.7  $\pm$ 1.2 mm (21  $\mu\text{L}$ ). However, the overall difference in Aggregation Effect between the different volumes was not very significant ( $p=0.130$ ). The 15  $\mu\text{L}$  sample volume being used all along, just like in the case of the prothrombin time assay (chapter 4), gave the best effect (4.0  $\pm$ 1.6 mm) and continued to be used as the assay sample volume. It should be noted that, even though not at statistically significant levels, the differences in the effect between 15  $\mu\text{L}$  and 12  $\mu\text{L}$  or 18  $\mu\text{L}$  (5.3 mm,  $p=0.038$ ), were better than that between 15  $\mu\text{L}$  and 21 $\mu\text{L}$  ( $p=0.323$ ). No overall improvement in aggregation effect was registered. Increased aggregation effect appeared to go along side with increased variability in travel distance.

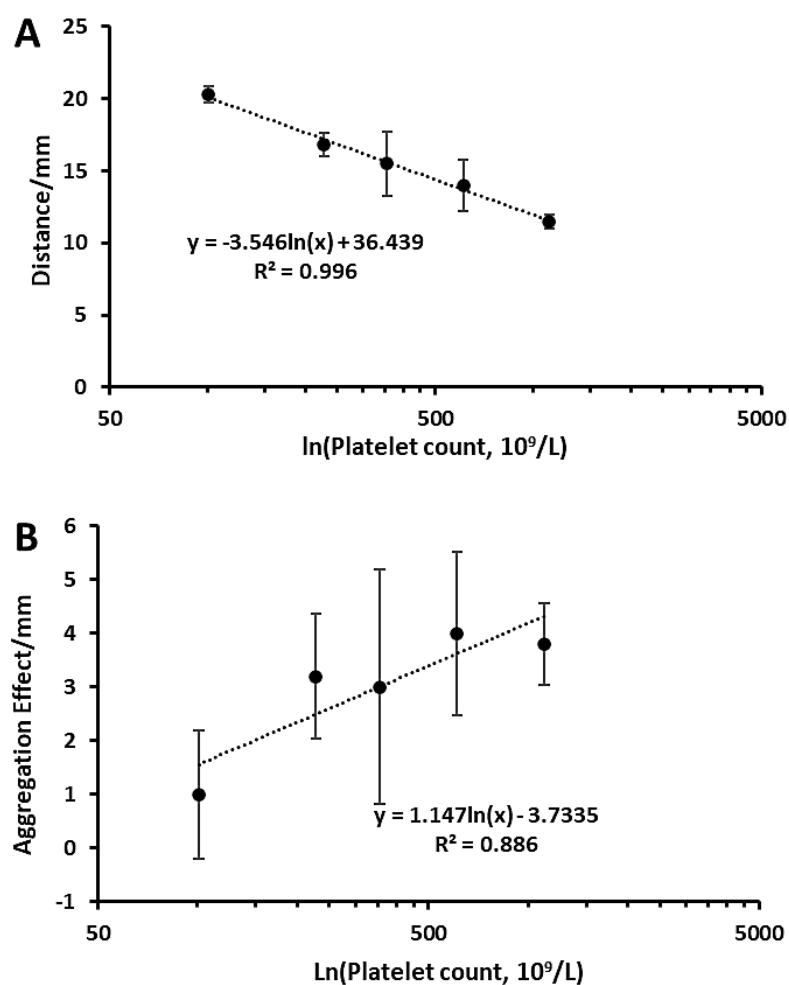
**Table 5.4.** Platelet aggregation effect as a function of sample volume on strips modified with ADP (500  $\mu\text{M}$ , 50  $\mu\text{L}$ ). Aggregation Effect determined by subtracting viscosity effect (1.8 mm) for the difference in distance travelled by control sample (CS) and test sample (TS) ( $p=0.130$ ).

Volume/ $\mu\text{L}$	TS/mm	CS/mm	Agg effect	SD/mm
12	10.7	14.2	1.7	0.9
15	14.5	20.3	4.0	1.6
18	17.7	21.2	1.7	0.9
21	21.5	26.0	2.7	1.2

### 5.2.10 Study of the effect of platelet count on the Aggregation Effect

A major aim of this study was to establish whether platelet count can be determined from the distance travelled by an aggregating plasma sample. While it has been demonstrated that platelet aggregation appears to lead to some change in sample flow at relatively high platelet count, the anticipation is that the magnitude of this effect would be proportional across a range of platelet counts relevant to clinical measurement. Samples with different platelet counts (101 to 1,119  $\times 10^9/\text{L}$ ) were prepared and tested on ADP modified strips (50  $\mu\text{L}$ , 500 mM) as well as TBS modified (50  $\mu\text{L}$ ) strips and the corresponding sample travel distances and aggregation effect determined.

As shown in Fig. 5.8A, the platelet count and distance travelled by the sample showed an inverse logarithmic relationship ( $r=0.996$ ), covering the entire platelet count range. However, the contribution to this effect was from both differences in sample viscosity, as well as platelet aggregation. Ultimately, any test method would have to be independent of viscosity effects. When Aggregation Effect was calculated according to Eq. 5.3 (Fig 5.8 B), this demonstrates that the Aggregation Effect increased with platelet count and the two had a direct logarithmic relationship. A correlation coefficient ( $r=0.886$ ) did appear to demonstrate a reasonable relationship. However, the increase in error again due to inherent strip variability, and the need to subtract the viscosity control again led to a significant increase in imprecision.



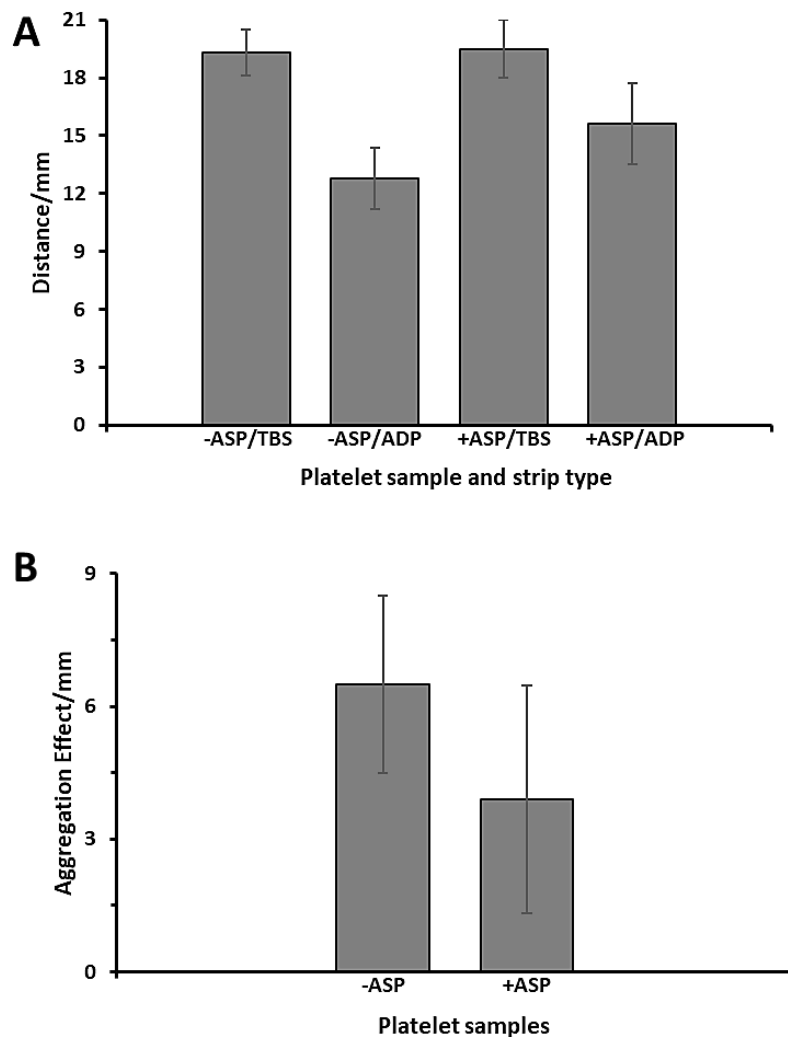
**Fig. 5.8.** Platelet count vs distance travelled by sample and Aggregation Effect. A) platelet count vs distance travelled by sample, B) platelet count vs Aggregation Effect. Platelet count appeared to show an inverse logarithmic relationship with distance travelled and a direct logarithmic relationship with Aggregation effect. Aggregation effect was considered to be the difference between the distance travelled on ADP modified (50  $\mu$ L, 500 mM) and TBS modified (50  $\mu$ L) strips. 15  $\mu$ L was used as sample volume.



### 5.2.11 The effect of the platelet antagonist aspirin on platelet aggregation on strip

There was now reasonable evidence that the platelet samples used were active and functional and were responding to ADP by adhering and aggregating on assay strips, and thus causing a reduction in sample distance as determined by the Aggregation Effect. These conclusions were based on quantitative platelet behaviour. Further proof of the validity of the fact that the effect was due to platelet aggregation would be to employ a platelet antagonist such as aspirin to eliminate platelet aggregation and see if the assay could distinguish the antagonist treated platelets from untreated ones. Platelets treated with the antagonist would aggregate less or not aggregate at all and result in faster flow rates, while untreated platelets would continue to aggregate normally, obstructing sample flow and lead to shorter distances. To test this, two different platelet samples were prepared, one treated with 2 mM aspirin and the other prepared in the usual way without aspirin. Aspirin inhibits platelet function by preventing the conversion of arachidonic acid to thromboxane  $A_2$ , a potent platelet activator that induces shape change and release reactions in platelets which are essential for adhesion and aggregation (Catherine, 2021). Both samples had identical platelet counts of approx.  $607 \times 10^9/L$ , and were tested on TBS and ADP modified strips and their travel distances recorded and compared (Fig. 5.9A).

On the TBS-modified control strips, both distances were very similar with the difference between the treated and untreated platelet samples of  $0.2 \pm 1.35$  mm ( $p=0.400$ ), indicating that there was no significant difference between the two distances, the difference was due to random variations in measurement. In the case of ADP-modified test strips, the difference between the treated and untreated samples was  $2.8 \pm 1.85$  mm ( $p=0.034$ ). This showed that there was a statistically significant difference between the distances, meaning the inhibited sample covered a longer distance than the functional sample, which confirms that the effect was due to the action of aspirin on activated platelets. Furthermore, as shown in Fig, 59B, the Aggregation Effect elicited by the platelet sample ( $6.5 \pm 2.0$  mm) appeared larger than that elicited by the aspirin treated platelet sample ( $3.9 \pm 2.6$  mm). However, again due to accumulation of errors involved in calculating the Aggregation Effect, precision was lost, and the two Aggregation Effects were not statistically distinguishable ( $p=0.164$ ).



**Fig. 5.9.** (A) Distance travelled by platelet (-ASP) and aspirin treated platelet (+ASP) samples (15  $\mu$ L) on TBS (50  $\mu$ L) and ADP (50  $\mu$ L, 500 mM) modified strips. (B) Aggregation Effect of a platelet sample (-ASP) compared to that of aspirin treated platelet sample (+ASP).

To sum up, activation and adhesion/aggregation of platelets on paper-based lateral flow strips have been studied and confirmed in this work. Platelets exposed to immobilised platelet agonists adhere and aggregate on the strips and reduce sample flow rate and distance travelled to a degree at which normal platelet samples could be distinguished from inactivated/dysfunctional platelet samples ( $p < 0.05$ ). In addition, the technique was found to be sensitive to sample platelet count. No comparative work has yet been seen in the literature. The current platelet function tests in used in hospitals and clinics such as VerifyNow, Plateletworks, Multiplate device, TEG platelet mapping, PFA 100/200, Sonorheometry (Bolliger *et al.*, 2021), Flow cytometry, Impact, Phosphorylated Vasodilator-stimulated phosphoprotein (VASP-P), and Microparticles (Choi *et al.*, 2014) are either laboratory based, expensive and/or require power, instrumentation and expertise and so not ideal for low resource and remote environments. The impedance

method developed by Chrono-Log Havertown (USA) (Van Werkum *et al.*, 2007) has the advantage of using whole blood instead of PRP just like TEG and PFA 100/200 and has shown a good correlation with optical aggregometry (Vinholt *et al.*, 2017; Blanc *et al.*, 2020) but it still requires about two minutes sample preparation, and over ten minutes turnaround time and most importantly, it is laboratory-based and requires power and expertise to operate. New methods of detecting platelet aggregation have been reported including spectroscopic determination of platelet aggregation (Tsujino *et al.*, 2019), Spectroscopic determination of platelet count (Kitamura *et al.*, 2018) and the use of a Microchip Flow Chamber (Iwanaga *et al.*, 2020). However, all of these are also expensive and technically complex to operate. This work, therefore, is novel and has laid down the foundation for the development of a new, simple, and low-cost paper-based lateral flow platelet function test that could detect platelet dysfunction as well as quantitative platelet defects like thrombocytopenia and thrombocythemia.

### 5.3 Conclusion

In this study, it has been clearly demonstrated that platelets adhere and aggregate on paper-based assay strips in response to agonists. In addition, this aggregation also appears to influence sample flow dynamics by reducing flow rate and distance. It has also been shown that the assay was able to distinguish between platelets treated with an antagonist (aspirin) from untreated ones ( $p < 0.05$ ). The treated platelet samples travelled longer distances (15.6 mm) than untreated platelets (12.8 mm) on ADP modified strips while on the buffer modified strip (control strip), there was not significant difference in the distance covered by the two different platelet samples ( $19.5 \pm 1.5$  mm and  $19.3 \pm 1.2$  mm, respectively,  $p = 0.400$ ). However, due to accumulation of errors and loss of precision, Aggregation Effect of platelets, though appeared to be larger ( $6.5 \pm 2.0$  mm) but was not significantly larger than that of aspirin treated platelets. The techniques also demonstrated sensitivity to platelet count by showing a strong correlation between platelet count and distance travelled by sample- ( $r = 0.996$ ). Due to the very small volume fraction of the platelets in samples, the response was small and that the approach used requires improvements in order to make it more analytically and clinically viable. However, these preliminary observations hold significant potential for platelet assays based on lateral flow paper platforms which might provide low-cost platelet function testing in resource scarce and remote environments.

## **6. OVERALL CONCLUSIONS AND FUTURE WORK**

## 6.1 Overall conclusions

In this work, two separate paper-based lateral flow assays have been developed for measuring different blood coagulation parameters using a visual readout format based on the distance travelled by the sample. A comprehensive study was also conducted on the aggregation of platelets on the lateral flow strips, which has laid a foundation for future work on lateral flow platelet analysis.

The first assay was a paper-based lateral flow device for measurement of fibrinogen in human plasma. In this device, the paper test strips were modified with exogenous thrombin, and the distance covered by a plasma sample was inversely proportional to the fibrinogen concentration. This device was capable of measuring fibrinogen across the entire clinically relevant range (0.5 to 7.5 mg/mL) within five minutes and showed a strong correlation ( $r=0.979$ ) with a routine method (Yumizen G FIB).

The second assay was the paper-based lateral flow prothrombin assay. Here, paper test strips were modified with a thromboplastin reagent and calcium chloride solution. Plasmas with normal PT values covered short distances ( $\leq 14$  mm) while plasmas with prolonged PT values covered longer distances ( $\geq 14$  mm). This assay also showed a strong correlation with an established clinical prothrombin time test in samples with PT values from 9.5 to 40.0 seconds. It could effectively distinguish abnormal plasmas from normal plasmas based on their PT values.

The third investigation looked at the potential for a paper-based lateral flow system for platelet function test. Here, the effect of platelet activation and aggregation on the paper strips were investigated. While the effect was relatively small, there did appear to be a change in sample flow as a result of platelet aggregation following activation with a number of agonists, particularly ADP. While the ability to use this to quantify platelet count was somewhat limited, its ability to differentiate between platelets that had been treated with or without an antagonist was quite definitive.

These coagulation and aggregation testing devices are compact, low cost, and very simple to operate in comparison to most, if not all coagulation testing devices currently available. In the case of platelet function testing, there are no other comparable techniques or devices yet available. As they are based on cellulose paper strips which are abundantly available and highly biodegradable, they also represent improved

environmental sustainability at a time when eradication of plastics is becoming particularly important. The devices also use small volumes of reagents and samples and have a short turnaround time of five minutes. These devices are therefore more suited to low resource settings which often lack laboratories and affordable diagnostic methods for bleeding and clotting disorders. These devices exhibit the potential to conduct simplified, low-cost, clinically reliable screening tests for coagulation disorders. However, they still require further developments to improve their sensitivity, precision, and stability to fully achieve these objectives.

## **6.2 Future work**

### **6.2.1 Improving the performance of the developed assay devices**

The performance of the developed devices, particularly the prothrombin and platelet function assays (Chapters 4 and 5, respectively) require further significant improvements. Each of these devices has a low precision and a narrow dynamic range which limit their performance. These analytical features could be further explored and enhanced by investigating the use of fibrinogen coated polystyrene/silica nanoparticles on test strip surfaces (Díaz-González and Escosura-Muñiz, 2021). Other cellulose-based paper types with different thicknesses and water flow rates such as Whatman grade 4 and grade DE81 should be investigated as well.

The fibrinogen assay (Chapter 3) was robust and had an adequate correlation with a routine method ( $r=0.979$ ), but its performance was based on artificially constructed and limited number of plasma samples (20 samples). In addition, only one type of thrombin reagent (lyophilised bovine thrombin from Clauss fibrinogen 50 kit) was fully explored in the development of the assay. The fibrinogen assay, therefore, should be further studied by using thrombin reagents from other sources and by adding calcium to the test strips. Its performance should also be re-evaluated using a large number ( $\geq 60$ ) of real patient samples. Prior to the COVID-19 pandemic, there had been a plan to analyse a bank of plasma samples for a study of post-partum haemorrhage at Cardiff Hospital, but which had to be cancelled due to the pandemic. Testing the performance of the device in such a cohort would demonstrate potential of the device to support maternal peri-natal care in low resource environments.

The investigation of platelet behaviour on lateral flow strips in response to agonists (Chapter 5) appeared to adequately set the foundation for developing a lateral flow

platelet function test. The inherent variability of the paper substrate which led to low precision in sample flow rate and the very small volume fraction of platelets in the sample (Pogorzelska *et al.*, 2020) which made it difficult for platelet aggregation to significantly alter sample flow behaviour on strips, were the main limitations of the envisioned paper-based lateral flow platelet function analyser. Modification of the strips with fibrinogen or fibrinogen coated nanoparticles (Sanfins *et al.*, 2014) before adding the agonist and/or using papers with different thickness and pore size distribution could improve both precision and Aggregation Effect. Furthermore, reconstituted lyophilised platelet samples instead of fresh platelet rich plasma samples were used in the investigation. After satisfactorily enhancing the aggregation effect and precision as explained in the first paragraph (section 6.2.1), assay performance should be re-evaluated using normal platelet samples and platelet samples from patients with different platelet defects such as thrombasthenia, thrombocytopenia, and thrombocythaemia.

The strip fabrication technique for all three devices, especially the reagent immobilisation and drying steps should also be improved so that these steps are conducted in an environment with constant temperature and humidity such as in an environmental chamber. Automated techniques for reagent deposition such as the use of microdroplet dispensers would improve reproducibility in the distribution of reagents on strip surfaces, as well drying of strips which would improve assay reproducibility. The flow monitoring window of the plastic holders could also be covered with a thin transparent plastic film to reduce the impact of humidity fluctuations and evaporation during device operation.

To omit the need for power, which is often an issue in remote places, the operation of the devices at a range of ambient temperatures instead of on a heating blocks set at 37°C should be explored further, and the devices should be developed with calibration ranges that suit such a range of ambient temperatures as might be found in low resource environments. The plastic holders could also be equipped with multiple reading scales applicable for these different ambient temperature ranges.

## 6.2.2 Development of a paper-based lateral flow activated partial thromboplastin assay

As explained in the introduction (section 1.4.3), aPTT is used to evaluate the intrinsic and common coagulation pathways, is sensitive to all of the haemophilia types (A, B, and C) and is used to monitor heparin therapy (Shirlyn, 2010). Coupled with the simple low-cost fibrinogen and thromboplastin assays developed in Chapters 3 and 4, the addition of an aPTT assay could allow a wider range of bleeding and clotting problems to be affordably screened in low resource and emergency settings. This assay could also therefore be developed and tested for use in the target settings. Development of lateral flow partial thromboplastin assay might begin with using the test strip design adopted for prothrombin assay device (Chapter 4, Fig 4.4C). The test strips might comprise a sample deposition zone and a fluidic flow channel on the top surface and a wax coated base that covers the sample deposition zone at the back surface. The strips might be modified with an aPTT reagent and investigated for alteration in flow behaviours of normal plasmas in comparison to control samples (serum and buffer). An anticipated challenge in lateral flow aPTT assay development could be the continuous flow of plasma along the fluidic channel after clotting process has seized as was encountered in the PT assay development (Chapter 4). It led to low sensitivity and precision and aPTT being a slower and longer clotting test (35 to 45 s) than PT (10 to 13 s) in normal plasmas (Leonardi, 2019b), this challenge could be even more severe and more difficult to alleviate than in PT. Methods of trapping the flowing serum in paper matrix such as modification of the paper strips with fibrinogen nanoparticles (Rejinold et al., 2010) or fibrinogen coated nanoparticles (Marucco *et al.*, 2014) could be employed. The identified clotting effect on fluid flow behaviour could be quantified and further enhanced by assessing different aPTT reagents, different reagent concentrations, different strip geometries, different paper types, and different sample volumes. Each of these parameters could be assessed individually using at least three plasma samples that differ in aPTT values. The parameters would be selected based on precision of plasma distances and how far apart the plasmas differ in flow rate/distance.

The device should be tested against an established routine aPTT method using normal plasmas and plasma samples from haemophilia patients and the assay performance determined using appropriate analytical parameters.

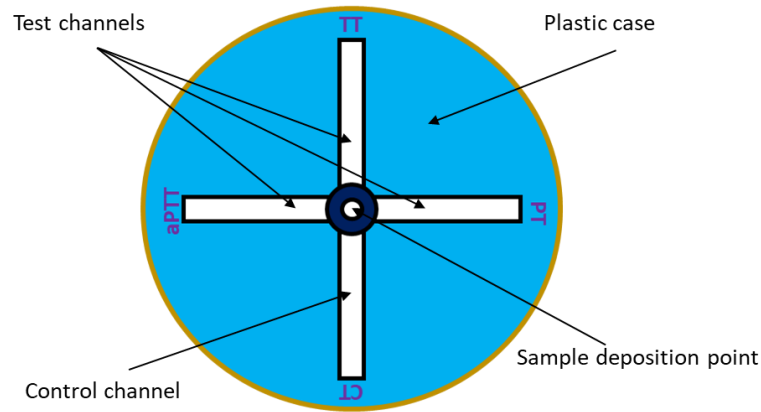


### 6.2.3 Development of a multiplexed lateral flow coagulation analyser

The three different lateral flow clot screening assays (fibrinogen/TT, PT, and aPTT) developed could be integrated into a multichannel device (Anfossi et al., 2018; Zhao *et al.*, 2016) with a single sample deposition zone (Fig. 6.1). The paper cartridge of the device could be circular in shape and bears four analytical channels (i.e., three test channels and a control channel) that join at the centre. Each test channel would conduct one of the clotting tests while the control channel would be used to normalise effects of temperature and humidity fluctuations as well to test for assay validity. The test channels would be modified with the appropriate reagent(s), while the control channel be modified with appropriate control materials. The multichannel paper cartridge could be sandwiched between two protective and reusable plastic discs to make it compact (Macaskie and Redwood, 2008). The upper plastic disk would bear a sample application window and a transparent window with millimetre reading scale along each channel.

Since platelets and other blood components interfere with clotting assays, to achieve adequate sensitivity and robustness, the multiplex clot screening device could be designed for PPP samples. At the sample zone where all the channels meet, the upper plastic protective disc could bear a perforated drainage piece (Zhao *et al.*, 2016). Since the individual testing channels would likely differ in optimum sample volume, the drainage piece could be designed and position in such a way that it would distribute the sample among the channels according to the sample volume requirement of the different channels. This could be achieved by using different drainage hole sizes toward the different channels. A sample chamber which would be placed on top of the drainage piece, could be designed to hold just the right sample volume so that the samples could be applied even without using a micropipette and the drainage holes would gently release and distribute the sample into the channels to ensure capillary rather than bulk flow into and along the channels.

The multiplex device would be calibrated using artificially constructed standard samples to define normal ranges after which it would be validated by testing on clinical samples and comparing the actual outcomes with the expected ones using statistical tests.



**Fig. 6.1.** Multiplexed lateral flow coagulation screening device showing thrombin time/quantitative fibrinogen channel (TT), prothrombin assay channel (PT), activated partial thromboplastin assay channel (aPTT), control test channel (CT), sample deposition point, and reusable strip housing plastic case.

#### 6.2.4 Development of lateral flow assay for detection of Von Willebrand Disease (vWD)

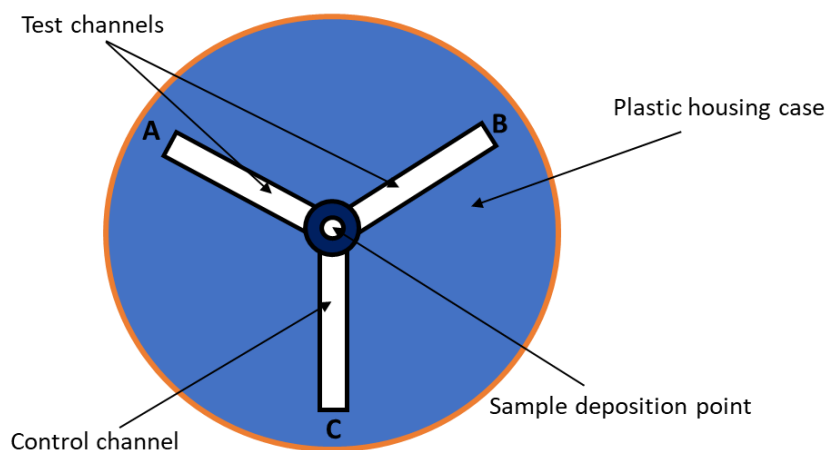
Von Willebrand's Factor (vWF) is a glycoprotein present in blood plasma at a normal concentration of about 10 µg/mL. It mediates adhesion of platelets to exposed collagen at the injured site via the GPIb receptor, as well as via fibrinogen and GPIIb/IIIa receptor. Dysfunction of vWF which leads to Von Willebrand disease (vWD), and/or dysfunction of the GPIb receptor called Bernard Soulier syndrome (BSS) result in either bleeding or thrombotic problems (Hoffbrand *et al*, 2015). The strip design used in the investigation of platelet behaviours on lateral flow strips (Chapter 5) could be used in the initial investigations. The test strips would be modified with ristocetin and collagen and tested for changes in the flow behaviour of normal PRPs samples compared to samples with defective GPIb and/or vWF. Collagen, being a highly hydrophobic material that greatly inhibits fluid flow on lateral flow strips but critical for vWF-mediated platelet adhesion, should be added to strip surfaces in a very dilute solution. A change in sample flow behaviour attributable to platelet adhesion and aggregation would be enhanced by assessing different collagen and ristocetin sources and concentrations as well as adding fibrinogen coated nanoparticles on test strips. Other analytical features such as sample volume, paper types and strip designs could also be explored to achieve optimum effect. The device could be validated with a cohort of PRP samples that includes normal and abnormal samples from vWD and BSS patients and comparing results with the expected outcomes.

### 6.2.5 Development of a multiplexed lateral flow platelet function analyser

Platelet adhesion/aggregation depend on both platelets and vWF and the multiplex analyser proposed here would be capable of detecting and differentiating inherent platelet defect and vWD. The two platelet assays (Chapter 5, and section 6.2.4), when fully developed could be integrated into a single device (Anfossi *et al.*, 2018; Zhao *et al.*, 2016) with one sample deposition point, two test channels and one control channel (Fig. 6.2). This device would be similar in shape to that of the one proposed for multiplex lateral flow coagulation analyser (section 6.2.3) but with three instead of four channels. One of the test channels would be coated with ristocetin and collagen and sensitive to Von Willebrand disease (vWD) and platelet defects such as Bernard Soulier syndrome (BSS) and thrombocytopenia. The other test channel will be coated with ADP and sensitive to platelet defects like thrombasthenia, thrombocytopenia, and aspirin ingestion. The control channel will be coated with an appropriate buffer, and it will be used to normalise environmental effects and to ascertain assay validity.

This device would be designed for testing PRP samples. Just like in the case of the multiplex coagulation analyser, it could be house in a plastic protective case that bears a sample deposition window and transparent windows with millimetre reading scales along the channels. It would also bear a sample chamber and a drainage piece.

The device will be calibrated to define normal and abnormal ranges and then validated by testing normal and patient samples and comparing actual and expected results.



**Fig. 6.2.** Multiplexed lateral flow platelet function analyser. A) analytical channel sensitive to Von Willebrand disease (vWD), Bernard Soulier syndrome (BSS) and thrombocytopenia, B) analytical channel sensitive to thrombasthenia, thrombocytopenia, and aspirin ingestion, C) control channel for normalising environmental effects and testing assay validity.

## 6.2.6 Deployment of the coagulation testing devices into low resource areas

Effective deployment of the proposed coagulation testing devices into a healthcare system in the intended regions would require a number of procedures including clinical and feasibility studies, securing regulatory and ethical approvals, cooperation of relevant stakeholders, training of healthcare personnels and so forth. The following strategies and procedures could be followed.

*Building partnership with key stakeholders:* For effective introduction and use of new diagnostic devices into a healthcare system, partnership and cooperation of key stakeholders in the target country/region have to be secured. Institutions such as the health ministry, relevant local NGOs, ethical and regulatory committees and so forth could be contacted and engaged in meeting and seminars in which the need for and how low-cost, multiplex, lateral flow coagulation screening devices would improve access to diagnosis and treatment for people with bleeding and clotting problems in the target communities. A strong need for the devices should be presented before the stakeholders via presentations, demonstrations, and discussions in order to ensure their cooperation.

*Conducting clinical assessment and feasibility studies:* Clinical assessment of the devices and the feasibility of effectively using them in the target communities should be conducted in conjunction with health ministry, and healthcare personnel in both public and private health facilities. NGOs could be engaged to secure funding for the process. In the clinical assessment, the performance of the devices within the target communities should be re-evaluated. The impact of the prevailing environmental conditions on operation and storage of the devices and should also be assessed and adjustments made accordingly.

*Securing ethical and regulatory approval:* Unfortunately, many developing countries especially those in West Africa do not have national level regulatory policies and guidelines for medical devices (Ekeigwe *et al*, 2019). However, where national level regulatory policies and guidelines do not exist, those within the WHO model (WHO, 2017) could be followed. The relevant regulatory policies and guidelines could be identified, and adjustments made accordingly in the design, labelling, packaging and usage of the devices. Other necessary procedures could be sorted and followed until approval is secure.

*Training healthcare personnel:* For proper handling and usage of the devices, healthcare personnel such as nurses and public health officers in target communities should be trained. Training on effective handling, storage, and operation of the devices could be conducted via workshops and seminars.

*Fabrication and distribution of the devices:* A building/venue for fabrication of the devices could be secured and furnished with a wax printer, workstations, and other necessary tools. The disposable paper test cartridges and reusable holders could be produced, packaged and distributed to the target area hospitals, clinics, and primary healthcare centres as needed.

## References

- Aizawa, P., Winge, S., & Karlsson, G. (2008). Large-scale preparation of thrombin from human plasma. *Thrombosis Research*, 122(4), 560–567. <https://doi.org/10.1016/j.thromres.2007.12.027>
- Akbar Dorgalaleh, Maryam Danshi, Jamal Rashidpanah, and E. R. Y. (2018). An Overview of Hemostasis. In *Congenital Bleeding Disorders* (pp. 3–26). Springer International Publishing. [https://doi.org/http://doi.org/10.1007/978-3-319-76723-9\\_1](https://doi.org/http://doi.org/10.1007/978-3-319-76723-9_1)
- Akyazi, T., Basabe-Desmonts, L., & Benito-Lopez, F. (2018). Review on microfluidic paper-based analytical devices towards commercialisation. *Analytica Chimica Acta*, 1001, 1–17. <https://doi.org/10.1016/j.aca.2017.11.010>
- Alnajrani, M. N., Aljohani, M. M., Chinnappan, R., Zourob, M., & Alsager, O. A. (2022). Highly sensitive and selective lateral flow aptasensor for anti-coagulant dabigatran etexilate determination in blood. *Talanta*, 236(September 2021), 122887. <https://doi.org/10.1016/j.talanta.2021.122887>
- Analytical Tools to Improve Optimization Procedures for Lateral Flow Assays. (2017). *Diagnostics*, 7(2), 29. <https://doi.org/10.3390/diagnostics7020029>
- Andersson, M., Andersson, J., Sellborn, A., Berglin, M., Nilsson, B., & Elwing, H. (2005). Quartz crystal microbalance-with dissipation monitoring (QCM-D) for real time measurements of blood coagulation density and immune complement activation on artificial surfaces. *Biosensors and Bioelectronics*, 21(1), 79–86. <https://doi.org/10.1016/j.bios.2004.09.026>
- Anfossi, L., Di Nardo, F., Cavalera, S., Giovannoli, C., & Baggiani, C. (2018). Multiplex lateral flow immunoassay: An overview of strategies towards high-throughput point-of-need testing. *Biosensors*, 9(1). <https://doi.org/10.3390/bios9010002>
- Anubhuti Saha and Shantanu Bhattacharya. (2020). Novel Paper Based Hand-Fabricated Point of Care Prothrombin Time Sensing Platform Using Pencil and Correction Pen. *ECS Meeting Abstracts*. <https://doi.org/10.1149/MA2020-01272020mtgabs>
- Bahadır, E. B., & Sezgintürk, M. K. (2016). Lateral flow assays: Principles, designs and labels. *TrAC - Trends in Analytical Chemistry*, 82, 286–306. <https://doi.org/10.1016/j.trac.2016.06.006>

- Bialkower, M., Manderson, C. A., McLiesh, H., Tabor, R. F., & Garnier, G. (2020). Paper Diagnostic for Direct Measurement of Fibrinogen Concentration in Whole Blood. *ACS Sensors*, 5(11), 3627–3638. <https://doi.org/10.1021/acssensors.0c01937>
- Bialkower, M., McLiesh, H., Manderson, C. A., Tabor, R. F., & Garnier, G. (2019). Rapid paper diagnostic for plasma fibrinogen concentration. *The Analyst*, 144(16), 4848–4857. <https://doi.org/10.1039/c9an00616h>
- Bialkower, M., McLiesh, H., Manderson, C. A., Tabor, R. F., & Garnier, G. (2020). Rapid, hand-held paper diagnostic for measuring Fibrinogen Concentration in blood. *Analytica Chimica Acta*, 1102, 72–83. <https://doi.org/10.1016/j.aca.2019.12.046>
- Bolliger, D., Lancé, M. D., & Siegemund, M. (2021). Point-of-Care Platelet Function Monitoring: Implications for Patients With Platelet Inhibitors in Cardiac Surgery. *Journal of Cardiothoracic and Vascular Anesthesia*, 35(4), 1049–1059. <https://doi.org/10.1053/j.jvca.2020.07.050>
- Catherine, S. (2021). Chemical Properties of Aspirin. *Journal of Clinical & Experimental Pharmacology Physical*, 11(1000), 2021.
- Chapin, J. C., & Hajjar, K. A. (2015). Fibrinolysis and the control of blood coagulation John NIH Public Access. *Blood Reviews*, 29(1), 17–24. <https://doi.org/10.1016/j.blre.2014.09.003>.Fibrinolysis
- Chen, X., Wang, M., & Zhao, G. (2020). Point-of-Care Assessment of Hemostasis with a Love-Mode Surface Acoustic Wave Sensor. *ACS Sensors*, 5(1), 282–291. <https://doi.org/10.1021/acssensors.9b02382>
- Chen, Y., Awasthi, A. K., Wei, F., Tan, Q., & Li, J. (2021). Single-use plastics: Production, usage, disposal, and adverse impacts. *Science of the Total Environment*, 752, 141772. <https://doi.org/10.1016/j.scitotenv.2020.141772>
- Choi, J.-L., Li, S., & Han, J.-Y. (2014). Platelet Function Tests: A Review of Progresses in Clinical Application. *BioMed Research International*, 2014, 1–7. <https://doi.org/10.1155/2014/456569>
- Colafranceschi, M., Papi, M., Giuliani, A., Amiconi, G., & Colosimo, A. (2006). Simulated point mutations in the A $\alpha$ -chain of human fibrinogen support a role of the  $\alpha$ C domain in the stabilization of fibrin gel. *Pathophysiology of Haemostasis*

and *Thrombosis*, 35(6), 417–427. <https://doi.org/10.1159/000102048>

- Cortet, M., Deneux-Tharoux, C., Dupont, C., Colin, C., Rudigoz, R. C., Bouvier-Colle, M. H., & Huissoud, C. (2012). Association between fibrinogen level and severity of postpartum haemorrhage: Secondary analysis of a prospective trial. *British Journal of Anaesthesia*, 108(6), 984–989. <https://doi.org/10.1093/bja/aes096>
- Dashkevich, N. M., Vuimo, T. A., Ovsepyan, R. A., Surov, S. S., Soshitova, N. P., Panteleev, M. A., Ataulakhanov, F. I., & Negrier, C. (2014). Effect of pre-analytical conditions on the thrombodynamics assay. *Thrombosis Research*, 133(3), 472–476. <https://doi.org/10.1016/j.thromres.2013.12.014>
- Díaz-González, M., & de la Escosura-Muñiz, A. (2021). Strip modification and alternative architectures for signal amplification in nanoparticle-based lateral flow assays. *Analytical and Bioanalytical Chemistry*, 413(16), 4111–4117. <https://doi.org/10.1007/s00216-021-03421-5>
- Doerge, L., Galm, M., & Horn, C. (2009). ( 12 ) *Patent Application Publication ( 10 ) Pub . No . : US 2009 / 0236238 A1*. 1(19).
- Dorgalaleh, A., Favaloro, E. J., Bahraini, M., & Rad, F. (2021). Standardization of Prothrombin Time/International Normalized Ratio (PT/INR). *International Journal of Laboratory Hematology*, 43(1), 21–28. <https://doi.org/10.1111/ijlh.13349>
- Douglas A, T. (2000). Coagulation and bleeding disorders: Review and update. *Clinical Chemistry*, 46(8 II), 1260–1269.
- Dudek, M. M., Kent, N., Gustafsson, K. M., Lindahl, T. L., & Killard, A. J. (2011). Fluorescence-based blood coagulation assay device for measuring activated partial thromboplastin time. *Analytical Chemistry*, 83(1), 319–328. <https://doi.org/10.1021/ac102436v>
- Dudek, M. M., Kent, N. J., Gu, P., Fan, Z. H., & Killard, A. J. (2011a). Development of a fluorescent method for detecting the onset of coagulation in human plasma on microstructured lateral flow platforms. *Analyst*, 136(9), 1816–1825. <https://doi.org/10.1039/c0an00907e>
- Dudek, M. M., Kent, N. J., Gu, P., Fan, Z. H., & Killard, A. J. (2011b). Development of a fluorescent method for detecting the onset of coagulation in human plasma on microstructured lateral flow platforms. *Analyst*, 136(9), 1816–1825. <https://doi.org/10.1039/c0an00907e>



- Dudek, M. M., Lindahl, T. L., & Killard, A. J. (2010). Development of a point of care lateral flow device for measuring human plasma fibrinogen. *Analytical Chemistry*, 82(5), 2029–2035. <https://doi.org/10.1021/ac902763a>
- Efremov, V., Lakshmanan, R. S., Donnell, J. O., & Killard, A. J. (2021). *Chemical and biological sensors Rapid Whole Blood Clot Retraction Assay on Quartz Crystal Microbalance*. 5(1), 2021–2024.
- Ekeigwe, Abigail; Clase, Kari; Byrn, Stephen R.; Shivanand, Paddy; and Ekeocha, Z. (2019). *Medical Devices Regulation in West Africa – A Situation Analysis*. <https://docs.lib.purdue.edu/birsfcm/1/>
- Ferrante, E. A., Blasier, K. R., Givens, T. B., Lloyd, C. A., Fischer, T. J., & Viola, F. (2016). A novel device for the evaluation of hemostatic function in critical care settings. *Anesthesia and Analgesia*, 123(6), 1372–1379. <https://doi.org/10.1213/ANE.0000000000001413>
- Gerbers, R. (2013). Development of Enhanced Lateral Flow test Devices for Point-of-Care Diagnostics. *University of Rhode Island*, 120. <http://digitalcommons.uri.edu/theses%0Ahttp://digitalcommons.uri.edu/theses/123>
- Giavarina, D. (2015). Understanding Bland Altman analysis. *Biochemia Medica*, 25(2), 141–151. <https://doi.org/10.11613/BM.2015.015>
- Guan, Y., Zhang, K., Xu, F., Guo, R., Fang, A., Sun, B., Meng, X., Liu, Y., & Bai, M. (2020). An integrated platform for fibrinogen quantification on a microfluidic paper-based analytical device. *Lab on a Chip*, 20(15), 2724–2734. <https://doi.org/10.1039/d0lc00439a>
- Guler, M. T., Isiksacan, Z., Serhatlioglu, M., & Elbuken, C. (2018). Self-powered disposable prothrombin time measurement device with an integrated effervescent pump. *Sensors and Actuators, B: Chemical*, 273(May), 350–357. <https://doi.org/10.1016/j.snb.2018.06.042>
- Han, D., Pauletti, G. M., & Steckl, A. (2014). *Blood coagulation screening using a paper-based microfluidic lateral flow device†*. September. <https://doi.org/10.1039/C4LC00716F>
- Harris, L. F., Castro-López, V., & Killard, A. J. (2013). Coagulation monitoring devices: Past, present, and future at the point of care. *TrAC - Trends in Analytical Chemistry*, 50, 85–95. <https://doi.org/10.1016/j.trac.2013.05.009>

- Harris, L., Lakshmanan, R. S., Efremov, V., & Killard, A. J. (2016). Point of care (POC) blood coagulation monitoring technologies. In *Medical Biosensors for Point of Care (POC) Applications*. Elsevier Ltd. <https://doi.org/10.1016/B978-0-08-100072-4.00009-5>
- Hegener, M. A., Li, H., Han, D., Steckl, A. J., & Pauletti, G. M. (2017). Point-of-care coagulation monitoring: first clinical experience using a paper-based lateral flow diagnostic device. *Biomedical Microdevices*, 19(3). <https://doi.org/10.1007/s10544-017-0206-z>
- Herrmann, R. P. (1979). Plasma Thrombin Assay using a Chromogenic Substrate in Disseminated Intravascular Coagulation due to Snake Bite Envenomation. *Thrombosis and Haemostasis*, 41(03), 544–552. <https://doi.org/10.1055/s-0038-1646807>
- Hoffbrand, A.V. and Steensma, D. P. (2019). *Hoffbrand's Essential Haematology* (8th ed.). WileyBlackwell.
- Hoffbrand, A. V. R. H. M. K. B. M. (2015). *Postgraduate Haematology* (7th ed.). WILEY.
- Hood, J. L., & Eby, C. S. (2008). Evaluation of a prolonged prothrombin time. *Clinical Chemistry*, 54(4), 765–768. <https://doi.org/10.1373/clinchem.2007.100818>
- Hyatt, C. E., & Brainard, B. M. (2016). Point of Care Assessment of Coagulation. *Topics in Companion Animal Medicine*, 31(1), 11–17. <https://doi.org/10.1053/j.tcam.2016.05.002>
- Ian J. Mackie, Steven Kitchen, Samuel J. Machin, G. D. O. L. (2003). Guidelines on fibrinogen assays. *British Journal of Haematology*, 396–404.
- Iwanaga, T., Miura, N., Brainard, B. M., Brooks, M. B., & Goggs, R. (2020). A Novel Microchip Flow Chamber (Total Thrombus Analysis System) to Assess Canine Hemostasis. *Frontiers in Veterinary Science*, 7(June), 1–16. <https://doi.org/10.3389/fvets.2020.00307>
- Jeong, S. G., Kim, J., Jin, S. H., Park, K. S., & Lee, C. S. (2016). Flow control in paper-based microfluidic device for automatic multistep assays: A focused minireview. *Korean Journal of Chemical Engineering*, 33(10), 2761–2770. <https://doi.org/10.1007/s11814-016-0161-z>

- Jeppesen, A. N., Kirkegaard, H., Ilkjær, S., & Hvas, A. M. (2016). Influence of temperature on thromboelastometry and platelet aggregation in cardiac arrest patients undergoing targeted temperature management. *Critical Care*, *20*(1), 1–10. <https://doi.org/10.1186/s13054-016-1302-9>
- Jiang, N., Ahmed, R., Damayantharan, M., Ünal, B., Butt, H., & Yetisen, A. K. (2019). Lateral and Vertical Flow Assays for Point-of-Care Diagnostics. *Advanced Healthcare Materials*, *8*(14), 1–19. <https://doi.org/10.1002/adhm.201900244>
- Jin, J., Quinton, T. M., Zhang, J., Rittenhouse, S. E., & Kunapuli, S. P. (2002). Adenosine diphosphate (ADP)-induced thromboxane A<sub>2</sub> generation in human platelets requires coordinated signaling through integrin  $\alpha\text{IIb}\beta\text{3}$  and ADP receptors. *Blood*, *99*(1), 193–198. <https://doi.org/10.1182/blood.V99.1.193>
- Killard, A. J. (2010). *A Lateral flow assay device for coagulation monitoring and method thereof* (Patent No. US 2012/0107851 A1).
- Kitamura, Y., Suzuki, M., Tsukioka, T., Isobe, K., Tsujino, T., Watanabe, T., Watanabe, T., Okudera, H., Nakata, K., Tanaka, T., & Kawase, T. (2018). Spectrophotometric determination of platelet counts in platelet-rich plasma. *International Journal of Implant Dentistry*, *4*(1). <https://doi.org/10.1186/s40729-018-0140-8>
- Kitchen, S., Geisen, U., Kappelmayer, J., Quehenberger, P., Drieß, J., Lowe, A., Jones, R., Boehm, J. G., Miles, G., & Rozsnyai, G. (2018). Evaluating the analytical performance of five new coagulation assays for the measurement of prothrombin time and activated thromboplastin time. *International Journal of Laboratory Hematology*, *40*(6), 645–654. <https://doi.org/10.1111/ijlh.12897>
- Ko, H., Park, S., & Kim, K. (2015). Aptamer-free electrochemical detection of thrombin based on coagulation reaction of ferrocene-labeled fibrinogen. *Journal of Electroanalytical Chemistry*, *742*, 70–73. <https://doi.org/10.1016/j.jelechem.2015.02.002>
- Kumar, S., Gallagher, R., Bishop, J., Kline, E., Buser, J., Lafleur, L., Shah, K., Lutz, B., & Yager, P. (2020). Long-term dry storage of enzyme-based reagents for isothermal nucleic acid amplification in a porous matrix for use in point-of-care diagnostic devices. *Analyst*, *145*(21), 6875–6886. <https://doi.org/10.1039/d0an01098g>

- Kumar, V., & Chapman, J. R. (2007). Whole blood thrombin: Development of a process for intra-operative production of human thrombin. *Journal of Extra-Corporeal Technology*, 39(1), 18–23.
- Lanza F, Beretz A, Stierlé A, Hanau D, Kubina M, C. J. (1988). Epinephrine potentiates human platelet activation but is not an aggregating agent. *Am J Physiol*, 1276–1288. <https://doi.org/10.1152/ajpheart.1988.255.6.H1276>
- Le Blanc, J., Mullier, F., Vayne, C., & Lordkipanidzé, M. (2020). Advances in platelet function testing—light transmission aggregometry and beyond. *Journal of Clinical Medicine*, 9(8), 1–17. <https://doi.org/10.3390/jcm9082636>
- Lee, H. J., Kim, J. E., Lee, H. Y., Lim, H. S., & Kim, H. K. (2014). Significance of local international sensitivity index systems for monitoring warfarin and liver function. *American Journal of Clinical Pathology*, 141(4), 542–550. <https://doi.org/10.1309/AJCP2RY1PIRRPUOW>
- Leonardi, M. J. (2019a). Laboratory Evaluation of Hemostasis Disorders. *Physician Assistant Clinics*, 4(3), 609–623. <https://doi.org/10.1016/j.cpha.2019.02.014>
- Leonardi, M. J. (2019b). Laboratory Evaluation of Hemostasis Disorders. *Physician Assistant Clinics*, 4(3), 609–623. <https://doi.org/10.1016/j.cpha.2019.02.014>
- Levi, M. (2018). Pathogenesis and diagnosis of disseminated intravascular coagulation. *International Journal of Laboratory Hematology*, 40(February), 15–20. <https://doi.org/10.1111/ijlh.12830>
- Levy, J. H., Szlam, F., Wolberg, A. S., & Winkler, A. (2014). Clinical use of the activated partial thromboplastin time and prothrombin time for screening: A review of the literature and current guidelines for testing. *Clinics in Laboratory Medicine*, 34(3), 453–477. <https://doi.org/10.1016/j.cll.2014.06.005>
- Li, H., Han, D., Pauletti, G. M., & Steckl, A. J. (2014). Point-of-care blood coagulation monitoring using lateral flow device. *18th International Conference on Miniaturized Systems for Chemistry and Life Sciences, MicroTAS 2014*, 1575–1577.
- Li, Hua, Han, D., Pauletti, G. M., & Steckl, A. J. (2018). Engineering a simple lateral flow device for animal blood coagulation monitoring. *Biomicrofluidics*, 12(1), 1–13. <https://doi.org/10.1063/1.5017496>

- Li, Hua, & Steckl, A. J. (2019). Paper Microfluidics for Point-of-Care Blood-Based Analysis and Diagnostics [Review-article]. *Analytical Chemistry*, 91(1), 352–371. <https://doi.org/10.1021/acs.analchem.8b03636>
- Limited, D. R., Results, R., & Use, I. (2022). Normal and Abnormal IQC Plasmas. *Diagnostics Reagents Limited*, 3–4.
- Lin, C.-H., Liu, C.-Y., Shih, C.-H., & Lu, C.-H. (2014). A sample-to-result system for blood coagulation tests on a microfluidic disk analyzer. *Biomicrofluidics*, 8(5), 052105. <https://doi.org/10.1063/1.4893917>
- Lo, K., Denney, W. S., & Diamond, S. L. (2006). Stochastic modeling of blood coagulation initiation. *Pathophysiology of Haemostasis and Thrombosis*, 34(2–3), 80–90. <https://doi.org/10.1159/000089929>
- Louka, M., & Kaliviotis, E. (2021). Development of an optical method for the evaluation of whole blood coagulation. *Biosensors*, 11(4). <https://doi.org/10.3390/bios11040113>
- Macaskie, L. E., & Redwood, M. D. (2008). ( 12 ) Patent Application Publication ( 10 ) Pub . No . : US 2008 / 0225123 A1 Patent Application Publication. *Privateaccess Point Containinga Sm Card*, 1(19), 11–14.
- Machovich, R. (1984). *The Thrombin* (Volume 1). CRC Press.
- Mahmud, M. A., Blondeel, E. J. M., Kaddoura, M., & MacDonald, B. D. (2018). Features in microfluidic paper-based devices made by laser cutting: How small can they be? *Micromachines*, 9(5), 1–12. <https://doi.org/10.3390/mi9050220>
- Manisha, H., Priya Shwetha, P. D., & Prasad, K. S. (2018). Low-cost Paper Analytical Devices for Environmental and Biomedical Sensing Applications. *Energy, Environment, and Sustainability*, 315–341. [https://doi.org/10.1007/978-981-10-7751-7\\_14](https://doi.org/10.1007/978-981-10-7751-7_14)
- Martinez, A. W., Phillips, S. T., Whitesides, G. M., & Carrilho, E. (2010). Diagnostics for the developing world: Microfluidic paper-based analytical devices. *Analytical Chemistry*, 82(1), 3–10. <https://doi.org/10.1021/ac9013989>
- Marucco, A., Turci, F., O'Neill, L., Byrne, H. J., Fubini, B., & Fenoglio, I. (2014). Hydroxyl density affects the interaction of fibrinogen with silica nanoparticles at physiological concentration. *Journal of Colloid and Interface Science*, 419, 86–94.

<https://doi.org/10.1016/j.jcis.2013.12.025>

Mehic, D., Pabinger, I., Ay, C., & Gebhart, J. (2021). Fibrinolysis and bleeding of unknown cause. *Research and Practice in Thrombosis and Haemostasis*, 5(4), 1–10. <https://doi.org/10.1002/rth2.12511>

Mikhailidis, D. P., Barradas, M. A., Maris, A., Jeremy, J. Y., & Dandona, P. (1985). Fibrinogen mediated activation of platelet aggregation and thromboxane A2 release: Pathological implications in vascular disease. *Journal of Clinical Pathology*, 38(10), 1166–1171. <https://doi.org/10.1136/jcp.38.10.1166>

Mohammadi Aria, M., Erten, A., & Yalcin, O. (2019). Technology Advancements in Blood Coagulation Measurements for Point-of-Care Diagnostic Testing. *Frontiers in Bioengineering and Biotechnology*, 7(December), 1–18. <https://doi.org/10.3389/fbioe.2019.00395>

Moss, A. V. H. and P. A. H. (2011). *Essential Haematology* (6th ed.). John Wiley & Sons.

National Institute for Health and Care Excellence. (2014). *Detecting, managing and monitoring haemostasis: viscoelastometric point-of-care testing (ROTEM, TEG and Sonoclot systems)*. August 2014. <https://www.nice.org.uk/guidance/dg13/resources/detecting-managing-and-monitoring-haemostasis-viscoelastometric-pointofcare-testing-rotem-teg-and-sonoclot-systems-1053628110277>

Neerman-Arbez, M., & Casini, A. (2018). Clinical consequences and molecular bases of low fibrinogen levels. *International Journal of Molecular Sciences*, 19(1). <https://doi.org/10.3390/ijms19010192>

Nieswandt, B., & Watson, S. P. (2003). Platelet-collagen interaction: Is GPVI the central receptor? *Blood*, 102(2), 449–461. <https://doi.org/10.1182/blood-2002-12-3882>

Palta, S., Saroa, R., & Palta, A. (2014). Overview of the coagulation system. *Indian Journal of Anaesthesia*, 58(5), 515–523. <https://doi.org/10.4103/0019-5049.144643>

Paniccia, R., Priora, R., Liotta, A. A., & Abbate, R. (2015). Platelet Function tests: A Comparative Review. *Vascular Health and Risk Management*, 11, 133–148. <https://doi.org/10.2147/VHRM.S44469>

- Papageorgiou, C., Jourdi, G., Adjambri, E., Walborn, A., Patel, P., Fareed, J., Elalamy, I., Hoppensteadt, D., & Gerotziafas, G. T. (2018). Disseminated Intravascular Coagulation: An Update on Pathogenesis, Diagnosis, and Therapeutic Strategies. *Clinical and Applied Thrombosis/Hemostasis*, 24(9\_suppl), 8S-28S. <https://doi.org/10.1177/1076029618806424>
- Pogorzelska, K., Krętowska, A., Krawczuk-Rybak, M., & Sawicka-Żukowska, M. (2020). Characteristics of platelet indices and their prognostic significance in selected medical condition – a systematic review. *Advances in Medical Sciences*, 65(2), 310–315. <https://doi.org/10.1016/j.advms.2020.05.002>
- Primpray, V., Chailapakul, O., Tokeshi, M., Rojanarata, T., & Laiwattanapaisal, W. (2019). A paper-based analytical device coupled with electrochemical detection for the determination of dexamethasone and prednisolone in adulterated traditional medicines. *Analytica Chimica Acta*, 1078, 16–23. <https://doi.org/10.1016/j.aca.2019.05.072>
- Qari, M. H. (2005). High throughput coagulation analysers review. *COMBINATORIAL CHEMISTRY & HIGH THROUGHPUT SCREENING*, 8, 353–360.
- Ramaswamy, B., Yeh, Y. T. T., & Zheng, S. Y. (2013). Microfluidic device and system for point-of-care blood coagulation measurement based on electrical impedance sensing. *Sensors and Actuators, B: Chemical*, 180, 21–27. <https://doi.org/10.1016/j.snb.2011.11.031>
- Rechner, A. (2009). *Stability, tromboplastin reagent with long-term* (Patent No. US2009/0162880 A1). <https://www.freepatentsonline.com/20090162880.pdf>
- Rejinold, N. S., Muthunarayanan, M., Deepa, N., Chennazhi, K. P., Nair, S. V., & Jayakumar, R. (2010). Development of novel fibrinogen nanoparticles by two-step co-acervation method. *International Journal of Biological Macromolecules*, 47(1), 37–43. <https://doi.org/10.1016/j.ijbiomac.2010.03.023>
- Rifai, N. (2018). *Tietz textbook of clinical chemistry and molecular diagnostics* (6th ed.). Elsevier.
- Roberts, D. E., McNicol, A., & Bose, R. (2004). Mechanism of Collagen Activation in Human Platelets. *Journal of Biological Chemistry*, 279(19), 19421–19430. <https://doi.org/10.1074/jbc.M308864200>
- Rojas-Murillo, J. A., Simental-Mendía, M. A., Moncada-Saucedo, N. K., Delgado-

- Gonzalez, P., Islas, J. F., Roacho-Pérez, J. A., & Garza-Treviño, E. N. (2022). Physical, Mechanical, and Biological Properties of Fibrin Scaffolds for Cartilage Repair. *International Journal of Molecular Sciences*, 23(17).  
<https://doi.org/10.3390/ijms23179879>
- Ruivo, S., Azevedo, A. M., & Prazeres, D. M. F. (2017). Colorimetric detection of D-dimer in a paper-based immunodetection device. *Analytical Biochemistry*, 538, 5–12. <https://doi.org/10.1016/j.ab.2017.09.009>
- Sajid, M., Kawde, A. N., & Daud, M. (2015). Designs, formats and applications of lateral flow assay: A literature review. *Journal of Saudi Chemical Society*, 19(6), 689–705. <https://doi.org/10.1016/j.jscs.2014.09.001>
- Sanfins, E., Augustsson, C., Dahlbäck, B., Linse, S., & Cedervall, T. (2014). Size-dependent effects of nanoparticles on enzymes in the blood coagulation cascade. *Nano Letters*, 14(8), 4736–4744. <https://doi.org/10.1021/nl501863u>
- Shih, C. H., Lu, C. H., Wu, J. H., Lin, C. H., Wang, Z. M., & Lin, C. Y. (2012). Prothrombin time tests on a microfluidic disc analyzer. *Sensors and Actuators, B: Chemical*, 161(1), 1184–1190. <https://doi.org/10.1016/j.snb.2011.11.025>
- Shirlyn B. McKenZie, J. L. W. (2010). *Clinical Laboratory Hematology* (2nd ed.). Pearson Education Inc.
- Smith, S. A., Comp, P. C., & Morrissey, J. H. (2006). Phospholipid composition controls thromboplastin sensitivity to individual clotting factors. *Journal of Thrombosis and Haemostasis*, 4(4), 820–827. <https://doi.org/10.1111/j.1538-7836.2006.01848.x>
- Smith, S. A., & Morrissey, J. H. (2004). Properties of recombinant human thromboplastin that determine the International Sensitivity Index (ISI). *Journal of Thrombosis and Haemostasis*, 2(9), 1610–1616. <https://doi.org/10.1111/j.1538-7836.2004.00897.x>
- Srivastava, A., & Kelleher, A. (2013). Point-of-care coagulation testing. *Continuing Education in Anaesthesia, Critical Care and Pain*, 13(1), 12–16.  
<https://doi.org/10.1093/bjaceaccp/mks049>
- Sunnersjö, L., Lindström, H., Schött, U., Törnquist, N., & Kander, T. (2023). The precision of ROTEM EXTEM is decreased in hypocoagulable blood : a prospective observational study. *Thrombosis Journal*, 1–8.



<https://doi.org/10.1186/s12959-023-00468-5>

Tsujino, T., Isobe, K., Kawabata, H., Aizawa, H., Yamaguchi, S., Kitamura, Y., Masuki, H., Watanabe, T., Okudera, H., Nakata, K., & Kawase, T. (2019).

Spectrophotometric determination of the aggregation activity of platelets in platelet-rich plasma for better quality control. *Dentistry Journal*, *7*(2).

<https://doi.org/10.3390/dj7020061>

Undas, A., & Ariëns, R. A. S. (2011). Fibrin clot structure and function: A role in the pathophysiology of arterial and venous thromboembolic diseases.

*Arteriosclerosis, Thrombosis, and Vascular Biology*, *31*(12), 88–99.

<https://doi.org/10.1161/ATVBAHA.111.230631>

Van Werkum, J. W., Hackeng, C. M., De Korte, F. I., Verheugt, F. W. A., & Ten Berg, J. M. (2007). Point-of-care platelet function testing in patients undergoing PCI: Between a rock and a hard place.

*Netherlands Heart Journal*, *15*(9), 299–305.

<https://doi.org/10.1007/BF03086004>

Verhovsek, M., Moffat, K. A., & Hayward, C. P. M. (2008). *Test of the Month*

*Laboratory testing for fibrinogen abnormalities. September*, 928–931.

<https://doi.org/10.1002/ajh.21293>

Vinholt, P. J., Nybo, M., Nielsen, C. B., & Hvas, A. M. (2017). Light transmission aggregometry using pre-coated microtiter plates and a Victor X5 plate reader.

*PLoS ONE*, *12*(10), 1–12. <https://doi.org/10.1371/journal.pone.0185675>

Wada, H., Matsumoto, T., & Yamashita, Y. (2014). Diagnosis and treatment of disseminated intravascular coagulation (DIC) according to four DIC guidelines.

*Journal of Intensive Care*, *2*(1). <https://doi.org/10.1186/2052-0492-2-15>

*WHO global model regulatory framework for medical devices including in vitro diagnostic medical devices.* (2017). World Health Organization.

<https://apps.who.int/iris/handle/10665/255177>

Winter, W. E., Flax, S. D., & Harris, N. S. (2017). Coagulation testing in the core laboratory. *Lab Medicine*, *48*(4), 295–313. <https://doi.org/10.1093/labmed/lmx050>

Yang, D. T., Robetorye, R. S., & Rodgers, G. M. (2004). Home prothrombin time monitoring: A literature analysis. *American Journal of Hematology*, *77*(2), 177–

186. <https://doi.org/10.1002/ajh.20161>

- Yetisen, A. K., Akram, M. S., & Lowe, C. R. (2013). *Paper-based microfluidic point-of-care diagnostic devices*. October 2015. <https://doi.org/10.1039/c3lc50169h>
- Zhao, Y., Wang, H., Zhang, P., Sun, C., Wang, X., Wang, X., Yang, R., Wang, C., & Zhou, L. (2016). Rapid multiplex detection of 10 foodborne pathogens with an up-converting phosphor technology-based 10-channel lateral flow assay. *Scientific Reports*, 6(February), 1–8. <https://doi.org/10.1038/srep21342>

## List of Publications and Presentations

Saidykhan, J., Selevic, L., Cinti, S., May, J.E., and Killard, A.J. (2021). Paper-based lateral flow device for the sustainable measurement of human plasma fibrinogen in low-resource settings. *Analytical Chemistry* 93:14007-14013.

Saidykhan, J., Pointon, L., Cinti, S., May, J.E., and Killard, A.J. (2022). Development of a paper-based lateral-flow prothrombin assay. *Analytical Methods*, DOI: 10.1039/D2AY00965J.

Saidykhan, J., Selevic, L., Cinti, S., May, J.E., and Killard, A.J. Paper-based lateral flow device for measuring fibrinogen in human plasma, AMYC Biomed, online, 3-5 Nov 2021.

Saidykhan, J. Improving the accessibility of blood coagulation testing using paper-based diagnostic technologies. 7th International Conference on Bio-Sensing Technology, Sitges, Spain, 22-25 May 2022. Oral presentation

Saidykhan, J., Selevic, L., Cinti, S., May, J.E., and Killard, A.J. Quantification of plasma fibrinogen using a paper-based lateral flow assay device. 7th International Conference on Bio-Sensing Technology, Sitges, Spain, 22-25 May 2022. Poster presentation.

Saidykhan, J., Pointon, L., Cinti, S., May, J.E., and Killard, A.J. Development of a paper-based lateral flow prothrombin assay. 7th International Conference on Bio-Sensing Technology, Sitges, Spain, 22-25 May 2022. Poster presentation.